UNIVERSIDADE TECNOLÓGICA FEDERAL DO PARANÁ

MARCELO DE OLIVEIRA

VISIBLE LIGHT COMMUNICATIONS: ANALYSIS OF COOPERATIVE COMMUNICATION AND AMPLIFICATION

DOCTORAL THESIS

CURITIBA

2022

MARCELO DE OLIVEIRA

VISIBLE LIGHT COMMUNICATIONS: ANALYSIS OF COOPERATIVE COMMUNICATION AND AMPLIFICATION

Comunicações por luz visível: análise de comunicação cooperativa e amplificação

Doctoral thesis submitted to the Graduate Program in Electrical and Computer Engineering of the Universidade Tecnológica Federal do Paraná as partial fulfillment of the requirements for the degree of "Doctor of Science (D.Sc.)" – Concentration area: Photonics in Engineering.

Advisor: Prof. Dr. Alexandre de Almeida Prado Pohl

Co-advisor: Prof. Dr. Paulo Miguel Nepomuceno Pereira Monteiro

CURITIBA
2022

-

Ministério da Educação
Universidade Tecnológica Federal do Paraná
Campus Curitiba

MARCELO DE OLIVEIRA

VISIBLE LIGHT COMMUNICATIONS: ANALYSIS OF COOPERATIVE COMMUNICATION AND AMPLIFICATION.

Trabalho de pesquisa de doutorado apresentado como requisito para obtenção do título de Doutor Em Ciências da Universidade Tecnológica Federal do Paraná (UTFPR). Área de concentração: Fotônica Em Engenharia.

Data de aprovação: 24 de Maio de 2022

Dr. Alexandre De Almeida Prado Pohl, Doutorado - Universidade Tecnológica Federal do Paraná

Dr. Glauber Gomes De Oliveira Brante, Doutorado - Universidade Tecnológica Federal do Paraná

Dr. Jair Adriano Lima Silva, Doutorado - Universidade Federal do Espírito Santo (Ufes)

Dr. Luis Carlos Vieira, Doutorado - Universidade Tecnológica Federal do Paraná

Dr. Luis Filipe Mesquita Nero Moreira Alves, Doutorado - Universidade de Aveiro

Documento gerado pelo Sistema Acadêmico da UTFPR a partir dos dados da Ata de Defesa em 29/07/2022.

ACKNOWLEDGEMENTS

First of all, my deepest gratitude to my father Mario and my mother Santina (*in memoriam*), who I wish was here to see me conclude this phase of my life. I would also like to thank my sisters Sandra and Sonia, who always supported me.

My sincere gratitude to my advisor Prof. Alexandre Pohl for the work guidance, patience and motivation during all these years, since my undergraduate times. From UTFPR, I would also like to thank David Farfán and Fernando Tosta for the support provided during my doctorate course, and to professor Luis Vieira for the support in the final stages of this work.

I would like to thank everyone who supported me during my time in Aveiro, specially to my co-advisor, Prof. Paulo Monteiro, and to the professors and colleagues from Instituto de Telecomunicações who helped me to develop this work: Fernando Guiomar, Isiaka Alimi, Jorge Silva, Luis Nero, Marco Fernandes and Paulo Santos.

This study was financed in part by the Coordenação de Aperfeiçoamento de Pessoal de Nível Superior - Brasil (CAPES) - Finance Code 001 and part by Conselho Nacional de Desenvolvimento Científico e Tecnológico (CNPq), process 305714/2016-3. Part of the experimental work was carried out at the Instituto de Telecomunicações, Aveiro, Portugal, through the research infrastructure ORCIP, supported by the European Regional Development Fund (FEDER) CENTRO-01-0145-FEDER-022141.

RESUMO

OLIVEIRA, Marcelo. Comunicações por luz visível: análise de comunicação cooperativa e amplificação. 122 f. Tese de doutorado – Programa de Pós-Graduação em Engenharia Elétrica e Informática Industrial, Universidade Tecnológica Federal do Paraná. Curitiba, 2022.

Comunicações sem fio por radiofrequência (RF) têm visto um grande crescimento na última década, onde usuários usufruem de altas taxas de dados e conveniência. No entanto, enquanto a demanda por recursos sem fios cresce, seja de usuários móveis ou de dispositivos da Internet das Coisas, essa faixa de espectro se aproxima da saturação. Na busca por novas soluções, as comunicações por luz visível (*visible light communications* – VLC) emergem como uma potencial tecnologia, explorando o espectro visível para transmitir informação. Porém, apesar de suas vantagens, o VLC ainda apresenta desafios que devem ser superados antes de sua aplicação no mundo real. Neste sentido, este trabalho contribui para o desenvolvimento de sistemas VLC por meio de um modelo de simulação versátil que permite o cálculo de parâmetros de desempenho, tais como potência recebida, razão sinal-ruído (*signal-to-noise ratio* – SNR), taxa de erro de bit (*bit error rate* – BER) e magnitude vetorial do erro (*error vector magnitude* – EVM), em ambientes personalizáveis. O modelo é então empregado para analisar enlaces VLC auxiliados por *relay* em que, além da fonte e do destino, um nó de *relay* é incluído no percurso para auxiliar o enlace de comunicação. Isso é alcançado por meio da técnica *amplify-and-forward* no nó relay, em que o sinal da fonte é amplificado e retransmitido para o destino, onde os sinais da fonte e *relay* são combinados e processados. Resultados de simulação mostram que a cooperação melhora o desempenho do enlace e pode permitir a comunicação em cenários em que originalmente não seria possível. Além de simulações, os enlaces VLC com cooperação foram testados experimentalmente. Empregando diferentes configurações de percurso, é demonstrado que valores de SNR melhoram entre 4 e 8 dB e valores de BER melhoram em até uma ordem de magnitude. Como amplificação é um importante aspecto da cooperação *amplify-and-forward* empregada, simulações de amplificação óptica e elétrica no VLC também são desenvolvidas. Uma comparação de ambas as técnicas é apresentada, com resultados mostrando que o desempenho de um amplificador óptico de 3.7 dB é comparável a um ganho de 50 dB apenas no domínio elétrico. Por fim, uma aplicação específica do VLC, o seu uso na transmissão de sinais *downlink* de padrões de redes móveis LTE (4G) e 5G, é avaliada. Resultados experimentais mostram valores de EVM de 7 e 12 dB abaixo do EVM limite, para 4G e 5G respectivamente, à distância de 3 m.

Palavras-chave: Comunicações por Luz Visível, VLC, Comunicação Cooperativa, Amplificação de Luz, LTE, 4G, 5G

ABSTRACT

OLIVEIRA, Marcelo. Visible light communications: analysis of cooperative communication and amplification. 122 p. Doctoral thesis – Graduate Program in Electrical and Computer Engineering, Universidade Tecnológica Federal do Paraná. Curitiba, 2022.

Wireless radio frequency (RF) communication has seen an enormous growth in the last decade, with users enjoying its high data rates and convenience. However, as the demand of mobile users and devices employed in the Internet of Things grows, the use of the radio frequency spectrum approaches saturation. In search for new solutions, visible light communication (VLC) emerges as a potential technology that exploit the visible spectrum to transmit information. However, despite its advantages, VLC still presents limitations that must be addressed before it is deployed in the real world. In this sense, this work contributes with the development of VLC systems by means of a versatile simulation model that enables the calculation of performance parameters, such as received power, signal-to-noise ratio (SNR), bit error rate (BER) and error vector magnitude (EVM) in customizable environments. The model is then employed to evaluate relay-assisted cooperative VLC links, in which, besides the source and the destination, a relay node is added to the path to support communication. This is accomplished by using the amplify-and-forward technique at the relay node, where the source signal is amplified and retransmitted to the destination, at which point both source and relay signals are combined and processed. Simulation results show that cooperation improves the link performance and even allow communication in cases where it wouldn't originally be feasible. Besides simulations, the cooperative VLC links were tested experimentally. Using different path configurations it is demonstrated that SNR improves by an amount varying from 4 to 8 dB and BER results improves by up to one order of magnitude. As amplification is an important aspect of the employed amplify-and-forward technique, a simulation of optical and electrical amplification in VLC links is also accomplished. A comparison of both schemes is presented with results showing that the performance of an optical amplifier of 3.7 dB is comparable to a gain of 50 dB solely in the electrical domain. Finally, a specific application of VLC in the transmission of standard downlink mobile signals for LTE (4G) and 5G is evaluated. Experimental results show EVM values of 7 and 12 dB below the EVM limit for 4G and 5G, respectively, at 3 m distance.

Keywords: Visible Light Communications, VLC, Cooperative Communication, Light Amplification, LTE, 4G, 5G

LIST OF FIGURES

LIST OF TABLES

LIST OF ABBREVIATIONS

3GPP	3rd Generation Partnership Project
AF	Amplify-and-forward
APD	Avalanche photodiode
ASE	Amplified spontaneous emission
AWG	Arbitrary waveform generator
AWG	Arbitrary waveform generator
AWGN	Additive white Gaussian noise
BPSK	Binary phase shift keying
CP-OFDM	Cyclic prefix OFDM
CP	Cyclic prefix
CSK	Color shift keying
DF	Decode-and-forward
DSP	Digital signal processing
EGC	Equal-gain combining
EVM	Error vector magnitude
FOV	Field of view
FR1	Frequency Range 1
FR2	Frequency Range 2
FSO	Free space optical
IFFT	Inverse fast Fourier transform
IM/DD	Intensity modulation and direct detection
IoT	Internet of Things
IR	Infrared
ISI	Intersymbol interference
LED	Lighting-emitting diode
LiFi	Light-fidelity
LOS	Line-of-sight
LTE	Long-Term Evolution
MCM	Multi-carrier modulation
MIMO	Multiple-input and multiple-output
MRC	Maximum Ratio Combining
NLOS	Non line-of-sight
NR	New Radio
NRZ	Non return to zero
OCDMA	Optical code-division multiple access
OFDM	Orthogonal frequency-division multiplexing
OFDMA	Orthogonal frequency division multiple access
OOK	On-off keying
OWC	Optical wireless communications
PAM	Pulse amplitude modulation
PAPR	Peak-to-average power ratio

PD	Photodiode
PPM	Pulse position modulation
PWM	Pulse-width modulation
QAM	Quadrature amplitude modulation
QoS	Quality of service
RF	Radio frequency
RMS	Root-mean-square
SC-FDMA	Single channel orthogonal frequency division multiple access
SC	Selection combining
SNR	Signal-to-noise ratio
SSBI	Signal-to-signal beating interference
TIA	Transimpedance amplifier
UE	User equipment
UV	Ultraviolet
V2I	Vehicle to infrastructure
V2V	Vehicle to vehicle
VANET	Vehicular ad hoc network
VLC	Visible light communications
VSA	Vector signal analyzer
VSG	Vector signal generator
WDM	Wavelenght division multiplexing
WLAN	Wireless local area network

LIST OF NOTATIONS

φ	Emission angle
I	Luminous intensity
dS	Light emitter area
$\varphi_{1/2}$	Half-power semiangle
m	Lambertian order
γ	Photodetector's responsivity
$Y(t)$	Received signal
$X(t)$	Transmitted signal
$h(t)$	Impulse response
$N(t)$	AWGN noise
$\otimes$	Convolution operation
θ	Incidence angle at the photodetector
A	Photodetector's detection area
d	Distance between transmitter and receiver
H	DC channel gain
$T_s(\theta)$	Optical filter gain
$g(\theta)$	Optical concentrator gain
FOV	Photodetector's field of view
n	Refraction index
P_r	Received optical power
P_t	Transmitted optical power
ρ	Reflectance factor
d_1	Distance between source and reflective surface
d_2	Distance between reflective surface and receiver
α	Angle between source and reflective surface
β	Angle between reflective surface and destination
σ^2_{total}	Total noise
σ_{shot}	Shot noise
$\sigma_{thermal}$	Thermal noise
P_{rISI}	ISI noise
q	Elementary charge
B	Noise equivalent bandwidth (or data rate)
I_{bg}	Backlight current
I_2	Noise bandwidth factor
k	Boltzmann constant
T_k	Absolute temperature
G	Open loop gain
η	Fixed capacitance of the photodetector by area unit
Γ	FET noise factor
I_3	Noise bandwidth factor
M	Order of M-QAM modulation

h_{sr}	Height between source and relay
h_{rd}	Height between relay and destination
G_{el}	Gain in electrical amplification
G_{op}	Gain in optical amplification
h	Planck's constant
ν	Wave frequency
η_q	Quantum efficiency
λ	Wavelength

CONTENTS

1 INTRODUCTION

Since the advent of mobile telephony, in the beginning of the 1980s and taking into account other largely widespread services so far, such as television and radio, the radio frequency (RF) spectrum is approaching its capacity limits (KARUNATILAKA *et al.*, 2015). Despite improvements that allowed a better utilization of the RF spectrum, reaching higher bits/s/Hz rates, this spectral efficiency is approaching saturation, without the allocation of new RF bands (HAAS, 2013), though recent efforts are pushing 5G beyond the 11 GHz spectrum (HONG *et al.*, 2017). In this scenario, a proposed solution is the use of other regions of the electromagnetic spectrum for data transfer. These techniques are called optical wireless communications (OWC) and refers to any technology in which the electromagnetic bands corresponding to visible light, infrared (IR) or ultraviolet (UV) are employed for communication (UYSAL; NOURI, 2014).

Among the categories of OWC, free space optical (FSO) communication (KHALIGHI; UYSAL, 2014) are systems that employ very narrow laser beams for long range communication, *e.g.*, among buildings, and have applications such as last-mile access networks, enterprise or campus connectivity, video surveillance, among others. Another category of OWC are the visible light communications (VLC), which refers to those techniques that employ visible light, *i.e*, electromagnetic waves with frequencies between 400 and 800 THz (wavelengths between 380 and 780 nm) (RAJAGOPAL *et al.*, 2012), and are suitable to short- and mid-range indoor communications. Using light sources, primarily LEDs (lighting-emitting diodes), information is transmitted through free space, in line-of-sight (LOS) links, or through reflections (non line-of-sight – NLOS) and is captured at the other end by photodetectors, typically photodiodes (PDs)

Examples of VLC can be traced back to pre-historical times, as smoke signals were employed to transmit a message, for instance (DIMITROV; HAAS, 2015). In 1880, Alexander Graham Bell presented the photophone, a device that was capable of modulating a voice message in a light signal (BELL, 1880). Recent progress began with the pioneer work of Gfeller and Bapst (1979), in which it was proposed a model for the OWC channel and demonstrated its potential for the development of indoor networks, taking advantage of hundreds of THz of available optical spectrum. Initially, however, research on OWC focused in the IR domain, due to the low power emitted by visible light devices at the time, making it unfeasible for communication purposes. This context

began to change with the invention of the blue LED, based on gallium nitride (GaN), by Shinji Nakamura in 1993 (NAKAMURA *et al.*, 1994), that led to the development of the white LED, which has high energetic efficiency and high power. White LEDs can be manufactured by a mix of red, green and blue lights or from blue LEDs with a layer of yellow phosphor (BESSHO; SHIMIZU, 2012), a technique that is more common due to the lower cost and complexity (WANG *et al.*, 2015a).

Until then, LEDs were typically employed only as indicative lights. However, with the white LEDs these devices began to be employed as environmental illumination sources (BESSHO; SHIMIZU, 2012). In 2001, Tanaka *et al.* considered for the first time its use for communication and illuminations simultaneously (TANAKA *et al.*, 2001), a feature that has become recurrent in the literature as, for instance, in the proposition of the LiFi (light-fidelity) standard (HAAS *et al.*, 2016).

The LiFi standard proposes to expand the VLC technology to become a complete LAN networking protocol with multiuser capacity and bidirectional access (DIMITROV; HAAS, 2015). The IEEE 802.15.7 standard (Institute of Electrical and Electronics Engineers, 2011), that defines VLC standards and protocols, is currently being revised to include LiFi (HAAS *et al.*, 2016). LiFi proposes the implementation in the environments of multiple access points called attocells (as a reference to the femtocells used in RF) (HAAS, 2013) to ensure the coverage of the whole space and therefore provide complete mobility to the user. It is estimated that the market for LiFi technology will be worth 75.5 billion dollars in 2023 (Global Market Insights, 2016).

Single carrier modulations typically employed in VLC, such as OOK (on-off keying), PAM (pulse amplitude modulation) and PPM (pulse position modulation) are equally usable in LiFi. However, as this technology intends to be a substitute or complement to existing WiFi networks, high data rate links are essential (HAAS *et al.*, 2016). Thus, in LiFi and in any VLC link in which high data rates are desired, the use of multicarrier modulations is very common. In the case of VLC, orthogonal frequency-division multiplexing (OFDM) is the default choice as multicarrier technique. In this method, parallel data streams are transmitted in different orthogonal subcarriers, therefore reaching higher rates with a simple equalization at the destination. Due to the inherent features of LED communication systems, adaptations are needed in OFDM, which was initially developed for RF communications. Thus, several OFDM methods specific for VLC have been proposed, such as DCO-OFDM (DC biased optical OFDM), ACO-OFDM (asymmetrically clipped optical OFDM) and ADO-OFDM (asymmetrically

clipped DC biased optical OFDM) (DISSANAYAKE; ARMSTRONG, 2013). Single carrier techniques are also employed (RAHMAN *et al.*, 2020), with the advantage of not having the the high peak-to-average power ratio (PAPR) of OFDM (HSIEH; SHIU, 2006).

There are also propositions of hybrid WiFi/LiFi models, in order to improve the reliability of the systems and provide a better quality of service (QoS) (HAAS *et al.*, 2016). This hybrid model also has the advantage of a possible solution to one of the main limitations in the design of VLC systems, which is the uplink from the user equipment (UE) to the access point (KARUNATILAKA *et al.*, 2015).

With increasing interest in VLC research, higher data rates are being pursued. The group of Tanaka *et al.*, mentioned early, that firstly proposed the use of LEDs for simultaneous communication and illumination, in 2003 presented a VLC system employing OOK capable of reaching up to 400 Mbps (TANAKA *et al.*, 2003). Vucic *et al.* (2010) showed a 500 Mbps system in a implementation based on DCO-OFDM and, later, a 800 Mbps system employing RGB LEDs, modulating each color separately (VUCIC *et al.*, 2011). Khalid *et al.* (2012), in a similar way, but with a larger DCO-OFDM band, demonstrated the first system with a rate higher than 1 Gbps, using a white LED with phosphor and, later, a system capable of up to 3.4 Gbps using a commercial RGB LED (COSSU *et al.*, 2012). Wang *et al.* (2015b) demonstrated a system with data rate of 4.5 Gbps using RGB LED, using wavelength division multiplexing (WDM) techniques and the RLS algorithm. Chun *et al.* (2016) implemented a system capable of reaching over 10 Gbps rates, also employing WDM and RGB LEDs, but with different color combinations. Bian *et al.* (2019) reported a 15.73 Gbps system with off-the-shelf LEDs after forward error correction codes over 1.6 m, employing OFDM and adaptive bit loading. Figure 1 presents this data rate evolution over time in a graphical manner. Nevertheless, it is prudent to note that in general these implementations are realized in non-practical scenarios and are better seeing as a proof of concept. A commercial set of access point and transmitter released in 2018 by the company pureLiFi, from the United Kingdom, provides data rates of around 40 Mbps, bidirectionally (Mobile World Live, 2018). LiFiMAX Flex, from Oledcomm, provides plug and play full-duplex LiFi connection with 100 Mbps download (LIFI.CO, 2022).

Possible application areas for VLC are numerous and, in parallel to research towards higher data rates and energy and spectral efficiency, specific practical applications has also being developed. These applications target medium range communications,

Figure 1 – Evolution over time of record VLC data rates reported in the literature. References: [1] Tanaka *et al.* (2003), [2] Vucic *et al.* (2010), [3] Vucic *et al.* (2011), [4] Khalid *et al.* (2012), [5] Cossu *et al.* (2012), [6] Wang *et al.* (2015b), [7] Chun *et al.* (2016), [8] Bian *et al.* (2019).

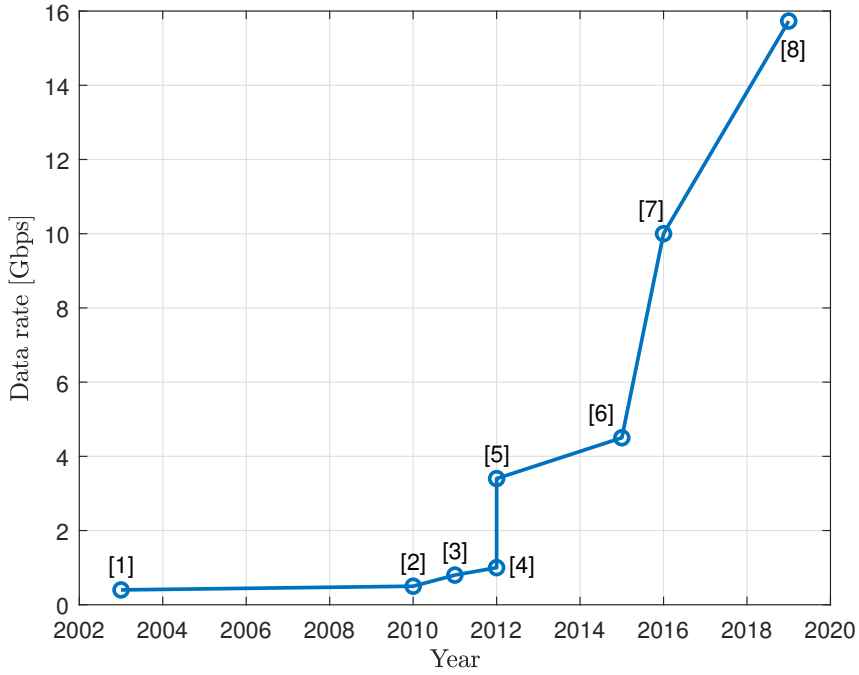

Source: The author.

i.e., in the range of meters (UYSAL; NOURI, 2014). In closed environments, it is possible to act as a wireless local area (WLAN) network, either as a unique solution or in hybrid LiFi/WiFi networks (HAAS *et al.*, 2016). At environments considered critical, such as airplane cabins (DIMITROV; HAAS, 2015) or hospitals (ZWAAG *et al.*, 2021), VLC becomes interesting due to the fact that it does not cause interference with RF waves. It is also possible to employ VLC in vehicular communications, either as vehicle to vehicle communication or between vehicle and infrastructure, such as semaphores (PREMACHANDRA *et al.*, 2010; UCAR *et al.*, 2016). Another potential application is underwater communications, in which VLC has many advantages over the usually employed acoustic communications which, besides its long range, has the limitations of low rates and high latencies (UYSAL; NOURI, 2014). There is also research towards assistive applications for visually impaired individuals, in which highly precise positioning sensors based on VLC may support safe displacement in public spaces (OKUDA *et al.*, 2014).

Unlike what is observed in RF links, visible light communications do not suffer from multipath fading (KAHN; BARRY, 1997). This happens due to the fact that the photodiode areas are millions of times larger than the visible light wavelengths, resulting in

a rich spatial diversity (KAHN; BARRY, 1997; KOMINE *et al.*, 2004; GHASSEMLOOY *et al.*, 2013). However, VLC links are prone to other adverse effects, such as intersymbol interference (ISI) and shadowing. VLC systems are prone to ISI effects specially as data rates or bandwidth grows (HSIEH; SHIU, 2006), while shadowing refers to regions of the environment where light does not reach with full power (in the VLC case, literally shadows), limiting communication performance (KOMINE *et al.*, 2004).

Cooperative communication techniques and relay-assisted communication are possible tools to diminish these undesired effects. In relay-assisted VLC, a relay device between the source and destination captures the source information, processes it and retransmits to the destination. Cooperative communication techniques were developed in order to reach spatial diversity in RF scenarios in which, for practical reasons, it is not possible to add more antennas to the system, specially in the receiver end (YANG; PANDHARIPANDE, 2013). Cooperative communication may also be employed in VLC links, in order to diminish harmful effects or to expand capacity and reach of the installed systems (YANG; PANDHARIPANDE, 2013, 2014; CUI *et al.*, 2016; NARMANLIOGLU *et al.*, 2017). In this scenario, there is also a relay, but the destination receives both source and relay information and combines them.

Relaying in VLC may extend communication distance in a hop-on-hop fashion and enable communication when there is no direct line-of-sight between source and destination. The relay may also act as a support to infrastructure, extending communication reach without additional backbone structure. In cooperative communication, the destination receives both the source and relay signals and combines them to improve performance of VLC systems, which may be quantified as improvement of BER or SNR values.

This work addresses cooperative communication in the context of VLC, creating a path by developing a platform for VLC simulations, which are employed to evaluate VLC cooperation. Cooperation is also analyzed by a experimental setup, analyzing different configurations. In order to implement cooperative communication in VLC, light amplification is required at the relay, which is the device that supports cooperation. In this sense, two possibilities of amplification, electric and optical, are simulated and compared.

Finally, the experimental setup is also employed to explore a practical application, in the form of transmission of LTE and 5G mobile signals. It was conducted the transmission of downlink signals of both technologies using VLC over varying distances to evaluate its communication performance.

1.1 OBJECTIVES

This work aims a step forward towards a wide adoption and popularization of the VLC technology, by providing results and tools to give support for such development, both theoretically and experimentally, using the cooperative cooperation technique as the main tool. In this way, specific objectives include:

1. Develop a flexible simulation model to evaluate different indoor scenarios with customizable parameters, such as environment dimensions and transmitter and receiver properties and implement a graphical interface to allow easy simulation of different scenarios;

2. Investigate the application of cooperative communication in VLC, analyzing simulation scenarios and proposing experimental setups;

3. Analyze means of light amplification, namely electric and optical, to compare the methods and study their advantages and limitations for deployment of cooperative VLC systems;

4. Study a specific application, the transmission of LTE and 5G, analyzing its applications and evaluating its performance and viability.

1.2 STRUCTURE OF THE DOCUMENT

This thesis is organized as follows. Chapter 2 contextualizes the VLC technology, reporting historical development, its operating principles and describing its applications, advantages and limitations. Largely employed in this work, the VLC channel model is described in detail.

In Chapter 3, the simulation model used throughout this thesis is described and its implementation is detailed, applying the model presented in the previous chapter. To illustrate the application of the simulation model, communication scenarios are defined, different parameters are applied and its results presented. Lastly, a graphical interface for intuitive VLC simulation is presented.

The next three Chapters addresses more specific aspects of VLC. In each chapter, a theoretical and background introduction is given, followed by the developed work in the theme of that Chapter. In Chapter 4, cooperative communication in the VLC context

is analyzed. Simulation scenarios are described and results presented. For the practical analysis, a experimental setup is proposed, in which different placement of components are defined to obtain SNR and BER values.

As signal amplification is necessary for the amplify-and-forward cooperative communication in VLC, in Chapter 5 electrical and optical amplification are described and compared, including simulations. More practical applications are the theme of Chapter 6. In this Chapter, 4G (LTE) and 5G mobile signals are experimentally transmitted using VLC and performance results are presented.

Finally, Chapter 7 concludes this thesis with comments on the achieved development and final considerations.

Below are listed the papers published along the development of this thesis:

1. M. de Oliveira, L. N. Alves, P. P. Monteiro and A. de A. P. Pohl, "*On the use of Amplification in Visible Light Communication Systems*," **2019 SBFoton International Optics and Photonics Conference (SBFoton IOPC)**, São Paulo, Brazil, 2019, pp. 1-4.

2. M. de Oliveira, M. A. Fernandes, P. Santos, F. P. Guiomar, L. N. Alves, P. P. Monteiro and A. de A. P. Pohl, "*Experimental Transmission of LTE Signal Using Visible Light Communications*," **2019 SBMO/IEEE MTT-S International Microwave and Optoelectronics Conference (IMOC)**, Aveiro, Portugal, 2019, pp. 1-3.

3. M. de Oliveira, P. P. Monteiro and A. de A. P. Pohl, "*Performance Improvement of VLC Systems Employing an Amplify-and-Forward Scheme*," **2019 22nd International Symposium on Wireless Personal Multimedia Communications (WPMC)**, Lisbon, Portugal, 2019, pp. 1-5.

4. F. C. B. Tosta, M. de Oliveira and A. de A. P. Pohl, "*Análise e caracterização de luminária LED aplicada em comunicação por luz visível*," **XXXVIII Simpósio Brasileiro de Telecomunicações e Processamento de Sinais - SBrT 2020**, Florianópolis, Brazil, 2020, pp. 1-4.

5. M. de Oliveira, F. C. B. Tosta, D. E. F. Guillen, P. P. Monteiro and A. de A. P. Pohl, "*Theoretical and Experimental Analysis of LED Lamp for Visible Light Communications*," **Wireless Personal Communications**, published May 20th 2022.

6. M. de Oliveira, L. C. Vieira, F. P. Guiomar, L. N. Alves, P. P. Monteiro and A. de A. P. Pohl, "*Experimental Assessment of the Performance of Cooperative Links in Visible Light Communications*," **Optics Communications**, Volume 524, 2022.

2 FUNDAMENTALS OF VISIBLE LIGHT COMMUNICATIONS

In this chapter, fundamental concepts related to VLC are presented. The VLC technology is contextualized and its theoretical concepts are detailed, such as the channel model and employed modulation formats.

2.1 VISIBLE LIGHT COMMUNICATIONS

The expression VLC typically refers to visible light communications in short and medium range and in a diffuse manner, using light sources such as LEDs, at indoor environments such as houses, offices, shopping malls etc. It is different from, for instance, the expression free space optical (FSO) communications, which usually refers to point-to-point LOS communications using high-power lasers (UYSAL; NOURI, 2014; GUPTA *et al.*, 2017) at long range distances, *i.e.*, up to several kilometers (KHALIGHI; UYSAL, 2014). FSO communications aims applications such as communication between buildings, between Earth and spaceships or between spaceships, in distances that may reach hundreds of kilometers, or even spatial and inter-satellite communications, such as between the Earth and the Moon (UYSAL; NOURI, 2014).

Figure 2 presents a general diagram of a VLC link. In general terms, the system diagram is similar to a RF system, but with some peculiarities for a visible light-based system. For instance, the LED must be driven by a signal that combines DC light to turn on the lights and a AC signal, the message. An optical filter is desirable before the photodetector. Noise is inherently added to the system, particularly the shot and thermal noises. The analysis of predominance of each noise source is given at Section 5.2.

As mentioned, VLC transmitters are light sources, mainly LEDs, either the small ones or large luminaires (in this case, typically combining communication and illumination). Blue LEDs with a phosphor layer may require a blue filter at the reception for a better performance. With RGB LEDs, each color can be modulated separately, taking advantage of the three LEDs presence to achieve better performances (ISLIM; HAAS, 2016). The receivers employ photodetectors, specially photodiodes (PDs), but image sensors, such as cameras, can also be used.

VLC links may employ parallel transmissions, *i.e.*, a MIMO (multiple-input multiple-output) system, in which multiple LEDs and photodetectors are simultaneously used in order to improve the VLC link performance (GHASSEMLOOY *et al.*, 2013;

Figure 2 – General diagram of a VLC link.

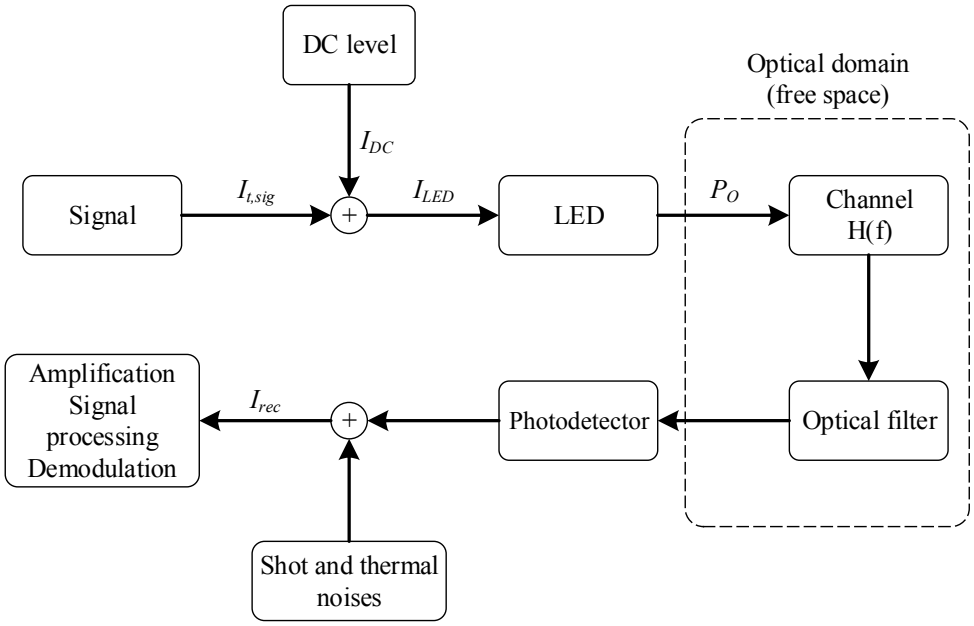

Source: Adapted from Karunatilaka *et al.* (2015).

KARUNATILAKA *et al.*, 2015). MIMO systems may, besides improving data rates, allow a flexibilization of the systems in order to allow higher mobility and less mechanical alignment restrictions. Also, it enables a wider variety of channel coding techniques (AZHAR *et al.*, 2013; JHA *et al.*, 2015). Table 1 summarizes a comparison of RF and VLC features, based on Kahn and Barry (1997).

Table 1 – Comparison between RF and VLC communications.

Property	Radio frequency	VLC
Available spectrum	~300 GHz	~400 THz
Spectrum regulation	Yes	No
Security	Limited	High
Coverage	High	Limited
Multipath distortion	Yes	Yes
Multipath fading	Yes	No
Path loss	High	Higher
Electromagnetic interference	High	None
Infrastructure	Access point	Illumination
Prevailing noise	Other users	Background light

2.1.1 Advantages and limitations of VLC

The research on VLC is stimulated due to the advantages of this technology. Below, some of these features are listed.

- Spectrum: with the growth in demand for wireless communications, the RF spectrum has become increasingly congested (OH, 2013). It is cheaper for mobile providers to acquire new spectrum bands than to invest in more base stations to increase capacity (BALDWIN, 2012); however, the RF spectrum is a limited resource. On the other hand, the visible light spectrum is near 10 thousand times larger than the radio wave spectrum, providing a vastly wider available band. While the RF spectrum consists of about 300 GHz of band, almost all regulated, in VLC there is about 400 THz of available and license free band (KARUNATILAKA *et al.*, 2015), what in practice may be considered virtually unlimited (KAVEHRAD, 2010; KUMAR; LOURENÇO, 2010). Figure 3 illustrates the electromagnetic spectrum.

Figure 3 – The electromagnetic spectrum, highlighting the visible light band.

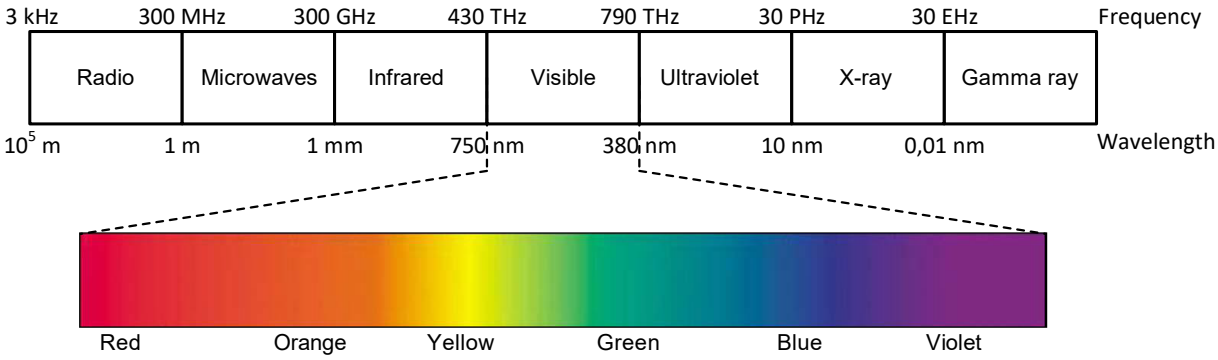

Source: Adapted from Pathak *et al.* (2015).

- Capacity: the spectral efficiency (bits/s/Hz) of wireless networks is approaching saturation, despite the manifold improvements in the last decades (HAAS, 2013). The demand for mobile data has been consistently growing, with an increase estimated of 6.3 times between 2013 and 2018, mostly outside Europe and the United States (Analysys Mason Limited, 2013). Thus, an imminent "RF spectrum crisis" was independently reported several times (Real Wireless, 2014). It is generally agreed that fourth generation (4G) systems and beyond will not depend only on one access technique, and VLC is a proposal with potential to support these technologies (KAVEHRAD, 2010; DIMITROV; HAAS, 2015). Moreover, in VLC it is easier to implement full-duplex channels, due to the directive propagation

characteristic of light which implies in lower levels of loop interference, while near all RF communications are half-duplex (NARMANLIOGLU *et al.*, 2017).

- Use of installed infrastructure: LED lamps have seen an ever growing presence in everyday life and it is expected to become the main source of illumination in the near future, in both indoor and outdoor environments and in applications such as billboards illumination, traffic lights, vehicular headlights, among others (UYSAL; NOURI, 2014). VLC links may be straightforward installed taking advantage of the already installed LED illumination infrastructure in many domestic and office environments, acting as both illumination and communication source simultaneously, as firstly reported in the work of Tanaka *et al.* (2001). With the installation of components in the front-end of the system, any LED lamp may become a VLC access point; since there are currently more than 10 billion LED lamps deployed around the world, therefore there are more than 10 billion potential VLC transmitters (KARUNATILAKA *et al.*, 2015). Cameras installed in modern smartphones may be used as receivers (LI *et al.*, 2018). Besides that, in some countries the electrical power grid may be used as a backbone for the VLC network, using the power-line communication technology (KUMAR; LOURENÇO, 2010).

- Cost: given that part of the infrastructure is already installed, there is already lower deployment costs. In addition, as the visible light spectrum is not regulated, there are no required license fees (UYSAL; NOURI, 2014). Although LED lamps usually cost more than conventional lamps, they have a higher lifespan, estimated in over 50 thousand hours, besides, as to be described in this Section, being more energy efficient (JOVICIC *et al.*, 2013; BALEJA *et al.*, 2015). Lastly, the cost of LED luminaires tends to drop in the next years (TUENGE, 2013).

- Energy: it is estimated that one third of all global energy consumption of electrical energy comes from illumination; therefore, the substitution of inefficient fluorescent and incandescent lamps is highly desired (KAVEHRAD, 2010). White LEDs, highly efficient illumination sources, are already widely available in the market. These devices requires up to 20 times less energy than conventional illumination sources, and up to five times less energy than fluorescent lamps. It is estimated that, if all light sources in the planet are replaced by LED sources, the global energy consumption would be cut up to 50% (KAVEHRAD, 2010), implying in a reduction of CO_2 emissions and the economy of over one trillion dollars (KIM; SCHUBERT, 2008). The telecommunications infrastructure is estimated to be

accountable for 3% of all yearly consumption of energy globally, becoming a concern both environmentally and economically (OH *et al.*, 2011). Between 60 and 80% of this energy is used in base stations, which are highly inefficient structures, in which over 80% of the energy is dissipated as heat, and only between 5 and 20% of the input energy is useful at the output (WU *et al.*, 2015). In this scenario, green technologies such as LEDs and VLC may contribute to the environment and the economy.

- Data security: Light waves do not penetrate opaque structures, which implies that it stays confined to a room. In this way, data are restricted to the internal environment, resulting in a inherent security at the physical layer, which is the most effective security mean (KAVEHRAD, 2010), at the same time providing mobility to the user. RF waves passes through walls and other structures and so may be vulnerable to eavesdropping by undesired receivers.

- Health safety: respecting the eye safety regulations, VLC communications presents no hazards to human health (DIMITROV; HAAS, 2015). This is not true for infrared communications, where high transmission power is not safe for eyes and skin, restricting data rates and distance ranges. Moreover, fluorescent lamps may release mercury in its disposal, resulting in severe health and environmental problems (KARUNATILAKA *et al.*, 2015).

- No interference with RF waves: optical radiation does not interact with other electromagnetic waves. In this way, light communications is safe in environments where RF radiation is limited due to the operation of critical systems, such as hospitals, airplane cabins or chemical and nuclear plants (KAVEHRAD, 2010; DIMITROV; HAAS, 2015).

Many challenges and limitations are inherent or exist in the current state of the art of VLC. Below are listed some of these aspects that needs more attention and studies in order to spread the use of this technology.

- Uplink: typically, most works in VLC literature focus in unidirectional transmission (DIMITROV; HAAS, 2015; PATHAK *et al.*, 2015). The design of an efficient uplink is one of the biggest challenges in this field. High power sources may not be suitable for portable devices, due to the limited energy of batteries, besides that a high light emission source near the user would be unpleasant and

hardly tolerated. Therefore, alternatives are being pursued. Modulation may be designed in a way that the communication is more energy efficient, reaching higher data rates and consuming less power and, therefore, avoiding a high quantity of light near the user (LIN *et al.*, 2016; YANG *et al.*, 2018; ZWAAG *et al.*, 2019). Another possibility is to use the RF channel for the uplink. Even though this keeps the use of the RF spectrum, a hybrid implementation with VLC may relieve a big chunk of the RF network traffic, given that the downlink is usually responsible for the major part of the data traffic (DIMITROV; HAAS, 2015). There is also the benefit of keeping the compatibility with traditional RF systems (RAHAIM *et al.*, 2011). However, hybrid RF/VLC links do not maintain some features of VLC, such as no interference with RF channels. Another proposal is the use of hybrid VLC/IR systems, using the infrared spectrum as the uplink channel (KARUNATILAKA *et al.*, 2015). Naturally, due to the inherent features of the infrared communication, this narrows the design in comparison to the data rate of the access point. An experimental VLC/IR system reached a data rate of 512 kbps in the IR uplink (PEREZ-JIMENEZ *et al.*, 2011). Alresheedi *et al.* (2017) proposes a system that uses adaptative directive IR beams in order to improve the uplink performance.

- Interference and noise: even though immune to RF interference, the optical wireless channel is subject to noise sources that may harm the performance of the system. If the system is installed in an environment that is illuminated by incandescent or fluorescent lamps, these will cause interference with the communication LEDs (KARUNATILAKA *et al.*, 2015). The environmental light causes shot noise at the receiver. Environments subject to natural sunlight may also be subject to background light noise. These noise sources may be mitigated with the use of optical filters and robust modulation formats (KAVEHRAD, 2010). The thermal noise is also relevant, due mainly to the electronic pre-amplifier at the transimpedance amplifier (TIA) (DIMITROV; HAAS, 2015). Also at the receiver, there is influence of noise caused by the photodiode, high pass filter and the power source (HUSSAIN *et al.*, 2015). It is also possible to exist interference between neighbor cells, which may be avoided by separating the sources between themselves by opaque objects (DIMITROV; HAAS, 2015). Finally, intersymbol interference (ISI) is also a concern, specially in environments with a high presence of reflections.

- Lights off: in VLC systems that combine illumination and data transmission simultaneously, one may wonder how communication may occur once lights are off. Due to the natural optical power limitation in this scenario, this topic

becomes a big challenge. One possibility is to keep the transmission with the light at a level low enough that it will not be perceived by human eyes. Through simulations, Borogovac *et al.* (2011) showed that a system like this is viable, maintaining practical performance with the light at an imperceptible level. As in the case of the uplink above, energy efficiency optimization techniques may also be applied, transmitting more information with less power, allowing a lower level of illumination (DIMITROV; HAAS, 2012). Another possibility is, in hybrid systems, alternate to IR or RF communication once lights are off (KARUNATILAKA *et al.*, 2015).

- Shadowing: as light does not go through opaque structures and the power received by reflections is very low (KAHN; BARRY, 1997), VLC systems are considered LOS. That is, it is expected that the transmitters have a direct line of sight to the receivers, what may not always be the case, especially considering scenarios in which the users demand mobility. A solution is to properly distribute the light sources all over the environment, in order to keep a constant and high signal-to-noise ratio (SNR) and always guarantee a LOS between the transmitter and receiver (HAAS *et al.*, 2016).

- Confinement: considered an advantage for security reasons, the confinement of light in the internal environment may also be inconvenient. In scenarios such as a house, typically there is not a high concern with security to the point of desiring the confinement of data among walls. Therefore, the installation of additional infrastructure is required to provide coverage for the whole house.

- Commercialization: one of the main challenges for a high scale distribution of VLC solutions in the market is the necessity of two different industries to work together, at the transmitter and receiver ends (JOVICIC *et al.*, 2013). At the same time that manufacturers of illumination equipment need to modify their equipment, manufacturers of consumer electronics, such as smartphones and computers, need to install high speed photodiodes in their products, as well as adopt an uplink solution to establish the communication link. Besides that, one of the big advantages of LED lamps, their high lifespan, turns out to generate a commercial problem: in short and medium term, sales are stimulated, but the market tends to stagnate in long term. One possibility for inserting VLC technologies in the market is the commercialization of solutions that does not require two industries to work simultaneously as, for instance, in the case of high precision positioning and pairing and data transfers

between devices (JOVICIC *et al.*, 2013). Once that receiver devices are widespread, the market for lamps and VLC-ready structures is stimulated.

2.1.2 Applications

Bellow, some of the specific applications employing VLC that are being researched nowadays are described as examples of the usefulness of the advantages that this technology may provide.

- Positioning: using VLC, it is possible to design low-cost positioning systems with precision of centimeters (JOVICIC *et al.*, 2013). It is an application that does not require high data rates, and therefore it may employ simpler systems, utilizing the installed infrastructure. In this application, receiver devices (such as smartphones) decode the localization information provided from installed lights and estimates the position related to each lamp. This way, triangulation algorithms may be employed to determine the position of the user and even the spatial orientation of the device (YOSHINO *et al.*, 2008). The main advantage in comparison to localization by WiFi (CHINTALAPUDI *et al.*, 2010) is that typically there are many LED lamps installed, unlike WiFi access points (PATHAK *et al.*, 2015). Practical use of this application includes the localization of products in shelves and corridors of stores and supermarkets, easily guiding users to the products and avoiding losses due to not finding something (JOVICIC *et al.*, 2013); assistive technologies, aiding the displacement of visually impaired people (OKUDA *et al.*, 2014); and vehicular communication, as will be seen below. As it is an application that requires low data rates, even conventional smartphone cameras may be used as receivers, not needing any additional hardware (LI *et al.*, 2018). A low cost proposal of a sensor connected to the microphone jack of a smartphone has been demonstrated by Chen *et al.* (2017).

- Vehicular communication: one trend for future transportation systems is the intercommunication between vehicles (V2V – Vehicle to vehicle) and between vehicles and infrastructures (V2I – Vehicle to infrastructure), sharing between each other information such as position and velocity, in order to, among other objectives, improve the traffic safety and collaborate for the dissemination of autonomous cars (YU *et al.*, 2013). VLC is a technology with a high potential to operate in this field due to the already installed infrastructure in vehicles and traffic signals and also

due to the low latency presented in VLC, what is essential to critical systems that demands high precision and response speed, as traffic safety does (UYSAL; NOURI, 2014). However, one must pay attention to the particular challenges in this field of application, such as severe climate conditions and the influence of sunlight (YU *et al.*, 2013). It may be presented also as an example of an application that has a big difficulty of commercialization, as previously explained. Is is estimated that vehicular networks requires a minimum market penetration of 10% of vehicles so that it begins to become viable (ERGEN, 2010).

- Underwater communications: wireless communications in underwater environments have many practical applications, such as vigilance, pollution monitoring, oceanographic research and climate change monitoring (KAUSHAL; KADDOUM, 2016). Typically, in these environments acoustic communications are employed due to the high attenuation of RF waves in water. However, even though these communications may reach long distances, in the order of kilometers, these technologies suffers from limitations such as low available band and high latencies (UYSAL; NOURI, 2014), with data rates typically below 35 kbps (COSSU *et al.*, 2017). On the other hand, underwater optical wireless communications may reach rates of tens of Mbps with distances of tens of meters, as well as low power consumption and low computational complexity. However, many specific features of these environments must be taken in consideration while modeling the channel and the system, requiring knowledge of the complex physio-chemical underwater environment (KAUSHAL; KADDOUM, 2016). In order to put together the advantages of light systems with the long range of acoustic systems, hybrid systems are also possible (JOHNSON *et al.*, 2014).

- Sensor networks: some of the VLC features are desirable for the design of networks of small devices, such as sensors and connected applications, as those of the Internet of Things (IoT). These relevant advantages include low power consumption, reliable LOS links and low latency. As communication between devices typically does not require high data rates, applications with light at non-visible levels are possible (PATHAK *et al.*, 2015; KADAM; DHAGE, 2016). Already deployed infrastructure may also be employed, as Jha *et al.* (2015) propose to use the camera and the LCD display of existing devices as receiver and transmitter. Implementations of device networks must pay attention to eventual limitation of application, such as shadowing and alignment between devices (specially if there is mobility among them), energy efficiency and interference between cells (PATHAK

et al., 2015).

2.1.3 Modulation

Due to the inherent physical properties of LED transmission and PD detection, a VLC system is a defined as of IM transmission and DD reception, know as an IM/DD system (DIMITROV; HAAS, 2015). IM refers to intensity modulation, where the information is coded in the intensity of the modulated light. DD means direct detection, a method in which the emitted light directly hits the detector, opposed to the heterodyne detection typically employed in RF systems. In DD, when excited by light, the photodetector generates a current proportional to the incident instantaneous power (KAHN; BARRY, 1997).

An IM/DD system implies that the modulation signal must be real-valued and non-negative unipolar. Therefore, not all existing techniques used in RF communications are usable in VLC. A LED may be modulated alternating between on and off states. In this way, the characteristics that can be modulated include the pulse width and the pulse interval. There may also exist illumination control over the intensity of the on and off states, without affecting the system performance (ISLIM; HAAS, 2016). Taking all precautions, these modulations are imperceptible to human eyes.

Techniques such as OOK, PWM (pulse-width modulation), PPM and PAM may be applied in a relatively straightforward manner (DIMITROV; HAAS, 2015). Figure 4 illustrates waveforms for the PAM and PPM modulations.

Due to its simplicity, OOK is the most employed technique in IM/DD systems (GHASSEMLOOY *et al.*, 2013). This modulation provides a good balance between performance and implementation complexity (HAAS *et al.*, 2016). In comparison, PPM is more energy efficient but has a lower spectral efficiency.

Single carrier techniques are suitable for transmissions at relatively low rates. As data rates increases, the ISI effect begins to become perceptible and deteriorate the system performance (ISLIM; HAAS, 2016). More elaborate modulation techniques are also needed because, due to eye safety regulations, it is not possible to increase optical power indefinitely, specially in indoor environments (GHASSEMLOOY *et al.*, 2013).

A modulation format that is unique to VLC is the color shift keying (CSK) (ISLIM; HAAS, 2016). RGB LEDs may be modulated in a manner that different intensities are applied to different colors, mapped for some given symbols. Figure 5 shows

Figure 4 – Examples of waveforms of the 4-PPM and 4-PAM modulations.

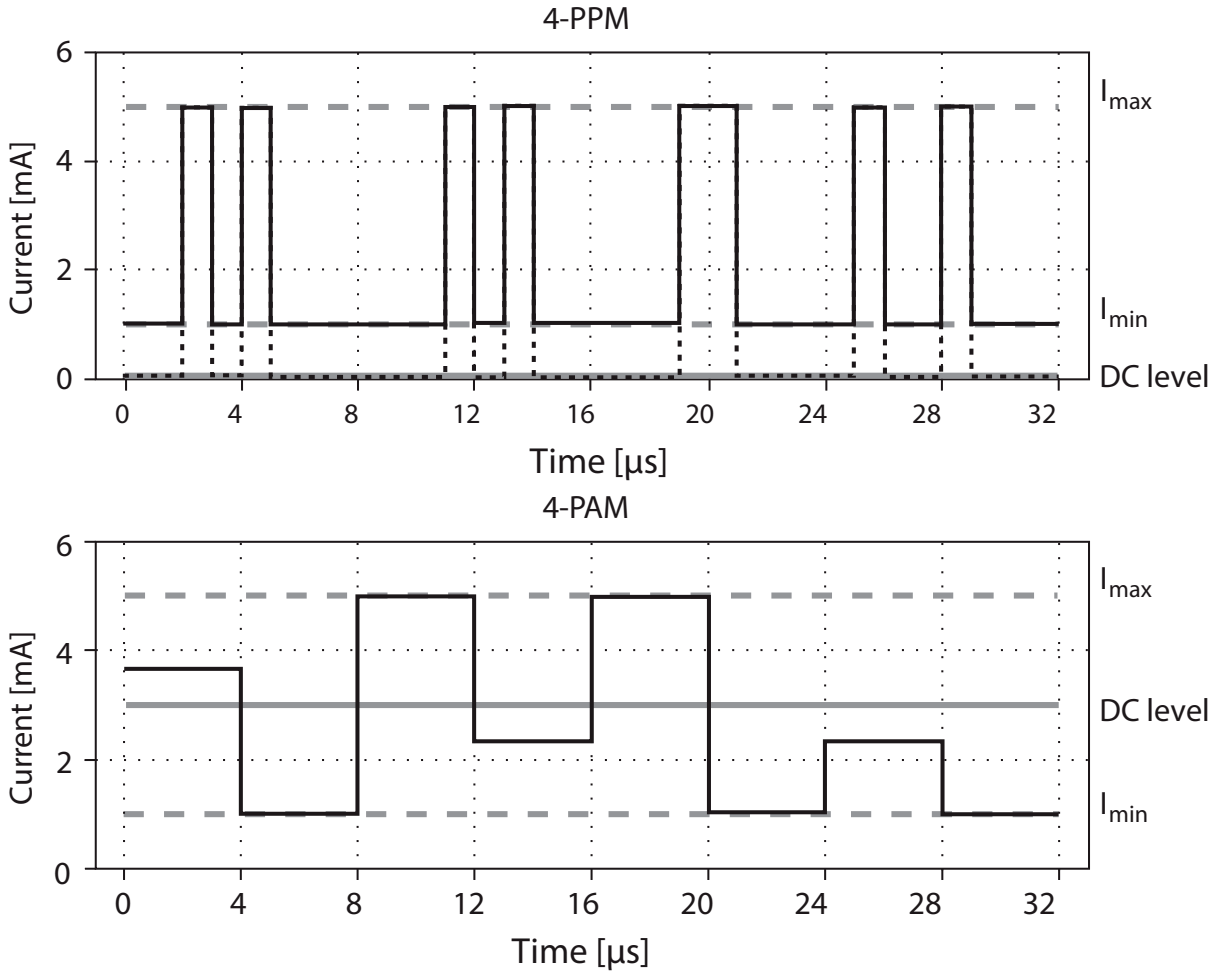

Source: Adapted from Dimitrov and Haas (2015).

the mapping for 4-CSK modulation.

The IEEE 802.15.7 standard recommends CSK as a modulation technique for VLC, proposing constellations up to 16-CSK, based on three tricolor LEDs (Institute of Electrical and Electronics Engineers, 2011). CSK is a technique that still needs more research, particularly in the receiver end, as the architecture is yet not fully addressed. It is considered complex and expensive when compared to OFDM (ISLIM; HAAS, 2016).

An undesired effect that occurs as modulation speeds increases is the symbol time becoming much smaller than the delay spread, resulting in ISI, due to the optical wireless channel becoming frequency selective. The intersymbol interference happens as a consequence of multiple copies of the transmitted symbols hitting the receiver at different time slots, therefore being susceptible to being interpreted as noise, making it harder for the receiver to decode the data. The multipath may be caused by reflection and refraction

Figure 5 – 4-CSK modulation mapped at the CIE 1931 color space.

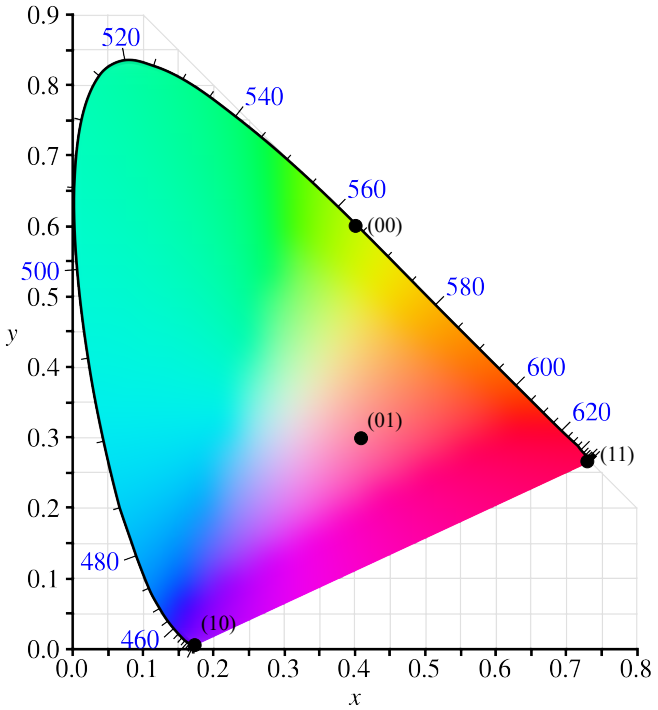

Source: Adapted from Islim and Haas (2016).

of electromagnetic waves. As visible light wavelengths are orders of magnitude smaller than the detection area of PDs, there is rich spatial diversity and there is no multipath fading, as the photodetector is equivalent to a two-dimensional array of antennas (KAHN; BARRY, 1997; DIMITROV; HAAS, 2015). However, the effects of multipath of NLOS links still generates distortion at the receiver, observed in practice as the effects of ISI. Simulation of multipath impulse response can be seen in Barry *et al.* (1993) and experimental characterization of the NLOS multipath effects can be seen in Kahn and Barry (1997). However, this component usually does not have much interference on the path loss exponent in scenarios with a strong LOS link, due to the higher power of the direct LOS component, specially as the distance between source and destination increases (KOMINE; NAKAGAWA, 2004; DIMITROV; HAAS, 2015)

A solution for this issue is the use of multi-carrier modulation (MCM) techniques. The idea behind these techniques is to divide the data packages in many subpackages and transmit them through different subchannels (GOLDSMITH, 2005). The number of subpackages is defined in a way that the symbol time of each subtransmission is longer than the delay spread. Equivalently, one can say that, in this way, the band of the subpackage is smaller than the coherence band of the channel.

Among the MCM techniques, OFDM is largely employed in VLC systems, firstly reported by Tanaka *et al.* (2001). The principle of employing orthogonal frequencies for transmission was initially proposed by Chang (1966). Many OFDM variations for VLC have been proposed in the literature, collectively called optical OFDM techniques. Among the advantages of employing OFDM in optical systems is its better energy efficiency, opposed to modulations such as OOK and PPM (DISSANAYAKE; ARMSTRONG, 2013).

As previously mentioned, the VLC waveforms need to be unipolar and real. To achieve this objective, optical OFDM implements techniques such as Hermitian symmetry (to ensure that the signal stays at the real domain) and DC level (to ensure that the system is unipolar) (DISSANAYAKE; ARMSTRONG, 2013; ISLIM; HAAS, 2016).

The more studied optical OFDM variations in the literature so far are ACO-OFDM, DCO-OFDM and ADO-OFDM (DISSANAYAKE; ARMSTRONG, 2013). Particularly, DCO-OFDM is typically employed as a comparison reference with other techniques due to its high spectral efficiency (ISLIM; HAAS, 2016).

2.1.4 VLC channel model

There are many diffuse VLC channel models proposed in the literature, based on different approaches (POHL *et al.*, 2000; ANGELOVA *et al.*, 2009; DING; KE, 2010; LEE; PARK, 2011; ZHOU *et al.*, 2014). The model to be described and employed in this work was first presented by Gfeller and Bapst (1979) and its current form was consolidated in the work of Kahn and Barry (1997). Initially proposed as models for infrared light, these models have also been adopted for visible light. This model or its variants are commonly employed in the literature (KOMINE; NAKAGAWA, 2004; ZENG *et al.*, 2008; TIWARI *et al.*, 2015; SHARMA *et al.*, 2017; SINDHUBALA; VIJAYALAKSHMI, 2017).

An LED is considered to behave as a Lambertian emitter (GFELLER; BAPST, 1979). The Lambert's cosine law stipulates that the luminous intensity of an ideal diffuse reflection surface is directly proportional to the cosine of the emission angle φ between the incidence direction of the light and the normal of the surface (DIMITROV; HAAS, 2015; GHASSEMLOOY *et al.*, 2018). Figure 6 illustrates this concept.

Mathematically, this law is given as

$$I(\varphi) = I_N \cos\varphi, \tag{1}$$

where I is the luminous intensity and dS is the light emitter area, as represented in

Figure 6 – Diagram of a Lambertian emitter.

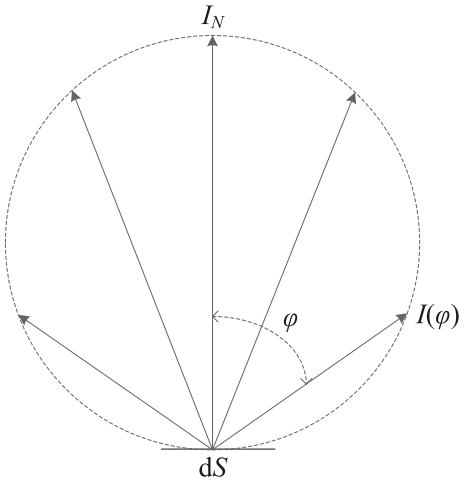

Source: Qiu *et al.* (2016).

Figure 6. This area doesn't need, necessarily, to be a light source; diffuse reflector surfaces may also be considered Lambertian sources (QIU *et al.*, 2016).

An important concept is the half-power semiangle $\varphi_{1/2}$, that is, the angle between the emission direction and the axis in which the luminous intensity is half of the axial intensity. This angle defines the Lambertian order m of the source (KAHN; BARRY, 1997; GHASSEMLOOY *et al.*, 2013; QIU *et al.*, 2016), defined as:

$$m = \frac{-\ln 2}{\ln(\cos \varphi_{1/2})}, \tag{2}$$

where ln represents the natural logarithm.

The general model of an optical wireless channel is given by (KOMINE; NAKAGAWA, 2004)

$$Y(t) = \gamma X(t) \otimes h(t) + N(t), \tag{3}$$

where γ is the photodetector's responsivity (given in A/W), $Y(t)$ is the received signal, $X(t)$ is the transmitted optical pulse, $h(t)$ is the channel impulse response, $N(t)$ is the additive white Gaussian noise (AWGN) and $\otimes$ represents the convolution operation.

Figure 7 illustrates the basic geometry of a LOS VLC model consisting of a transmitter and a receiver. Besides the concepts previously presented, in this diagram θ is the incidence angle between the optical ray and the normal to the photodetector's surface, A is the area of detection of the photodetector, d is the distance between transmitter and receiver and FOV is the field of view of the photodetector, the angle in which the photodetector receives the emitted light in the environment.

Figure 7 – Basic geometry of a LOS VLC model.

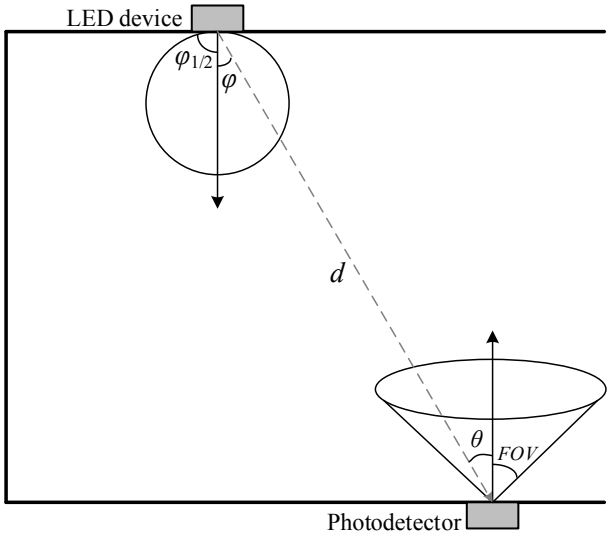

Source: The author.

The impulse response $h(t)$ is given as function of the channel DC gain H (GFELLER; BAPST, 1979; KAHN; BARRY, 1997; KOMINE; NAKAGAWA, 2004):

$$H_{los}(0) = \int_{-\infty}^{\infty} h(t)dt. \tag{4}$$

The DC gain is given by:

$$H_{los}(0) = \begin{cases} \frac{A(m+1)}{2\pi d^2} cos^m(\varphi) T_s(\theta) g(\theta) \cos(\theta), & 0 \leq \theta \leq \text{FOV} \\ 0, & \text{otherwise} \end{cases}, \tag{5}$$

where $T_s(\theta)$ and $g(\theta)$ represents, respectively, gains of the optical filter and concentrator, in case they are installed in the system. It should be noted that, as expected, if the incident light ray is outside the photodetector's FOV, it does not generate current at the reception. This equation may also be seen as the path loss of the communication link. In conventional indoor environments, the gain of the optical concentrator is given as (KAHN; BARRY, 1997)

$$g(\theta) = \begin{cases} \frac{n^2}{\sin^2 \text{FOV}}, & 0 \leq \theta \leq \text{FOV} \\ 0, & \text{otherwise} \end{cases}, \tag{6}$$

where n is the refraction index of the reflective surface.

The received optical power P_r for a LED is derived from the transmitted optical power P_t:

$$P_r = H(0)P_t. \tag{7}$$

The received optical power considering reflections is obtained using the P_r of the LOS link and the P_r caused by reflections (KOMINE; NAKAGAWA, 2004):

$$P_r = \sum^{\text{LEDs}} \left\{ P_t H_{los}(0) + \int_{\text{walls}} P_t H_{ref}(0) \right\}. \tag{8}$$

For the model considering power received from reflections, refer to the geometry of Figure 8. The DC gain for one reflection is given by

$$dH_{ref}(0) = \begin{cases} \frac{(m+1)A}{2\pi d_1^2 d_2^2} \rho dA_{\text{wall}} \cos^m(\varphi) \cos(\alpha) \cos(\beta) T_s(\theta) g(\theta) \cos(\theta), & 0 \leq \theta \leq \text{FOV} \\ 0, & \text{otherwise} \end{cases} \tag{9}$$

where ρ is the reflectance factor of the reflective surface; d_1 is the distance between the source and the reflective surface and d_2 is the distance between the reflective surface and the destination; α and β are, respectively, the incidence angles from the source to the reflective surface and from the reflective surface to the photodetector.

Figure 8 – Basic geometry of VLC model considering reflections.

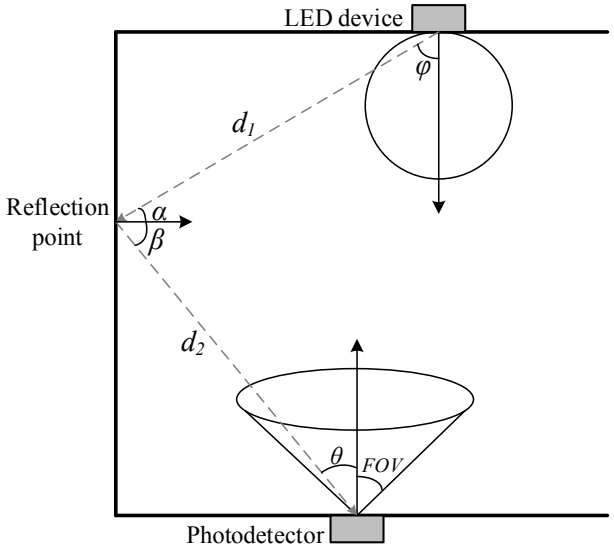

Source: The author.

2.1.4.1 Signal-to-noise ratio, bit error rate and error vector magnitude

For VLC systems, the signal-to-noise ratio (SNR) is defined as (KOMINE; NAKAGAWA, 2004; KUNG *et al.*, 2009; LEE; JUNG, 2012)

$$\text{SNR} = \frac{\gamma^2 P_r^2}{\sigma_{total}^2}, \tag{10}$$

where σ^2_{total} is the total root-mean-square (RMS) noise at the receiver, to be described below. The power received from all the LEDs in the system is

$$P_r = \int_0^T \left(\sum_{i=1}^{\text{LEDs}} h_i(t) \otimes X(t) \right) dt. \tag{11}$$

In order to obtain the SNR of the system, it is needed to define a noise model. Even in works that employ the same models based on those of Gfeller and Bapst (1979) and Kahn and Barry (1997), different approaches are presented for the definition of the total noise σ^2_{total} (KOMINE; NAKAGAWA, 2004; LEE; JUNG, 2012; SINDHUBALA; VIJAYALAKSHMI, 2017). In this work it is employed the model described by Komine and Nakagawa (2004), that defines the total noise as

$$\sigma^2_{total} = \sigma^2_{shot} + \sigma^2_{thermal} + \gamma^2 P^2_{rISI}, \tag{12}$$

where σ^2 corresponds to the variance of each noise source. σ_{shot} is the shot noise, $\sigma_{thermal}$ is the thermal noise and P_{rISI} is the ISI noise, caused by reflections. Similar to P_r (Equation (11)), this interference is given as

$$P_{rISI} = \int_T^{\infty} \left(\sum_{i=1}^{\text{LEDs}} h_i(t) \otimes X(t) \right) dt. \tag{13}$$

The shot noise, also known as Poisson noise, describes the fluctuation in the number of detected photons, and therefore the variation in the photocurrent generation. It is caused by the light sources of the optical path (LED source and others) (KAHN; BARRY, 1997; DIMITROV; HAAS, 2015). This variance is given by

$$\sigma^2_{shot} = 2q\gamma(P_r + P_{rISI})B + 2qI_{bg}I_2B, \tag{14}$$

where q is the elementary charge, B is the noise equivalent bandwidth (sometimes considered as data rate), I_{bg} is the backlight current and I_2 is the noise bandwidth factor.

The thermal noise happens due to the electronic pre-amplification in the front-end of the receiver, *i.e.*, the TIA (KAHN; BARRY, 1997; DIMITROV; HAAS, 2015). The thermal noise is modeled considering the use of a PIN/FET TIA (KOMINE; NAKAGAWA, 2004) and is expressed as

$$\sigma^2_{thermal} = \frac{8\pi k T_k}{G}\eta A I_2 B^2 + \frac{16\pi^2 k T_k \Gamma}{g_m}\eta^2 A^2 I_3 B^3, \tag{15}$$

where the two terms represent, respectively, noise of the feedback resistor and from the

FET channel. k is the Boltzmann constant, T_k is the absolute temperature, G is the open loop gain, η is the fixed capacitance of the photodetector by area unit, Γ is the FET noise factor and I_3 is the noise bandwidth factor. Both shot and thermal noises are given by squared amperes (A^2).

The BER is calculated using equations that use the SNR as a parameter. In the presented simulations, it is employed to calculated the BER for OOK and M-QAM (quadrature amplitude modulation) modulations. Equation (16) defines the BER for the OOK-NRZ (OOK non return to zero) (KOMINE; NAKAGAWA, 2004; GHASSEMLOOY *et al.*, 2013) and Equation (18) defines the BER for M-QAM (NARMANLIOGLU *et al.*, 2017).

$$\mathrm{BER_{OOK}} = Q(\sqrt{\mathrm{SNR}}), \tag{16}$$

where:

$$Q(x) = \frac{1}{\sqrt{2\pi}} \int_x^\infty e^{-y^2/2} dy. \tag{17}$$

$$\mathrm{BER_{M-QAM}} = \frac{\sqrt{M}-1}{\sqrt{M}\log_2\sqrt{M}} \mathrm{erfc}\left(\sqrt{\frac{3\mathrm{SNR}}{2(M-1)}}\right), \tag{18}$$

where M is the order of the M-QAM modulation and

$$\mathrm{erfc}(x) = \frac{1}{\sqrt{\pi}} \int_{-x}^{x} e^{-t^2} dt. \tag{19}$$

The error vector magnitude (EVM) is defined as the RMS value of the difference between ideal symbols and the received symbols, *i.e.*, their difference of position in the constellation (SHAFIK *et al.*, 2006a).

Mathematically, the EVM can be given as

$$\mathrm{EVM_{RMS}} = \frac{\frac{1}{N}\sum_{n=1}^{N} |S_n - S_{0,n}|^2}{\frac{1}{N}\sum_{n=1}^{N} |S_{0,n}|^2}, \tag{20}$$

where S_n is the normalized n-th symbol in the transmitted symbol stream, $S_{0,n}$ is the ideal, normalized constellation point of the n-th symbol and N is the number of unique symbols in the constellation (SHAFIK *et al.*, 2006b).

This variation may be represented as a percentage or in dB; the latter is employed in the presented results presented in this work. This relationship is given by Equations

(21) and (22).

$$\mathrm{EVM}_{\mathrm{RMS}} = 100 \times 10^{\mathrm{EVM}_{\mathrm{dB}}/20}. \tag{21}$$

$$\mathrm{EVM}_{\mathrm{dB}} = 20 \times \log_{10}\left(\frac{\mathrm{EVM}_{\mathrm{RMS}}}{100}\right). \tag{22}$$

The mathematical model presented in this chapter will be employed in the remaining of this document, in the form of MATLAB scripts. In the next chapter, the simulation model employing the channel model to simulate various scenarios is described.

3 VLC SIMULATIONS

In this chapter, the developed simulation model used in this thesis is presented in detail. First, the simulation model is described not considering reflections, following by further development considering them, presenting examples for each case. Lastly, a MATLAB graphical interface to ease VLC simulation is presented.

The scenario considered to simulate the VLC channel is an indoor environment of given dimensions, with one or more LED sources at the ceiling of the room. Given the sources and their attributes, the effects upon a surface of a given height, usually the equivalent height of a work desk, are calculated and relevant parameters, such as received power, SNR and BER are obtained (KOMINE; NAKAGAWA, 2004; GHASSEMLOOY *et al.*, 2013; BUI *et al.*, 2016).

In the simulations to be presented, the scenario is a closed room of dimensions 5×5×3 m and a reception surface is a desk with height of 0.85 m, *i.e.*, distant 2.15 m of the ceiling. The room is represented with coordinates from –2.5 to +2.5 in each axis, therefore the central coordinate being $(x,y) = (0,0)$, while $z = 3$ represents the position of the luminaires at the ceiling and the receiver plane is at $z = 0.85$. The receiver plane is divided in a grid, in order to calculate the parameters in all the grid points and obtain a general vision of the environment. The parameters used in these simulations are based in the works of Komine and Nakagawa (2004) and Ghassemlooy *et al.* (2018). Table 2 lists the parameters referring to the environment, to the transmitter and the receiver.

Table 2 – Simulation parameters for transmitter and receiver.

	Parameter	Value	Unit
Environment	Dimensions	5×5×3	m
	Receiver plane	0.85	m
Transmitter	Transmit power (P_r)	72	W
	Half-power semiangle ($\varphi_{1/2}$)	70	°
	Central luminous intensity	0.73	cd
Receiver	FOV	70	°
	PD detection area (A)	1	cm^2
	Optical filter gain	1	
	Refraction index of PD lens (n)	1.5	
	PD responsivity (γ)	0.54	A/W

For the calculation of SNR and BER, the noise model is employed for the system, which is presented in Equations (10), (12), (14) and (15). Table 3 compiles all these

parameters, as well as its units and the values employed in the simulations.

Table 3 – Noise parameters for simulation.

Parameter	Symbol	Value	Unit
Elementary charge	q	1.6×10^{-19}	C
Boltzmann constant	k	1.3606×10^{-23}	J/K
Fixed capacitance	η	112	pF/cm^2
FET transconductance	g_m	30	mS
Backlight current	I_{bg}	5100	µA
Data rate	B	100	Mbps (or MHz[1])
Absolute temperature	T_k	300	K
Open loop gain	G	10	
Noise factor	I_2	0.562	
Noise factor	I_3	0.0868	

3.1 NO REFLECTIONS

For the simulations, two scenarios are considered. In the first one, only one light source is positioned in the center of the room, at coordinate (0, 0). In the second scenario, four symmetrically positioned luminaires are employed at coordinates (-1.25, -1.25), (1.25, -1.25), (-1.25, 1.25) and (1.25, 1.25). Figure 9 illustrates the luminaire distribution. As seen in Table 2, it is considered a 5×5 m room. The simulation model is based on the works of Kahn and Barry (1997), Komine and Nakagawa (2004) and Ghassemlooy *et al.* (2018).

The simulations presented in Figures 10 and 11 show the incident optical power P_r in the receiver plane, for one and four sources, respectively, calculated from Equations (5) and (7). The plots show that there is a significant difference when more sources are installed in the environment, providing a higher optical power available at the receiver surface. Table 4 presents the average, minimum and maximum power for both scenarios, as well as the total transmitted power for each case. In practice, it should be noted that power may not be raised indefinitely, due to limitations in illumination standards and possible saturation in the photodetector's sensibility.

Using the information of the received power, as well as the results of noise calculation using parameters listed in Table 3, it is possible to obtain the SNR for these two cases. In these simulations, in which the ISI noise is not calculated, this component is obtained from the values of the graph presented in Figure 12, which are based on the

[1]In some works, B is used as "equivalent background noise" and is given in Hz.

Figure 9 – Luminaires placed at the ceiling of a 5×5 m room.

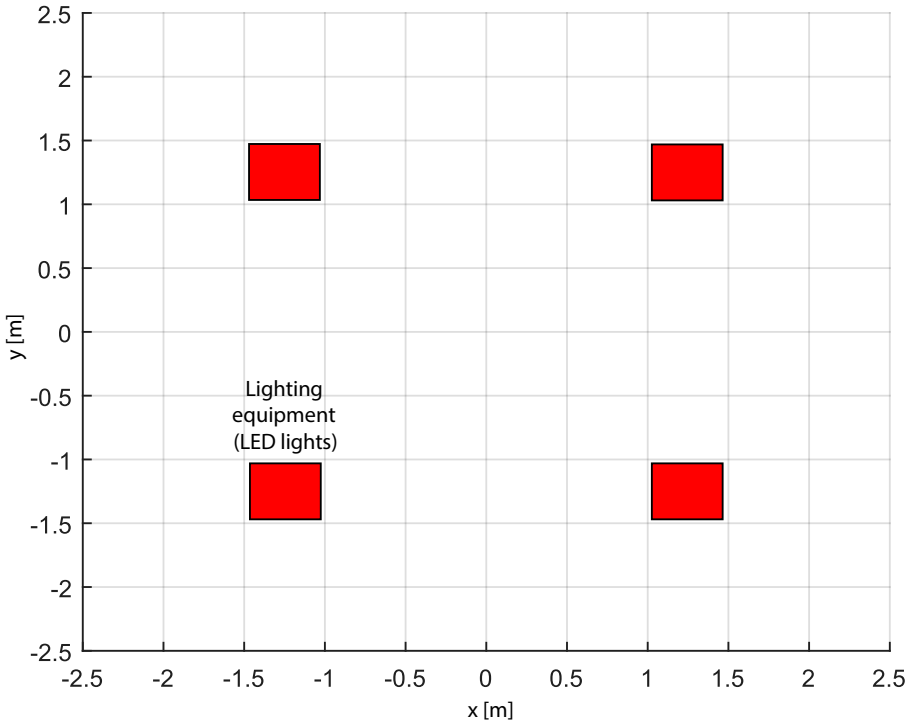

Source: Adapted from Komine and Nakagawa (2004).

Figure 10 – Optical power distribution upon a surface considering one source.

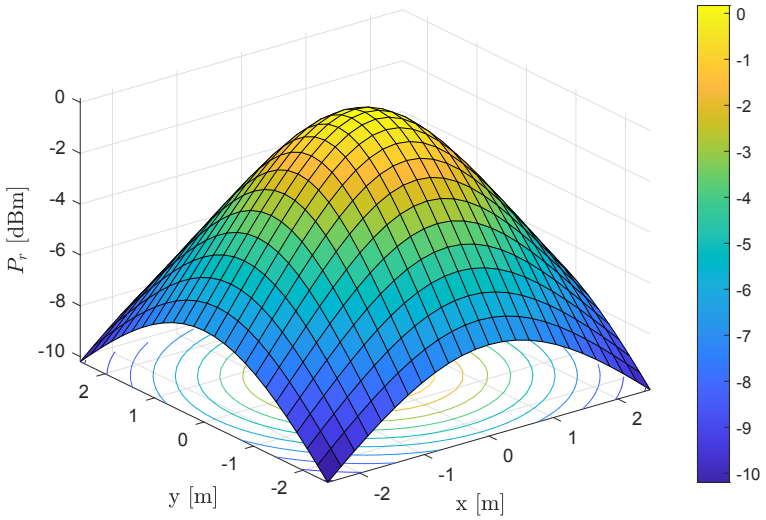

Source: The author.

noise Equations (14) and (15). From Figure 12, it is possible to see that the ISI noise is dominant for most data rates, being surpassed by the thermal noise from the FET channel in the order of 10^{10} bps. The plots presented in Figures 13 and 14 shows the SNR (in dB) for one and four sources, respectively.

As expected, considering that the signal-to-noise ratio is a function of the received

Figure 11 – Optical power distribution upon a surface considering four sources.

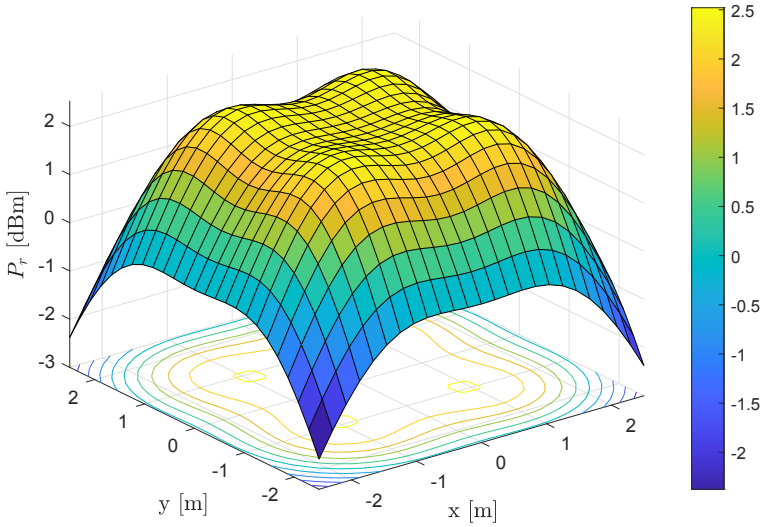

Source: The author.

Table 4 – Transmit and received power values for one and four sources.

	Number of sources		
	1	4	
Total P_t	72	288	W
Minimum P_r	–10.2	–2.40	dBm
Maximum P_r	0.17	2.21	dBm
Average P_r	–4.83	0.96	dBm

power, the SNR distribution has a similar behaviour. Table 5 lists the minimum, mean and maximum SNR for each case.

Table 5 – SNR values, in dB, for the scenarios considering one and four sources.

	Number of sources	
	1	4
Minimum SNR	–5.75	9.85
Maximum SNR	14.99	19.07
Average SNR	4.98	16.57

Finally, once that SNR values are obtained, it is possible to calculate the system's performance in terms of bit error rates. BER values were obtained, according to Equations (16) and (18), for the OOK and 8-QAM modulations formats (4-QAM presents the same performance as OOK). The results for one and four light sources are presented, respectively, in Figures 15 and 16.

Comparing Figures 15 and 16 the notable performance difference between the

Figure 12 – Noise as function of data rate.

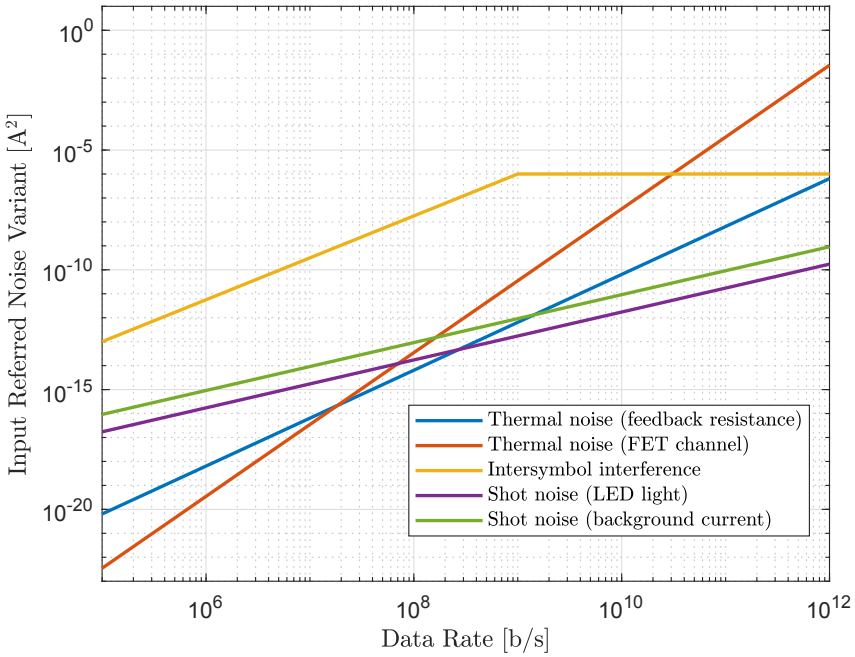

Source: The author, adapted from Komine and Nakagawa (2004).

Figure 13 – SNR distribution upon reception surface for one source.

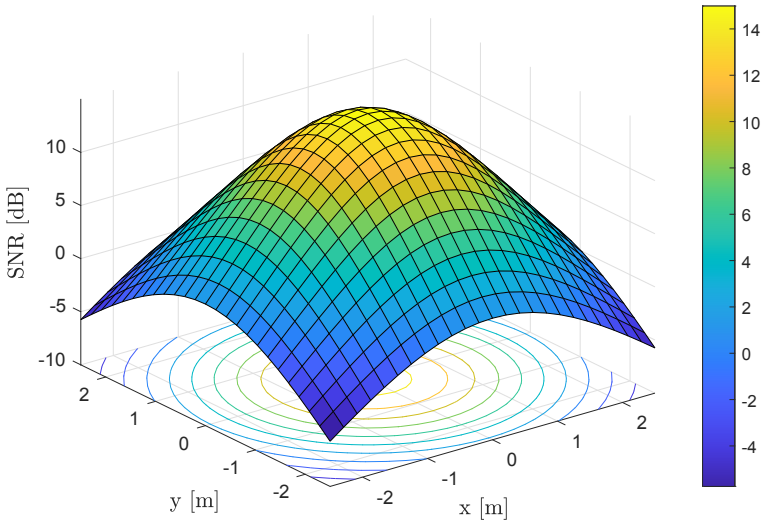

Source: The author.

two scenarios is perceived. Using one light source, the system performance drastically drops outside the room's center for both modulation formats. Particularly, for the 8-QAM modulation (Figure 15b), the best BER performance is in the order of 10^{-3}, which may not be acceptable depending on the adopted minimum performance quality criterion. Therefore, a scenario with just one lamp, even with higher transmission power, may be undesirable, with a limited performance and restricted user mobility.

Figure 14 – SNR distribution upon reception surface for four sources.

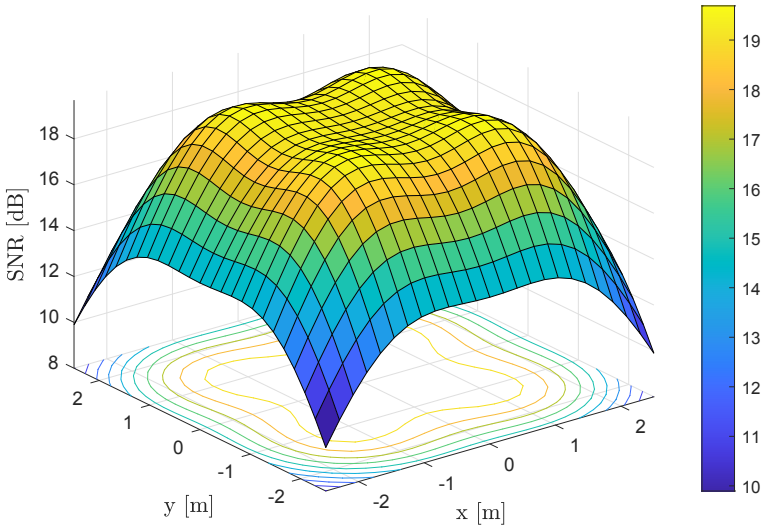

Source: The author.

On the other hand, in Figure 16, with four light sources, the system performance is considerably high all over the environment, presenting low BER values only at the extremities of the room, of the order of 10^{-4} for OOK and 10^{-2} for 8-QAM.

3.2 SCENARIO CONSIDERING REFLECTIONS

The consideration of reflections has two main implications for VLC channel analysis: the received power is different (typically, slightly higher, less than 1 dBm in the employed conditions in the previous examples) and, by taking it into account, it is possible to obtain a more accurate value for the ISI noise, instead of using a graph such as Figure 12. Therefore, more accurate SNR and BER values are obtained, specially given that, for most data rates, the ISI noise is the dominant noise, as can be seen in Figure 12. For these calculations, it is employed the same model as before, but considering the first reflected rays as calculated by Equation (9). The reflection calculation considers the light beams that hits a wall, is reflected and arrives at the PD inside its FOV. Light beams after the first reflection arrive at the PD with negligible optical power (KOMINE; NAKAGAWA, 2004).

In this section, it will be presented the results for 4 lamps, at the same position as presented in Figure 9. One new parameter is needed in this context, which is the reflectance factor ρ, where is adopted the value 0.8 for the walls, as in Ghassemlooy *et al.* (2018). The reflective surfaces also behave as a Lambertian emitter (GFELLER; BAPST,

Figure 15 – BER values for one light source for the (a) OOK and (b) 8-QAM modulation formats.

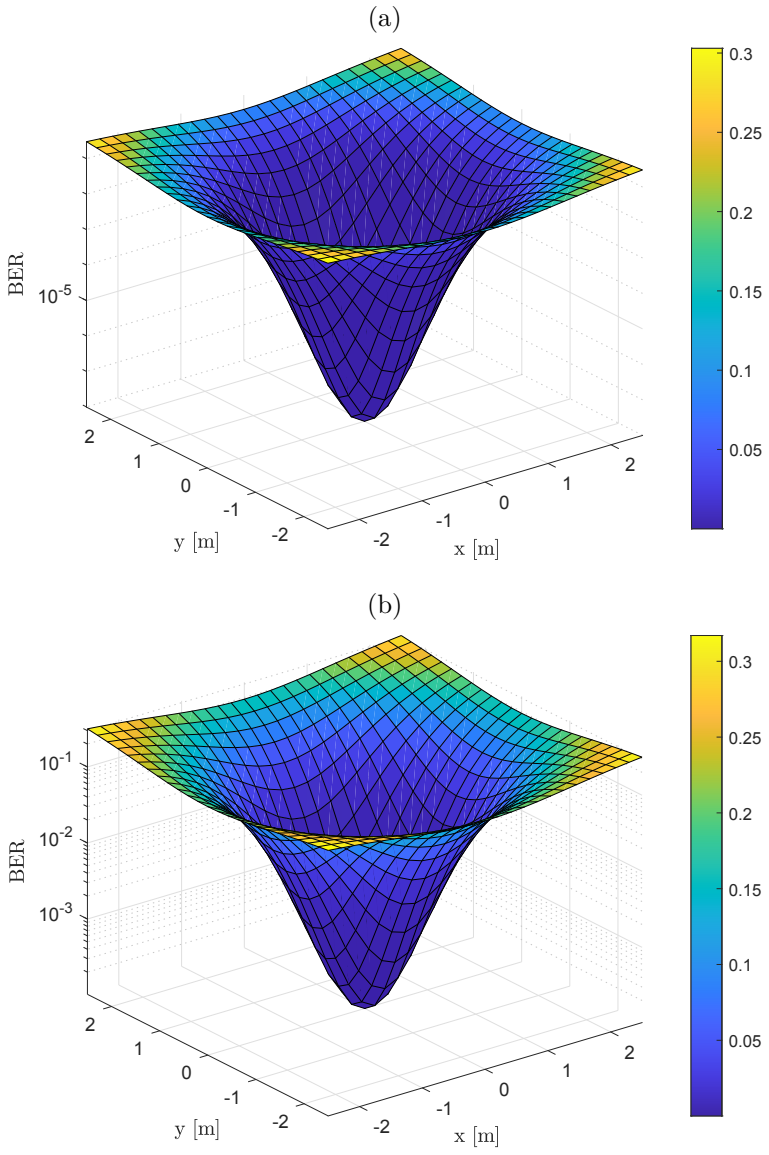

Source: The author.

1979; HUSSEIN *et al.*, 2016). Figure 17 shows the distribution of received power.

Similarly, Figure 18 plots the SNR and Figure 19 the BER for OOK and 8-QAM taking into account the reflections on the walls. Table 6 provides, for a numerical comparison the minimum, average and maximum received power and SNR considering reflections and not.

It can be seen that the average received power presents a gain of about 0.7 dBm in this context, and the maximum value raises from 2.21 dBm to 2.77 dBm. However, this higher measured received power does not reflect in an improved communication

Figure 16 – BER values for four light sources for the (a) OOK and (b) 8-QAM modulation formats.

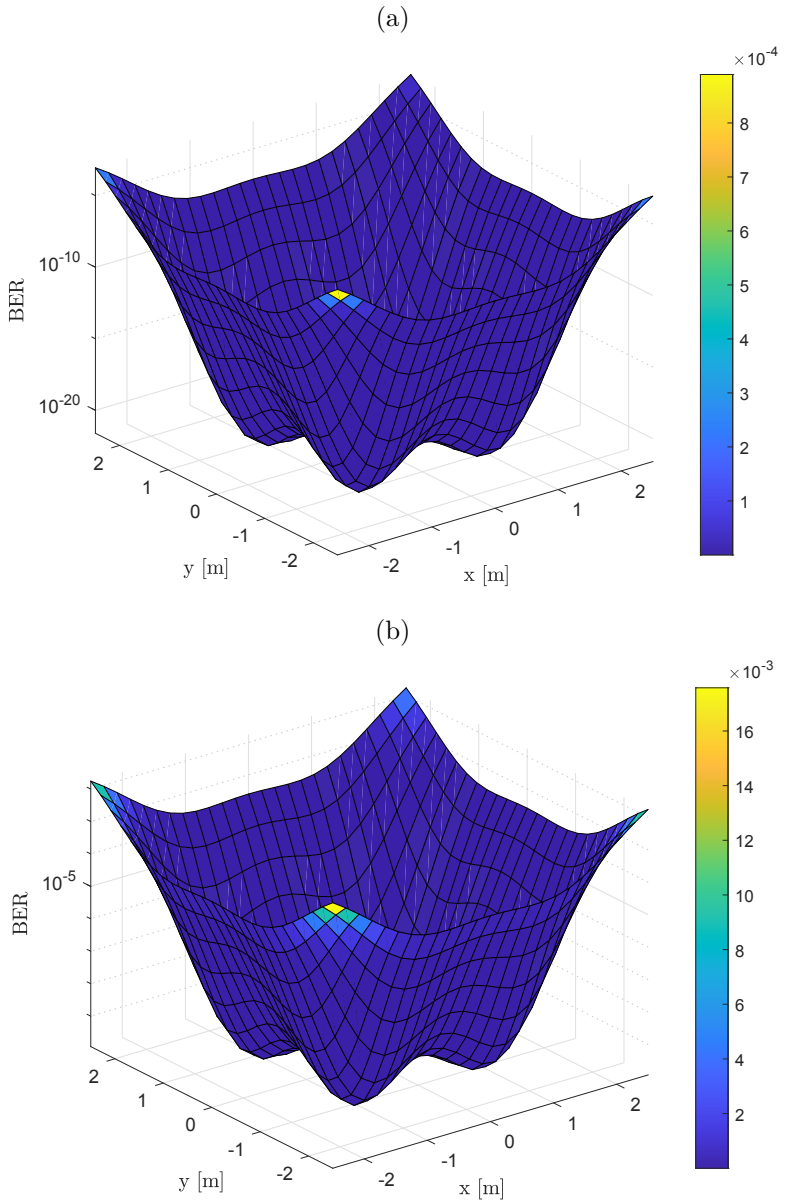

Source: The author.

performance. This is due to the more accurate calculation of the ISI noise, presented in Equation (12), which was previously extracted from Figure 12. Whereas in the previous section the common value of 10^{-8} A^2 was employed for the whole environment, in this Section each point of the grid has its own received reflected power and, therefore, its own ISI noise value. The average ISI noise ($\gamma^2 P_{rISI}^2$), considering all the environment, is 2.29×10^{-8}, which is similar to the value from Figure 12. Minimum and maximum values are, respectively, 9.89×10^{-9} and 3.53×10^{-8}.

Figure 17 – Optical power distribution for four sources considering reflections.

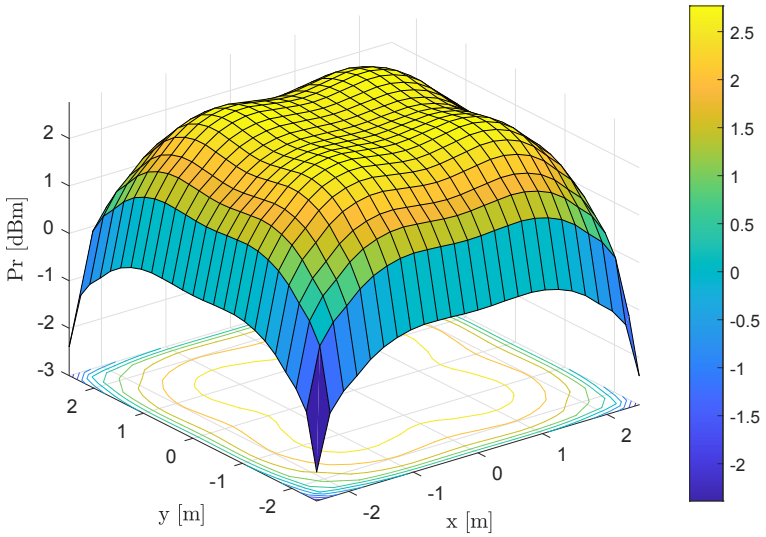

Source: The author.

Figure 18 – SNR distribution in reception surface considering reflections.

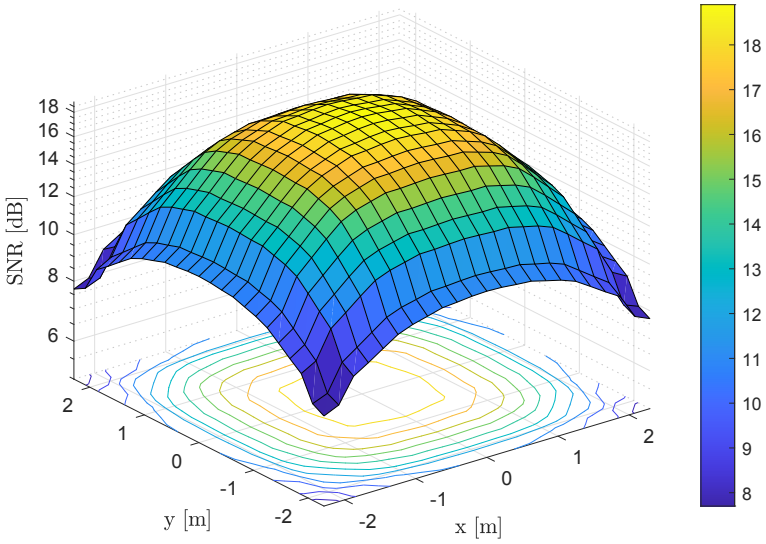

Source: The author.

3.3 GRAPHICAL INTERFACE FOR VLC SIMULATION

In order to quickly evaluate different scenarios and parameter changes, a graphical interface was developed in MATLAB for VLC simulation, as presented in this chapter.

The customizable parameters are the room width (x) and length (y) and the distance from the ceiling to the measured surface, or the height (z); for the transmitter, the LED's optical power (P_r) and the half-power semiangle; for the receiver, the FOV and the photodiode's area (A) can be varied. Also, the app allows to choose between one

Figure 19 – BER values, considering reflections, for the (a) OOK and (b) 8-QAM modulation formats.

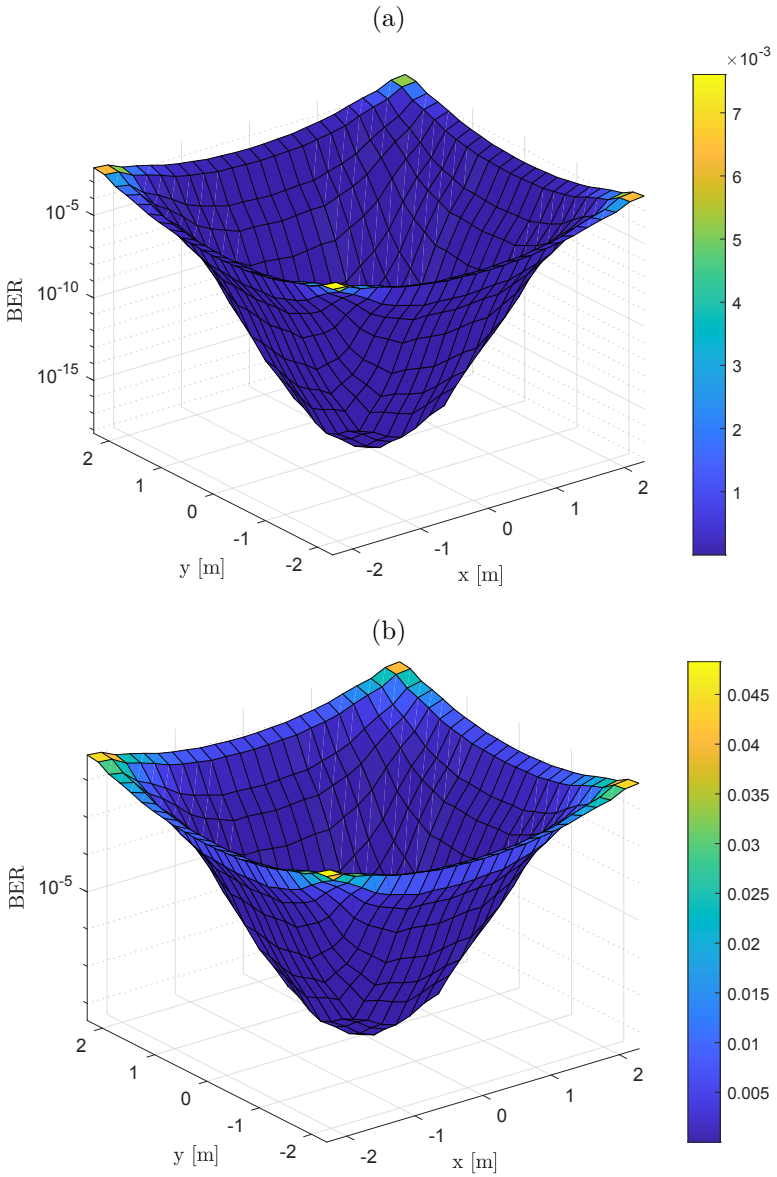

Source: The author.

and four sources and to consider or not the reflections.

Figure 20 presents an example of the application. In this example, the parameters are the same as in Tables 2 and 3. It is observed that the average, maximum and minimum P_r and SNR values are as presented in Tables 4 and 5.

Two more examples are shown in the following screenshots. In Figure 21 it is presented an example of a simulation with one source and considering reflections, a scenario that was not presented before, and Figure 22 presents a scenario with different values for the environment, transmitter and receiver parameters, as seen in the screenshot.

Table 6 – Comparison of received power considering reflections. P_r in dBm and SNR in dB.

	Reflections?		Difference
	No	Yes	
Minimum P_r	–2.40	–2.39	0.01
Maximum P_r	2.21	2.77	0.56
Average P_r	0.96	1.73	0.77
Minimum SNR	9.85	7.7	2.15
Maximum SNR	19.07	18.9	0.17
Average SNR	16.57	13.81	2.76

Figure 20 – Example of the VLC simulation graphical interface with parameters as presented in this chapter.

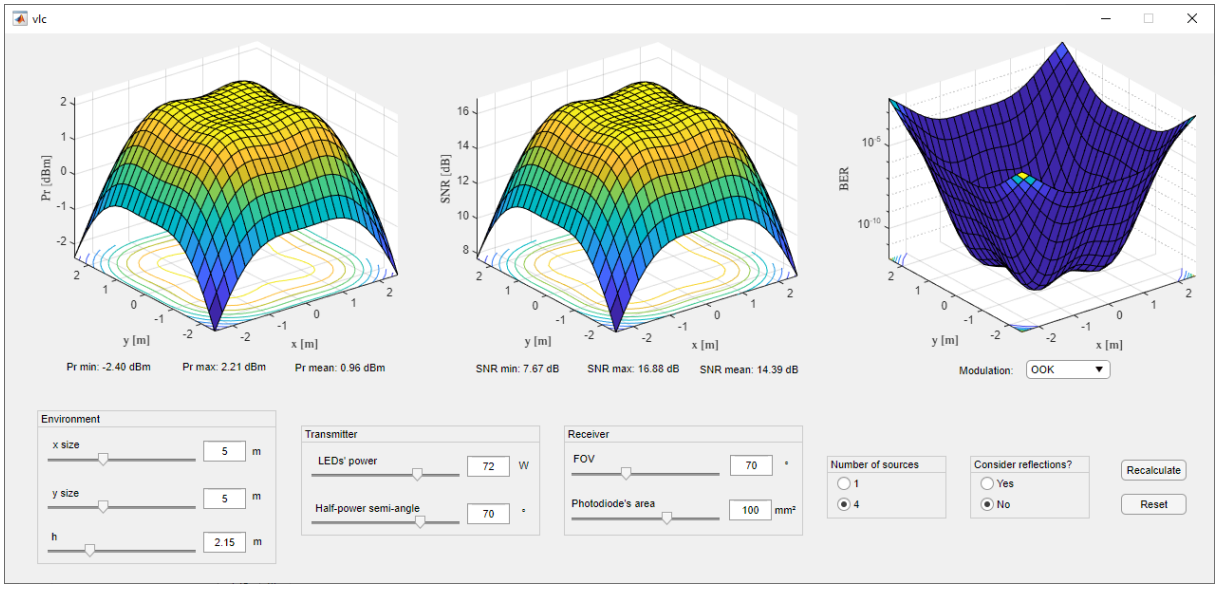

Source: The author.

3.4 CHAPTER CONCLUSIONS

In order to design and validate communication systems, simulation models are essential. The developed VLC simulation model allows the evaluation of environments with variable characteristics, such as room size, position of transceiver elements or reflectance factor of walls. Also, it is possible to simulate transceiver components (*i.e.*, LEDs and photodetectors) with varying parameters, such as emission optical power, emission and incidence angles, half-power semiangles, photodetection areas and others. In this way, the simulation model allows for a degree of flexibility for the evaluation of VLC systems. Finally, the graphical interface allows the quick simulation of basic scenarios.

In the next chapters, the VLC channel model and simulations presented in this

Figure 21 – Second example of VLC graphical interface.

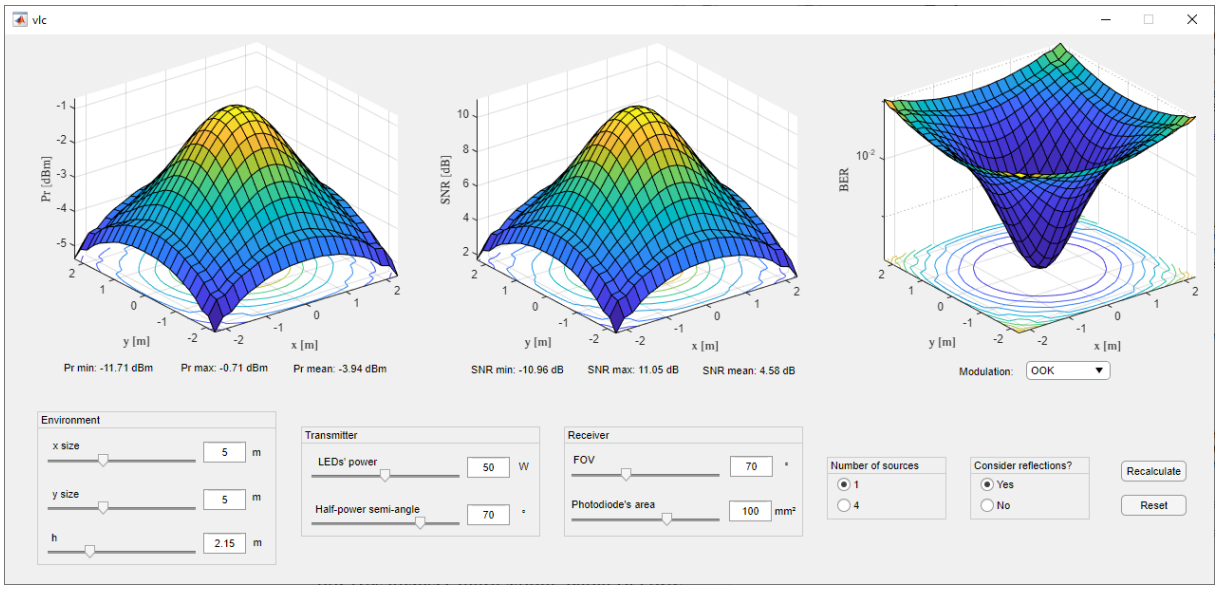

Source: The author.

Figure 22 – Third example of VLC graphical interface.

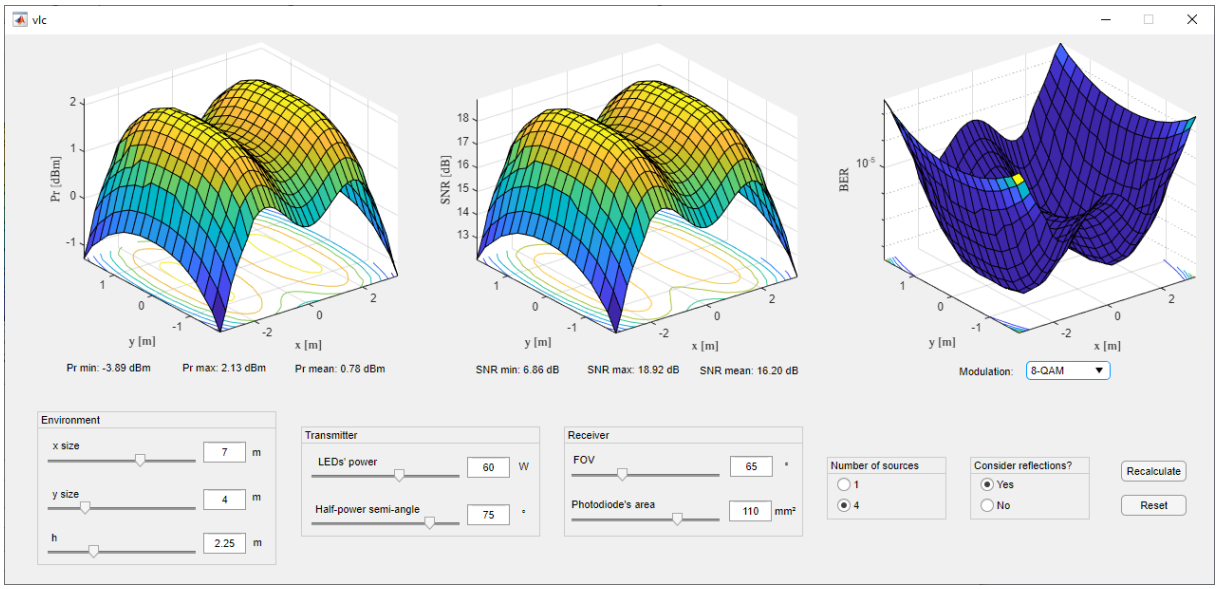

Source: The author.

chapter are employed to simulate and validate more specific scenarios and applications. Further on, the developed model may be employed for a variety of cases and applications to be proposed and validated, as the portable MATLAB code allows it to be readily adapted.

4 COOPERATIVE COMMUNICATION IN VLC

In this Chapter, cooperative simulation scenarios are described, using the simulation environment presented in Chapter 3, as well as laboratory experiments considering the amplify-and-forward (AF) technique.

4.1 COOPERATIVE COMMUNICATION

Cooperative communication is a technique whose purpose is to obtain spatial diversity in telecommunication systems in scenarios such as when it cannot be obtained due to the impossibility of the installation of multiple antennas (NOSRATINIA *et al.*, 2004). The RF communication channel is subject to statistical variation in time and as a consequence it is prone to fading. By installing multiple antennas at the transmitter and/or receiver, multiple paths are obtained and the probability of a communication failure decreases. In order to take advantage of spatial diversity's benefits, it is necessary to guarantee that the multiple paths are independent, which requires the antennas to be distanced by a given minimum distance that is a function of the wavelength λ (GOLDSMITH, 2005). However, spatial diversity is not always possible to be implemented, particularly in small devices, such as cellphones and small network sensors. Typically, in these devices there is no available space for the installation of various antennas and it may also be impracticable due to the higher power consumption for these additional antennas (NOSRATINIA *et al.*, 2004). Moreover, it is not expected that the user admits a bigger pocket device in order to obtain a better performance.

Therefore, cooperative communication is as a technique employed to obtain the benefits of spatial diversity even with only one antenna at the network elements (SENDONARIS *et al.*, 2003; LANEMAN *et al.*, 2004). The basic principle is the sharing of resources from the network nodes, creating a virtual array of antennas. In this scenario, it can be installed relays at the system, *i.e.*, devices that only retransmits the information between transmitter and receiver in order to provide robust communication (COVER; GAMAL, 1979). Alternatively, the user's device may also operate as relays, scenario in which it is usually employed the term cooperative communication. Figure 23 illustrates this principle.

At the destination, the information packages from different sources and paths must be combined, with combination techniques distinguishing themselves in the approach

Figure 23 – Basic elements of a cooperative communication system: source (*S*), relay (*R*) and destination (*D*).

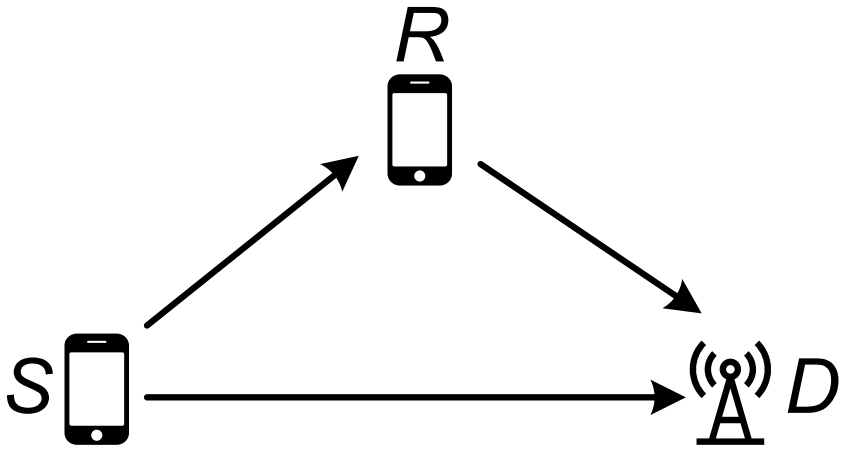

Source: Adapted from Nosratinia *et al.* (2004).

of weighting each received signal. Among such techniques, there is the selection combining (SC), equal-gain combining (EGC) and the maximum ratio combining (MRC) (GOLDSMITH, 2005). In the absence of interference, MRC is considered the optimal combining scheme. However, there is the challenge of knowing in detail all the fading parameters of the channel (SIMON; ALOUINI, 2005). On the other hand, EGC doesn't present this complexity and its performance may be similar to MRC, but it is a technique limited in practice to modulations of equal power symbols (GOLDSMITH, 2005; SIMON; ALOUINI, 2005). In SC, the decision is made by the signal which presents the highest SNR at the receiver. It is the simplest of these techniques, but its performance is poorer.

As for the implementation of cooperative communication, various protocols have been proposed, which are categorized according to what the relay does with the received information before retransmitting it (LANEMAN *et al.*, 2004):

- Amplify-and-forward (AF): it is the simplest cooperation strategy. The relay only transmits the information received from the source applying a determined power gain, in order to compensate the path loss over the source-relay channel, as illustrated in Figure 24. However, this strategy also tends to amplify the system noise.

- Decode-and-forward (DF): in this protocol, the relay attempts to decode the information before retransmitting it, therefore eliminating the channel attenuation and the effects of noise at the reception. Figure 25 illustrates this process.

Figure 24 – Illustration of the amplify-and-forward protocol.

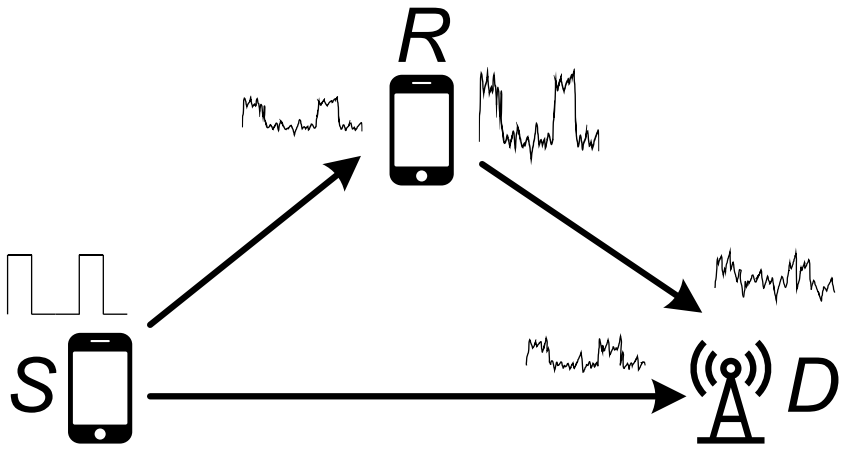

Source: Adapted from Nosratinia *et al.* (2004).

Figure 25 – Illustration of the decode-and-forward protocol.

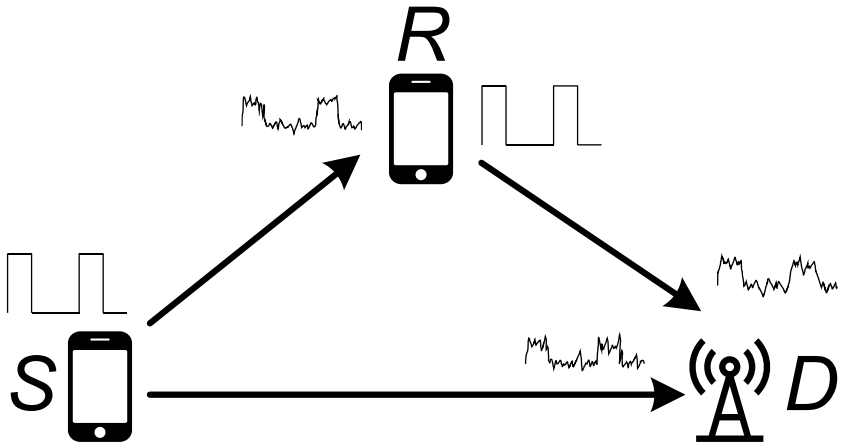

Source: Adapted from Nosratinia *et al.* (2004).

DF presents variations, such as:

- Fixed decode-and-forward (FDF): the relay always acts in the communication, independent of the performance of the source-destination channel and if the relay correctly decoded or not the source information.
- Selective decode-and-forward (SDF): the relay estimates if it correctly received the source information and only retransmits it if it considers that it was successful.
- Incremental decode-and-forward (IDF): the destination notifies the relay if it correctly received the source information; in this way, the retransmission only occurs if necessary.

The performance of the AF, FDF and SDF protocols are presented in Figure 26, as well as the performance of direct transmission for comparison purposes. This simulation shows the BER as function of the SNR considering BPSK (binary phase shift keying) modulation and MRC over a wireless channel subject to Rayleigh fading. It is assumed that the source, relay and destination are equally distanced and the channels have equal and unitary energy. For a fair comparison, the source and relay transmit with half the power of the direct source-destination power in direct transmission.

Figure 26 – BER as function of SNR for the cooperative communication protocols AF, DFD and SDF, compared to direct transmission.

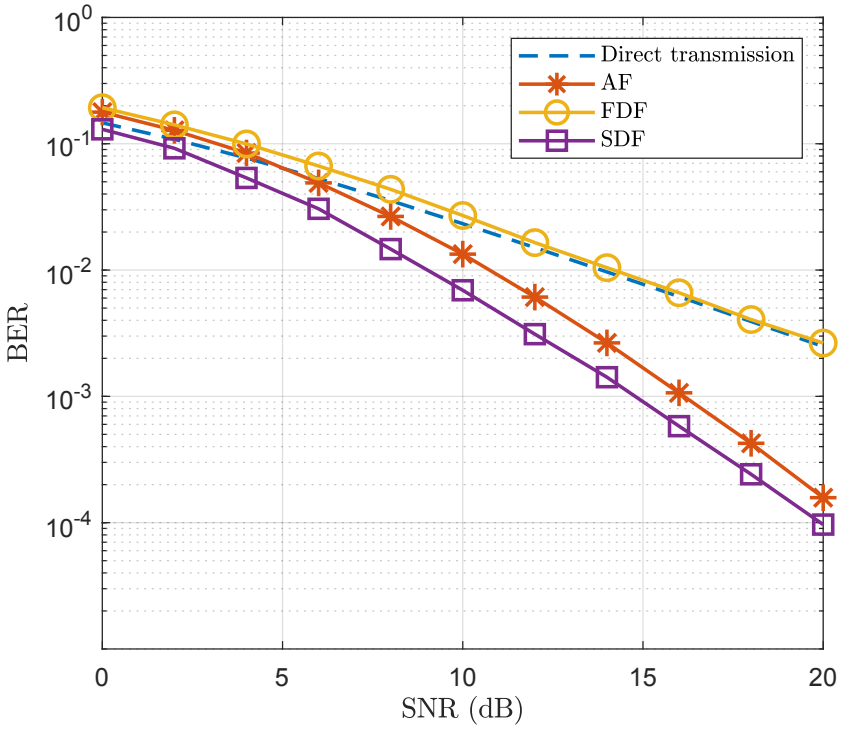

Source: The author.

It is noticed in the plot of Figure 26 that the FDF protocol presents a performance even worse than the direct transmission, which is preferred to the cooperation in such case. This happens because when always decoding and forwarding the information from the source, the eventual communication errors are also propagated. On the other hand, AF and SDF present a performance improvement in the communication of the direct transmission at the source and relay. Although AF presents an inferior performance compared with SDF, its implementation is simpler, given that a decodification of the source information is not needed.

4.1.1 Cooperative communication in VLC

As mentioned in Chapter 1, spatial diversity in VLC is typically high, due to the fact that the photodetection area of the receivers are millions of times higher than the wavelengths λ of the light that is detected (KAHN; BARRY, 1997; KOMINE *et al.*, 2004; GHASSEMLOOY *et al.*, 2013). Although the physical properties of the VLC systems mitigates multipath fading effects, there are still the effects of multipath distortion (ISI), specially in NLOS links (KAHN; BARRY, 1997). Moreover, the communication distance may be narrowed due to the high path losses at the optical wireless channel and also by the light being blocked by opaque structures, ceasing the communication at all. Therefore, cooperative communication techniques may be employed in VLC systems in order to improve the communication performance or even making it feasible in contexts which otherwise it would not be viable.

The application of cooperative communication techniques in VLC is a recent theme in the literature. Previously, it also had been studied in FSO channels (ABOU-RJEILY; SLIM, 2011). In VLC, specifically, the first related works are those of Yang and Pandharipande, in 2013 and 2014 (YANG; PANDHARIPANDE, 2013, 2014), in which they analyzed, respectively, triangular and linear topologies, as illustrated in Figure 27. The linear scenario may be interpreted as a communication between luminaires installed in light poles in a street or installed in corridors or small rooms, while the triangular topology can be interpreted as a room where a user equipment receives the signal from the source and one from a relay, that could be, for instance, a reading lamp near the user.

Analytically, the difference between these topologies is that, in the linear, the power from the source that is received at the destination is negligible. In this way, the first case may be considered as a relay-assisted system, as the receiver only receives the signal from the relay, while the triangular topology is a cooperation system, given that the destination receives both source and relay signals and combines them to generate spatial diversity. In both works the authors analyze the theoretical BER for these scenarios for the AF and DF protocols, and significant performance gains are observed in the performance of the BER as function of the relay luminaire position.

Since then, other works have been published presenting analysis and applications of cooperative systems in cooperative VLC. A recurrent theme addresses optical variations of OFDM in combination with relay-assisted transmission, which has been shown very efficient (KIZILIRMAK *et al.*, 2015; KAZEMI; HAAS, 2016; NARMANLIOGLU *et al.*, 2017; NA *et al.*, 2018). Another important analysis in this scenario is the

Figure 27 – Cooperation topologies as proposed in the works of Yang and Pandharipande: (a) linear topology and (b) triangular topology.

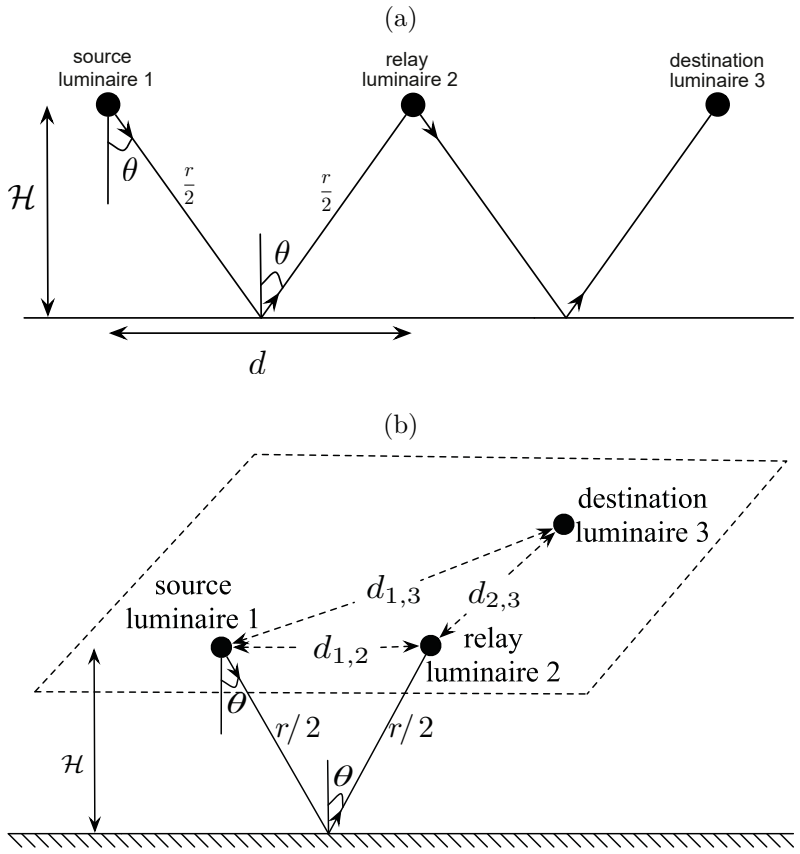

Source: Adapted from Yang and Pandharipande (2013, 2014).

allocation of power between the main source and the relay, essential for optimizing resources and power, and also to perform fair comparisons between direct and relay-assisted communications (YANG; PANDHARIPANDE, 2014; KIZILIRMAK *et al.*, 2015; NARMANLIOGLU *et al.*, 2017; NA *et al.*, 2018). Mobile applications are also possible, as Pešek *et al.* (2018) studied the possibility of VLC cooperation between mobile users, which act as relays to cooperate among themselves, resulting in significant gains in coverage, data rate and BER. Na *et al.* (2018) demonstrate that cooperative VLC has potential to improve the performance and flexibility of future 5G mobile systems. Deng *et al.* (2020) investigate a scheduling framework for cooperative VLC to mitigate inter-channel interference. Tiwari *et al.* (TIWARI *et al.*, 2015) analyze the use of cooperation in an uplink context, which is a challenge in VLC due to the lower power at the user equipment. As for the cooperation technique, works analyze AF (KIZILIRMAK; UYSAL, 2014; VATS *et al.*, 2017), DF (YANG; PANDHARIPANDE, 2013) or both schemes (NARMANLIOGLU *et al.*, 2015; KIZILIRMAK *et al.*, 2015; PEŠEK *et al.*, 2018; HAO *et al.*, 2020), typically presenting better results for DF.

Experimental research on cooperative VLC has seen limited coverage in the literature, mostly in relay assisted fashion, also called multi-hop, that is, a relay or set of relays that retransmits the signal and the final destination only receives the signal of one information source. That is the case of the work of Sejan and Chung (2020) which transmits a signal through four relay nodes until the destination. Similarly, Namonta and Cherntanomwong (2016) develop a system with repeaters to extend the communication distance.

Some specific applications for cooperative communication systems in VLC published in the literature are presented below.

- Underwater communications: the use of relays has been studied as a mean to improve the performance of underwater communications, including acoustic communications (KAUSHAL; KADDOUM, 2016). Besides increasing the communication distance, it is also possible to reduce power consumption with this method. Han *et al.* (2008) demonstrated an improvement of up to 5 dB using the AF protocol. Carbonelli *et al.* (2009) implemented a multi-hop system of underwater cooperation with the DF protocol and demonstrated that its performance is superior than direct transmission. As previously mentioned, underwater communications are one of the applications in which VLC has benefits. However, it was also said that optical wireless communications has a disadvantage in this context, which is the small communication reach. In this way, this is the main purpose for the research towards relaying communication in this scenario in recent literature. Vavoulas *et al.* (2014) analyzed a path loss model in the underwater environment, proposing a node network acting as relays to share information. Jamali *et al.* (2016) characterized the performance of underwater communications with relays using OCDMA (optical code-division multiple access), reporting a 32 dB improvement and a BER of 10^{-6} in a two relay system at a distance of 90 m. It is a field yet to be explored, but with potential to improve the reach of underwater VLC links.

- Vehicular communications: besides the advantages and possibilities of VLC in the traffic system, there are also challenges, specially the need of a LOS link. A traffic scenario is very dynamic, with vehicles changing their positions constantly, what compromises the existence of a LOS link at all times. Therefore, the use of relays is a possibility for the creation of VANETs (vehicular ad hoc networks). Cui *et al.* (2016) simulated a model considering both V2V and V2I communication in a scenario of lane change. In this case, it was observed that both V2V and V2I were

improved with cooperation; furthermore, in the V2I scenario, the communications would be interrupted considering only LOS links. Authors have employed the DF protocol and MRC combination.

- Uplink: one of the main challenges of VLC systems, the uplink channel may be improved employing cooperation techniques. Placing the relays in the path between the user and the receiver cause the path losses to be mitigated. Even with a low optical power in the user's device, the performance may be improved given that the travel distance is smaller. Besides that, as the relay is not immediately close to the user, high optical power values may be used, which otherwise would be prohibitively inconvenient for the user. Tiwari *et al.* (2015) proposed a relay-based uplink model, where the relays are placed in the walls of the environment, which receive the information of the users and transmit it to the receiver in the ceiling, where a matched filter decides about the received signal. In this case the relay acts as the only source of transmission between the user and the receiver, not existing a cooperation technique. Yang *et al.* (2018) proposes an AF cooperation system using the Bussgang theorem, with the relay being a luminaire placed next to the user. Authors employed M-QAM modulation and the multicarrier technique DCO-OFDM. In both works the results demonstrated that the uplink performance was improved.

Other scenarios where cooperative communication in VLC may be useful include:

- Shadowing: the shadowing in an environment may be constant, as in a particular part of a room that does not receive enough light to reach a desired performance, or doesn't receive light at all. Also, shadowing may be variable, for instance, when a person moves around the room, blocking the line of sight between transmitter and receiver. In this way, the installation of relays in determined locations in the environment may help to mitigate the phenomenon and support the communication to keep constant and avoid inconvenience to the mobility of users.

- Confinement: as light does not passes through opaque structures, environments outside the area illuminated by the main transmission infrastructure are not covered by the access point, demanding the installation of a new main transmission infrastructure. However, in some adjacent environments a portion of light from the main source is received. Although insufficient for the user, this light may be employed by a cooperation element. Therefore, a relay may act as a retransmitter in

an environment next to that in which the main infrastructure is installed, reducing costs.

4.2 SIMULATIONS

In Figure 28, a scheme of the cooperative VLC model used in the simulations is presented. Part of these results were published in (OLIVEIRA *et al.*, 2019). The scenario is described as an indoor environment, as presented in Chapter 3, but with a relay element near the receiver, which could be interpreted as a desk light in the work desk of the user. The center of the room, at the floor, is the coordinate $(0, 0, 0)$.

Figure 28 – Indoor cooperative VLC model.

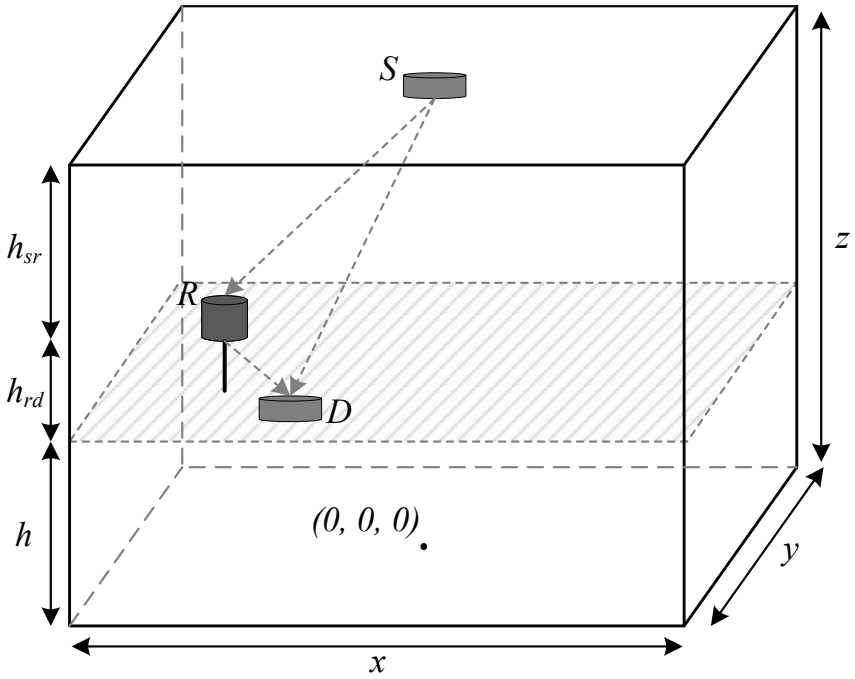

Source: The author.

In this scheme, a few new parameters are introduced. h_{sr} is the height between the source (here, positioned at the ceiling) and the relay, and h_{rd} is the height between the relay and the destination. Note that these are not the *distances* between the elements, but the distances between the planes, at the z coordinate, in which they are placed.

This work considers an AF approach, *i.e.,* the relay applies a gain to the received signal from the source and retransmits it to the destination. In the destination, the signals are combined using MRC, in which the total SNR is the sum of the SNRs of both source-destination (sr) and source-relay-destination (srd) paths (BRENNAN, 2003;

KIZILIRMAK *et al.*, 2015):

$$\mathrm{SNR}_{AF} = \mathrm{SNR}_{sd} + \mathrm{SNR}_{srd}. \tag{23}$$

The considered scenario is the room with one luminaire. This is chosen due to the worse link performance in this context, as presented in Figure 15. Scenarios with four luminaires, such as in Figure 16, would not be so improved by cooperation, since the overall communication performance in most of the area may already be considered satisfactory. Table 7 lists the parameters employed in the cooperative communication simulation.

Table 7 – Simulation parameters of environment, transmitter and receiver.

Parameters		Value	Unit
Environment	Dimensions ($x \times y \times z$)	5×5×3	m
	Receptor surface height (h)	0.85	
	Relay height from the surface (h_{rd})	0.5	m
Transmitter	Position ($x \times y$)	$(0, 0)$	
	Total transmit power (P_r)	72	W
	Half-power semiangle ($\varphi_{1/2}$)	70	°
Receiver	FOV	70	°
	PD's area of detection (A)	1	cm^2
	Optical filter gain	1	
	PD's lens refraction index (n)	1.5	
	PD's responsivity (γ)	0.54	A/W
Relay	Position ($x \times y$)	$(-1.875, -1.875)$	
	Half-power semiangle ($\varphi_{1/2}$)	40	°
	Gain	30	dB

Both receivers (at the relay and at the destination) are modeled with the same properties. The relay's lamp is different, presenting lower transmit power (the received power times the gain) and a narrower half-power semiangle of 40°, as in (NARMANLIOGLU *et al.*, 2017).

Results for three coordinates are presented, namely, P1, P2 and P3 which corresponds, respectively, to the coordinates $(-1.875, 1.875)$, $(-2.3, 0)$, and $(-1.25, 1.25)$ in the room (se Figure 28). Figure 29 graphically illustrates this coordinates for a visual reference and Figure 30 presents the SNR and BER for the scenario without cooperation.

Once parameters for this scenario are defined, analysis of the amplifier application is changed according to the position of the relay. For these simulations, amplitude gains that provides reasonable values of amplification and improved BERs are pursued. If a high

Figure 29 – Representation of evaluated coordinates for cooperative communication.

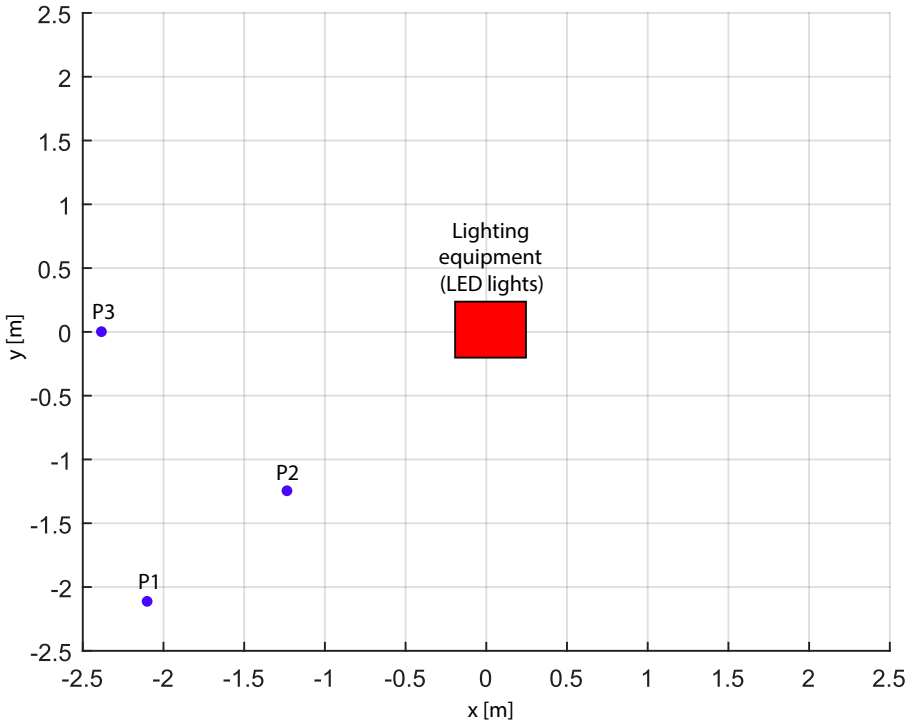

Source: The author.

gain is defined in a region where the BER is already low, the resulting BER values would be exaggeratedly low. In practice, this means that SNR is saturated, as was observed in the experimental results conducted for this work, where increasing the value of the LED's supply current, from a given point onwards, actually resulted in a poorer performance at the receiver. Therefore, a BER of the order of 10^{-5} is aimed at each point, with a height of 0.5 from the relay plane to the receiver plane.

First, P1 is evaluated. This coordinate is located near a corner of the room and is the most distant location from the transmitter of the evaluated points. To reach a BER at the order of 10^{-5}, a gain of 34 dB is employed. The SNR and BER plots are shown in Figure 31. In these and in the next plots, the graphs are shown in different angles in order to ease the visualization of the cooperation performance.

Coordinates P2 and P3 are closer to the source and, therefore, a lower gain is required for the target BER of 10^{-5}. Figures 32 and 33 present the SNR and BER plots. The employed gains are 33.5 and 29 dB, respectively, for P2 and P3.

Therefore, in scenarios like these, where there are areas in an environment that do not receive enough optical power from the source to provide satisfactory communication performance, cooperative communication has the capability to enable the user to stay

Figure 30 – (a) SNR and (b) BER values for the proposed scenario, without cooperation.

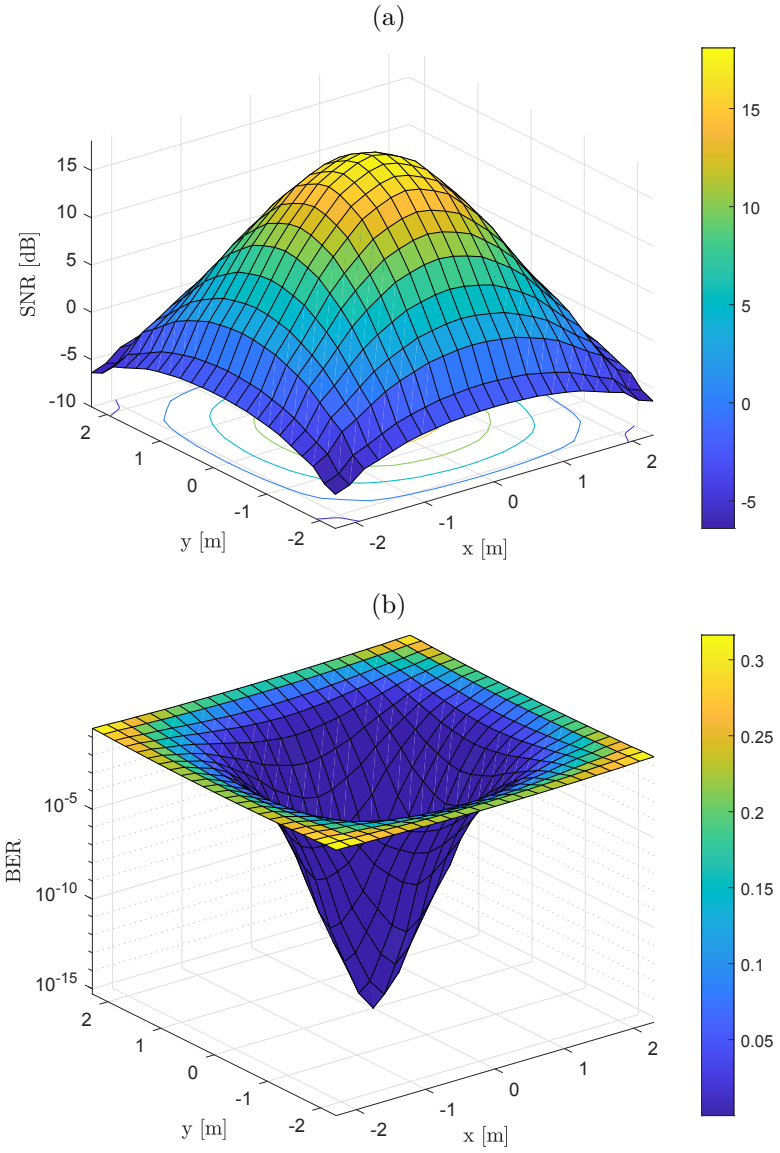

Source: The author.

at places of the room where communication wasn't possible before. Naturally, this is limited by the minimum received optical power at the given coordinate and the electric gain circuitry of the system.

This analysis takes a few assumptions into consideration. First, these simulations does not consider the use of lenses or other optical devices that improve light detection. Also, it does not consider amplification of the photocurrent at the destination. Therefore, in practical systems, the necessary amplification gain at the relay may be smaller. Commercial amplifiers with gain in the order 35 dB are available, such as Mini-Circuits ZHL-72A+ (Mini-Circuits, 2019). Given that most VLC signals, due to LED's physical

Figure 31 – (a) SNR and (b) BER values considering a relay positioned at $(-1.875, 1.875)$ and an amplification of 34 dB.

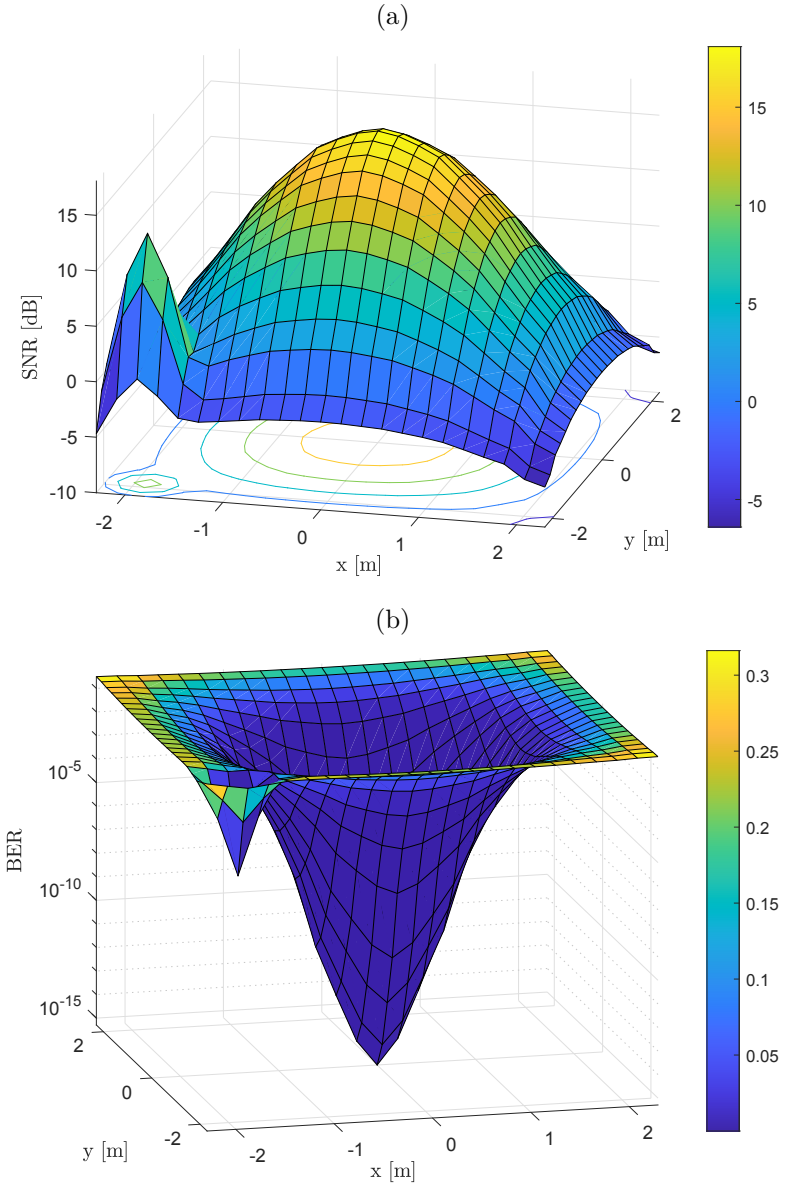

Source: The author.

characteristics, operates at relatively low frequencies (< 10 MHz), specific amplification circuitry may be constructed without higher complexity.

4.3 EXPERIMENTAL RESULTS

In this Section the cooperative communication experimental setup is described, as well as practical results employing offline combining. Results are divided into two categories: SNR and BER measurements.

Figure 32 – (a) SNR and (b) BER values considering a relay positioned at $(-2.3, 0)$ and an amplification of 33.5 dB.

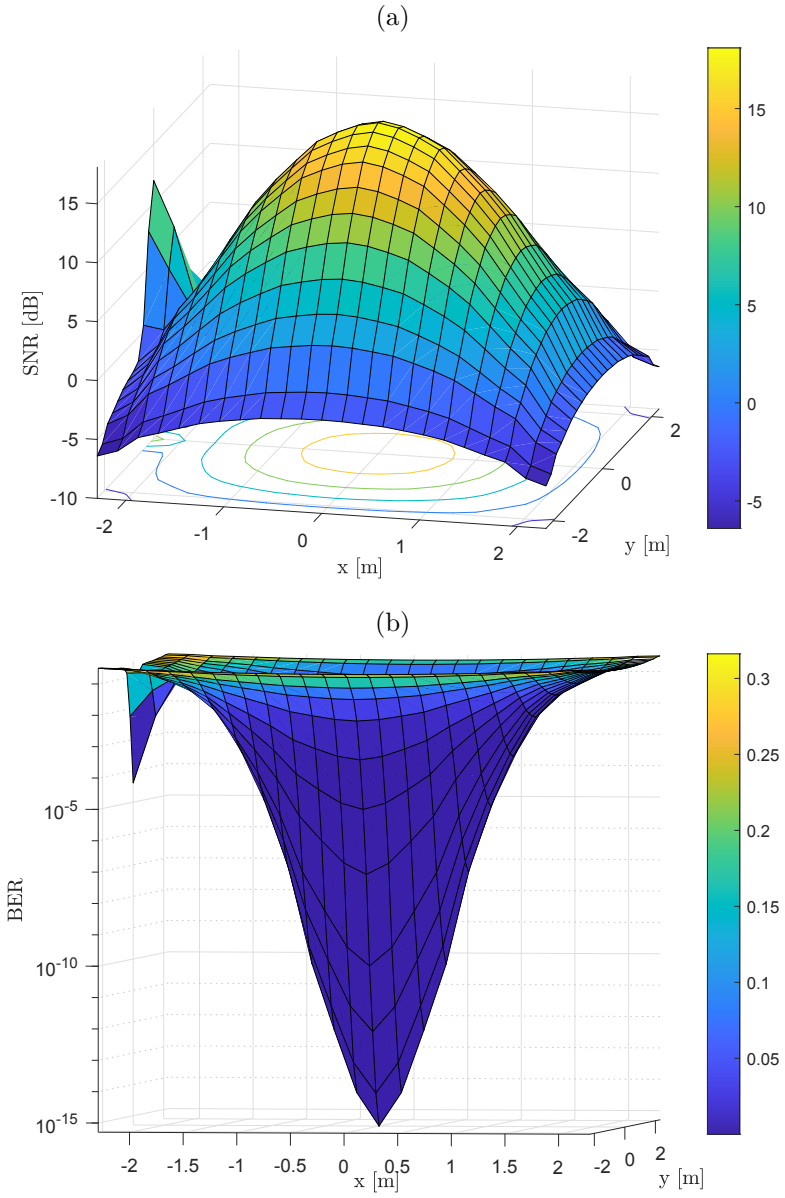

Source: The author.

4.3.1 Experimental setup for SNR measurements

At the transmitter side, the LED transmitter is the SP-02-T9 SinkPAD II module from Luxeon Star LEDs (Luxeon Star LEDs, 2015). The module consists of seven white LEDs, model LX18-P150-3 (Lumileds Holding B.V., 2017). In this experiment, the ZX85-12G-S+ bias-t from Mini-Circuits (Mini-Circuits, 2013) is employed. These signals are combined by using a bias-T, whose output DC (illumination) + AC (communication) drives the LED. An in-depth analysis of the illumination and communication performance

Figure 33 – (a) SNR and (b) BER values considering a relay positioned at $(-1.25, 1.25)$ and an amplification of 29 dB.

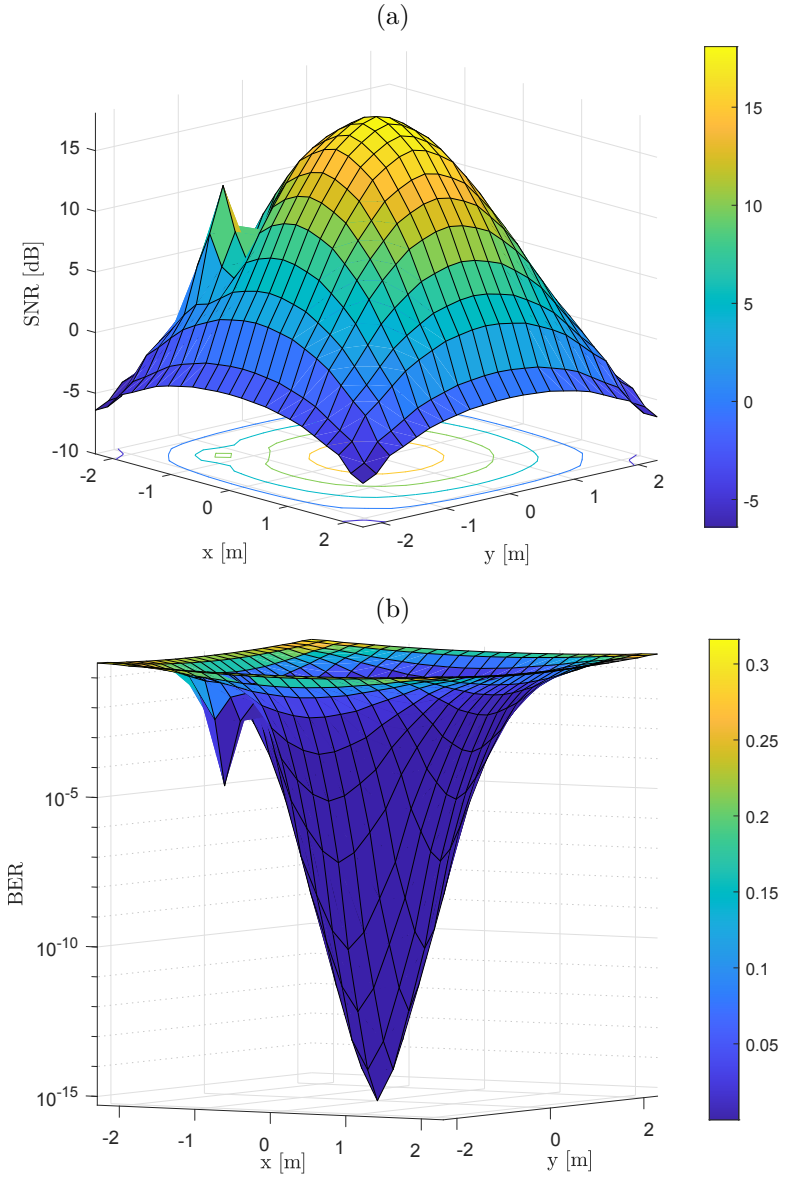

Source: The author.

of the same luminaire by our research group is published in Tosta *et al.* (2020).

At the receiver side, it is employed the Hamamatsu C12702 series photodetectors, using a C12702-12 and a C12702-11 model (Hamamatsu Photonics, 2017). These modules use an APD (avalanche photodiode) as the detector, applying a high gain (> 30 dB) to the generated photocurrent. The main difference between them is the photodetection area, which is 7.1 mm^2 ($\varnothing$ 3 mm) for the C12702-12 and 0.78 mm^2 ($\varnothing$ 1 mm) for the C12702-11, respectively. They also differ in their bandwidth, but not in the frequencies employed in this work.

In Figure 34, the block diagram of the experimental setup is presented. For both SNR and BER measurements, each signal (direct and relay) is captured separately. Direct signal is captured with only the source luminaire turned on, and relay signal is captured alone by blocking the source's light from the destination with an opaque structure.

Figure 34 – Block diagram of the cooperative communication VLC experimental setup for SNR measurement.

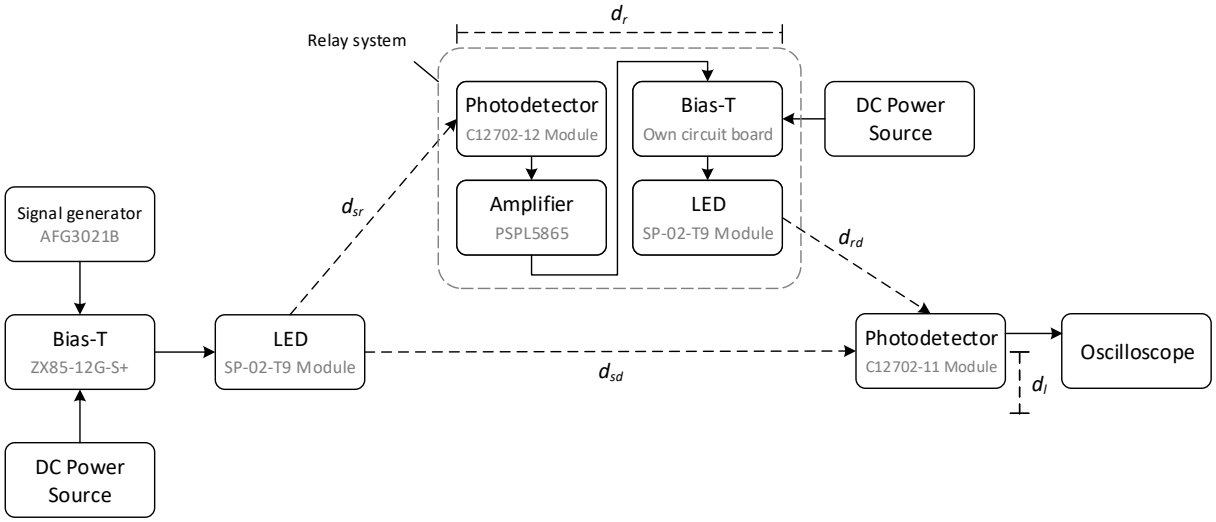

Source: The author.

As observed in Figure 34, the relay system is composed of four elements. First, the light from the transmitter is detected by the photodetection module at the relay system. The output of the module is composed solely by the modulated part of the transmitted signal (*i.e.*, there is no DC level). Therefore, this is similar to the input signal from the signal generator that serves as input for the transmitter, but with a significantly lower amplitude. Consequently, in order to input this signal in the next luminaire, it needs to be amplified. Tektronix's PSPL5865 amplifier is employed, which provides a linear gain of circa 26 dB (Tektronix, 2015). Then, this signal goes to a bias-t that drives the LED module, as in the source, and the amplified modulated optical signal reaches the destination photodetector, whose output is observed at an oscilloscope. Figure 35 shows a picture of the VLC cooperative communication workbench.

Due to the electronics between the received signal at the relay receiver and the retransmitter, there is a delay in the reception of the relayed signal at the destination, in comparison with the source signal. Therefore, the analysis is conducted off-line, by independently measuring each signal in the destination and combining them through signal processing using MATLAB.

The electrical input power of the LED luminaires was implicitly reduced in order

Figure 35 – VLC cooperative communication setup in the laboratory.

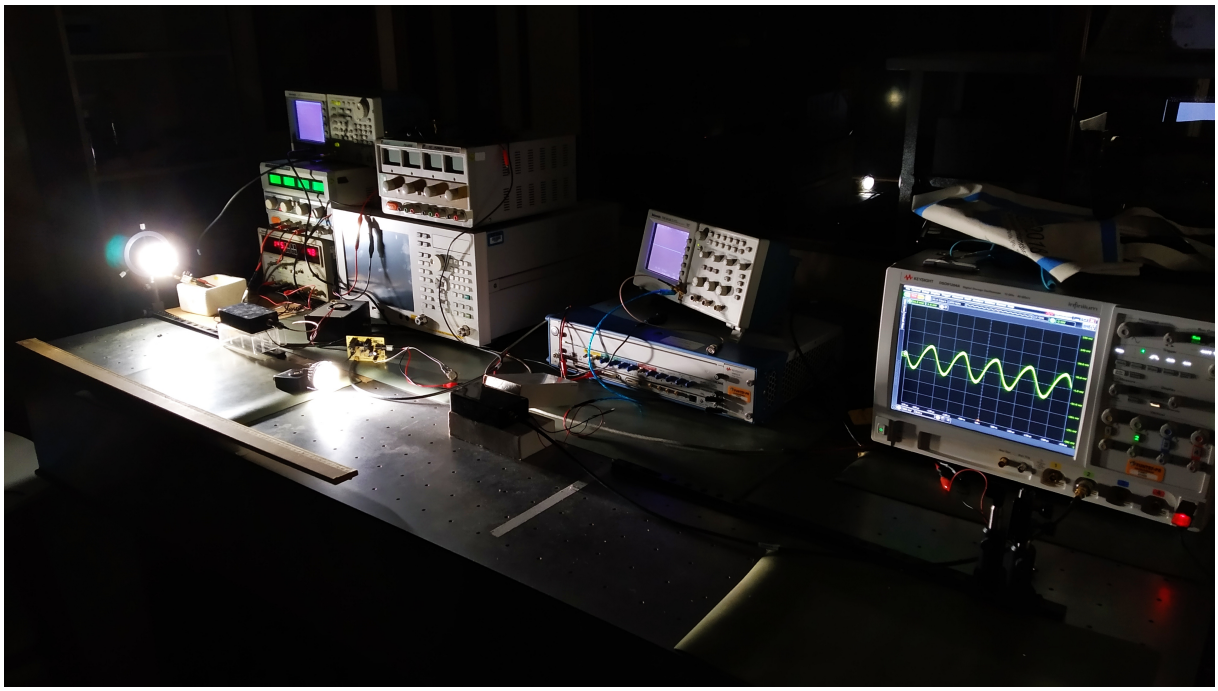

Source: The author.

to analyze the system performance. If the lamps were supplied with the power that would output optimal results, there wouldn't be performance deterioration in the available measurable distances at the laboratory working bench.

4.3.1.1 Experimental configurations and results for SNR measurements

In order to evaluate experimentally the VLC cooperative communication, different arrangements of components were defined and are discussed is this Section. The general setup is presented in the previous Section, in Figure 34, and in this Section specific distances and positions are described. Four experimental configurations were designed to evaluate different situations of cooperative communication in VLC.

To evaluate the performance of each of the configurations, SNR values are estimated from the measured peak voltage of each experiment, by transmitting a standard 1 MHz sine wave. From the photodetector's datasheet (Hamamatsu Photonics, 2017), it is obtained the photoelectric sensitivity of 10^4 V/W. From this value and the measured received voltages, it is inferred the received optical power and calculate the SNR with Equation (10), with $\gamma = 0.42$ A/W and a total noise obtained from Figure 12.

In the diagrams of Figures 37, 39, 41 and 43, solid lines mean fixed distances while

dashed lines refer to variable distances. The variable distances were increased in steps of 10 cm for experiments 1 to 3, and steps of 1 cm for experiment 4. Each experiment is described and is followed by the results as a SNR plot. The SNR results are presented for direct transmission, relay-only transmission and cooperative source + relay combined. For a reference for all configurations, refer to Figure 36.

Figure 36 – Reference block diagram of the experimental configurations.

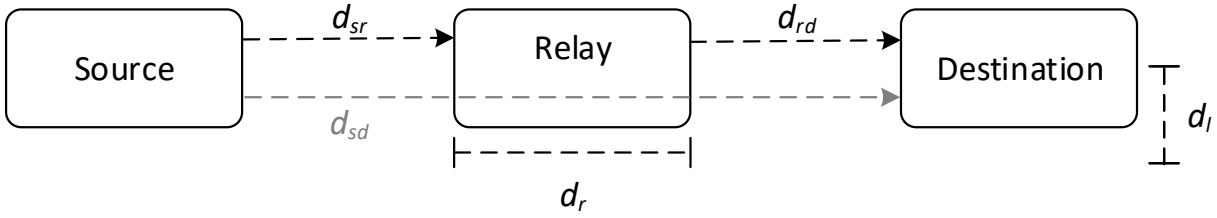

Source: The author.

d_{sr} is the distance from the source to the relay's photodetector; d_{rd} is the distance from the relay's LED module to the destination; d_{sd} is the distance of the direct transmission, *i.e.*, from source to destination; d_r is the distance from the relay's receiver to its transmitter; and d_l is a lateral displacement, employed at configuration 4 only.

Table 8 summarizes the values of the distances variations in each configuration. For configurations 1 to 3, all elements are aligned. A small height variation of about 5 cm between the source LED module and the relay components is employed so that there is no blocking between source and destination. Only in configuration 4 there is a lateral variation, by moving the destination.

Table 8 – Distance between elements for the SNR measurements. Values in centimeters.

Configuration	d_{sd}	d_{sr}	d_r	d_{rd}	d_l
1	$60+d_{rd}$	40	20	40 to 120	0
2	140	10 to 50	$(50-d_{sr})+30$	60	0
3	140	10 to 50	10	$(50-d_{sr})+80$	0
4	125	40	40	25 (aligned)	0 to 11

In the first experiment, the distance from source to relay is fixed, while the position of the destination is increased. This setup is depicted in Figure 37.

The objective of this configuration is to evaluate how cooperation affects a user equipment if it is moved away from both source and relay, in comparison with only the source acting. This configuration mimics a scenario in which source and relay are

Figure 37 – VLC cooperative communication experimental scheme for SNR 1: varying distance of destination.

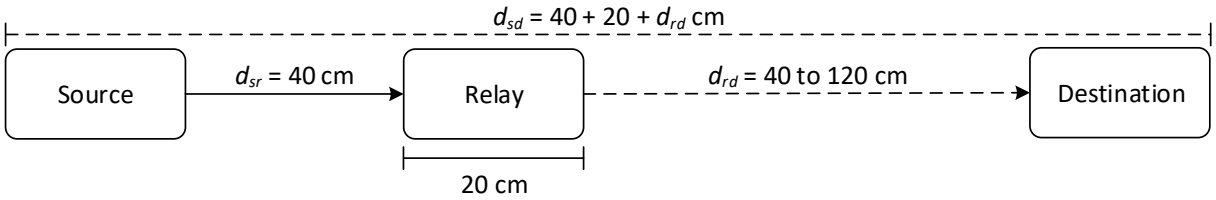

Source: The author.

positioned at fixed locations (in a room, for instance), while the user is moving, and considering that the relay is closer to the user than the source is. Figure 38 presents the results.

Figure 38 – SNR versus distance for experimental scheme 1.

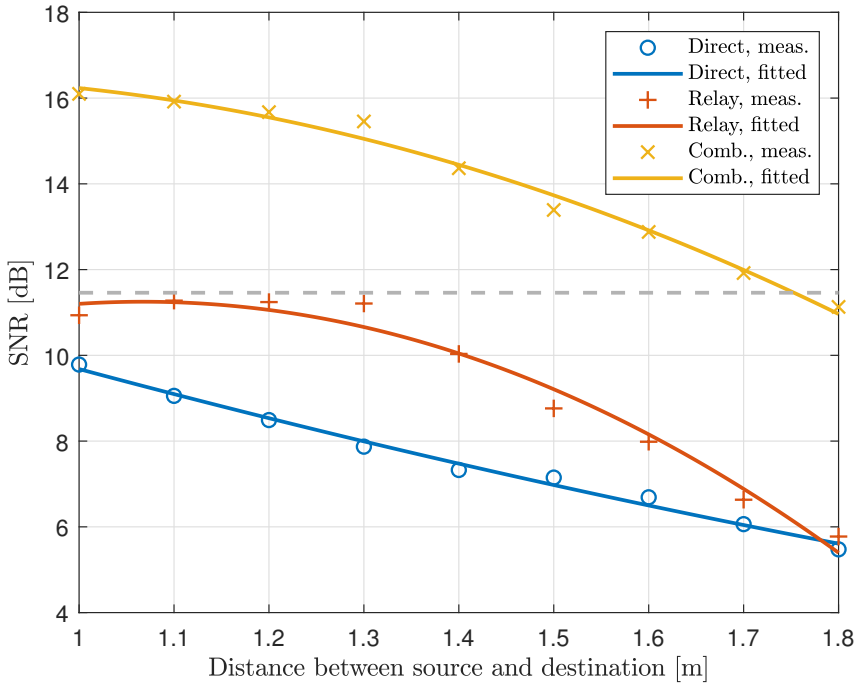

Source: The author.

Analyzing the plot in Figure 38, it can be seen that the cooperation significantly improves the performance of the received signal. Another noteworthy aspect is that, at the maximum measured distance, both direct-only and relay-only SNRs are relatively low, in which communication could be compromised; however, the resulting cooperative SNR is still relatively high, with an increase of approximately 6 dB, providing an estimated BER in the order of 10^{-5} for OOK at the maximum measured distance $d_{sd} = 1.8$ m. For reference, the SNR required for this BER is presented in this and the following plots as a dashed gray line.

The second configuration is depicted in Figure 39.

Figure 39 – VLC cooperative communication experimental scheme for SNR 2: varying position of the relay reception.

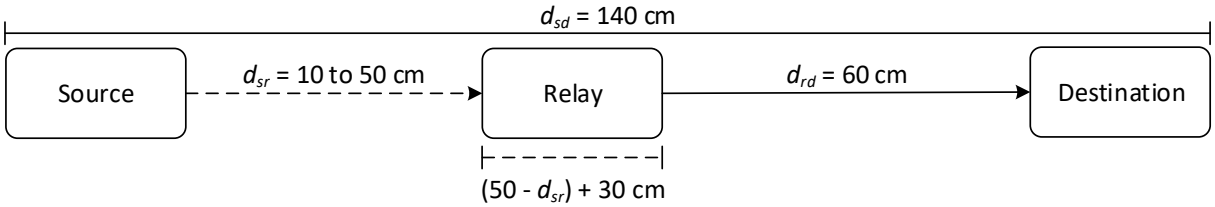

Source: The author.

In this case, the distance between the source and the relay reception is varied, while the relay LED and the destination are fixed. This means that the received power at the relay changes, decreasing as this distance increases. The distance between source and destination is 140 cm and between the relay LED and destination is 60 cm. The purpose of this experiment is to analyze the effect of the relay receiving different power values to drive the relaying LED. Results are presented in Figure 40.

Figure 40 – SNR versus distance for experimental scheme 2.

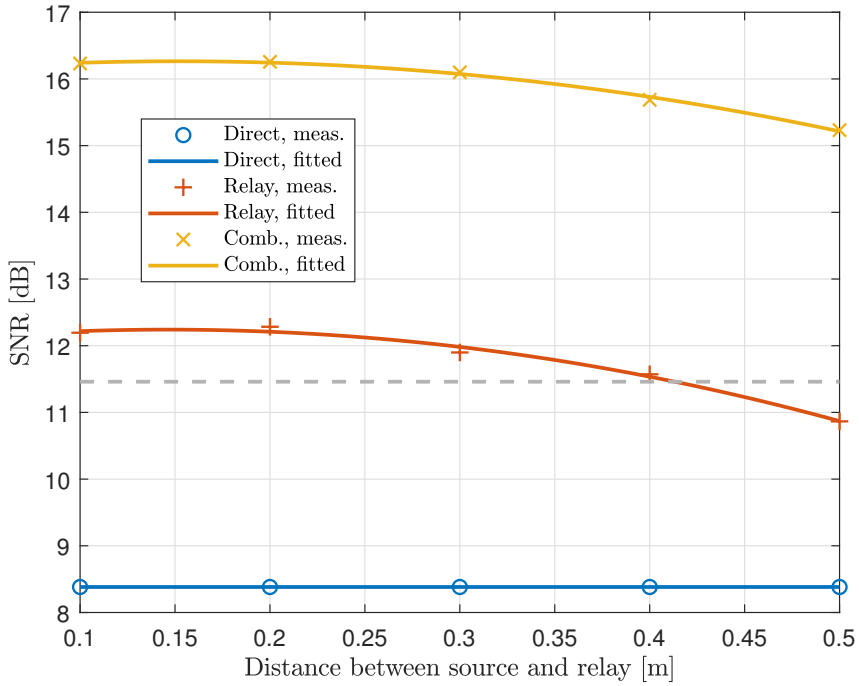

Source: The author.

For distances up to 20 cm, there is a very small variation of SNR. From this point onwards, the relayed signal starts to decrease the link performance. In all cases, the received power from the source at the relay is enough to provide a satisfactory

output at the relay to guarantee communication, which is further improved if the receiver is illuminated by both source and relay. There is a maximum SNR improvement of approximately 8 dB when the receiver detects both light sources.

Next, experiment 3 is illustrated in Figure 41. This experiment is somewhat similar to experiment 2, but in this case both relay elements (receiver and source) are moved together, starting close to the source and moving towards destination.

Figure 41 – VLC cooperative communication experimental scheme for SNR 3: varying position of the relay reception and transmission.

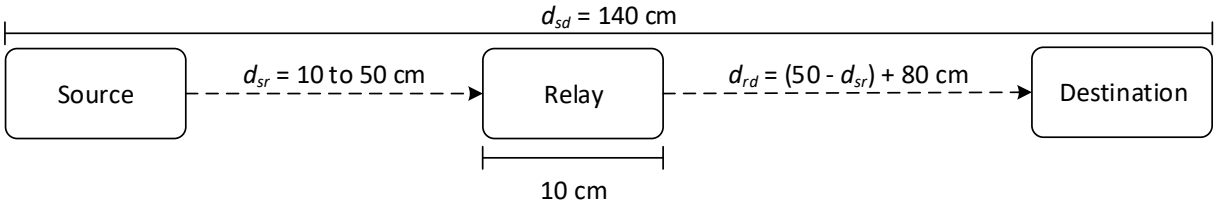

Source: The author.

In this experiment, it is intended to observe the behavior of the system while changing the position of the relay, *i.e.*, it aims to verify if there is an optimal point for the relay position. Results are presented in Figure 42.

Figure 42 – SNR versus distance for experimental scheme 3.

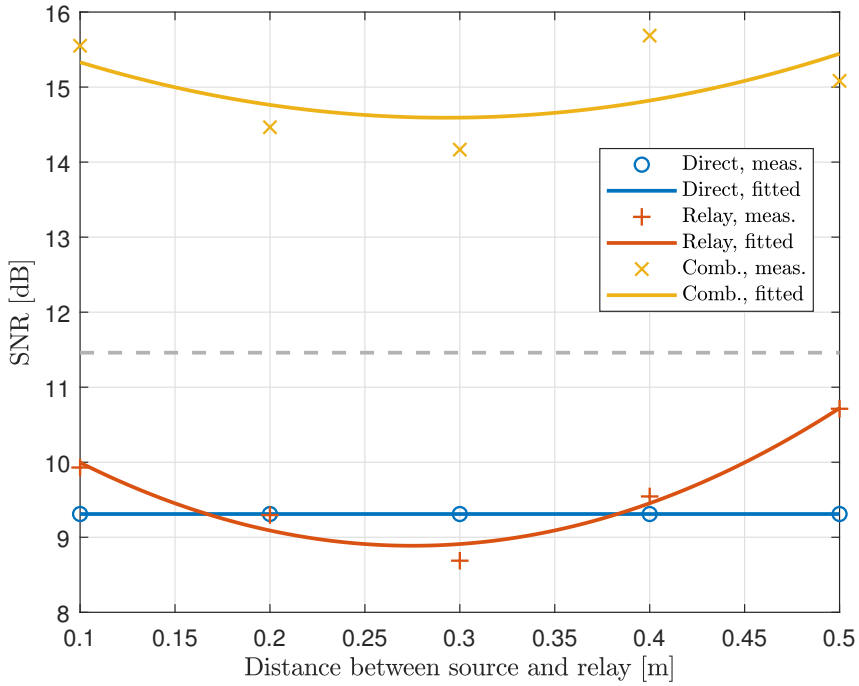

Source: The author.

It can be observed that the position of the relay has an impact upon the

performance and that a incorrectly positioned relay delivers a worse performance than the direct, source-only transmission, even if the relay is closer to the destination than the source. This is due a trade-off that occurs when the relay is repositioned: when it is close to the source, it receives a higher optical power, but the path loss in the relay-destination is also high; as it is pushed towards the destination, it receives less optical power from the source, but the path loss becomes smaller. When combining both source and relay power, the system performance improves up to 6 dB, which can be optimized by adjusting the relay position.

Lastly, experiment 4 intends to observe the impact of the relay system when the components are not in a straight line, by moving the destination module laterally, from 0 to 11 cm. All other distances were fixed, *i.e.*, all components are aligned, except for a small angle variation due to the destination's lateral displacement. The scheme is depicted in Figure 43.

Figure 43 – VLC cooperative communication experimental scheme for SNR 4: varying lateral position of the destination.

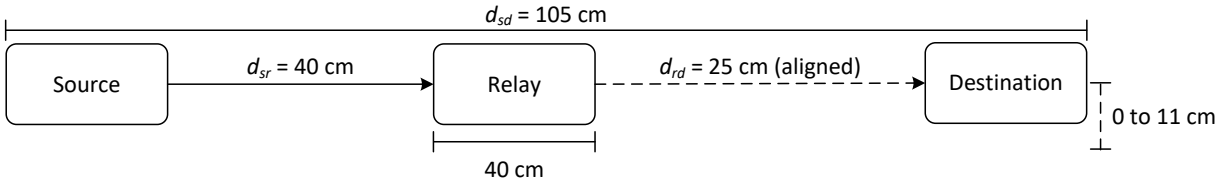

Source: The author.

In this experiment, the photodetector modules (as in Figure 34) were exchanged with each other, in order to improve performance at the receiver by employing the detector with the larger area at the destination, which is subject to angle variations. Figure 44 presents the performance results, as a function of the lateral displacement at the destination.

In this configuration, the variation of direct SNR is negligible. It can be observed that the relay improves the overall SNR, even if its performance quickly becomes poorer as the destination is moved away from the center. The performance for not aligned VLC systems, such as the setup used in this experiment can be further improved by employing lenses at the receiver.

Analyzing the results it can be seen that, at least for closer distances, the relay by itself can provide communication coverage. This is particularly useful because it allows the relay to act as infrastructure support, in the sense that it can act as the sole VLC access point in a room or part of a room. This is relevant for the deployment of VLC

Figure 44 – SNR versus lateral displaced distance for experimental scheme 4.

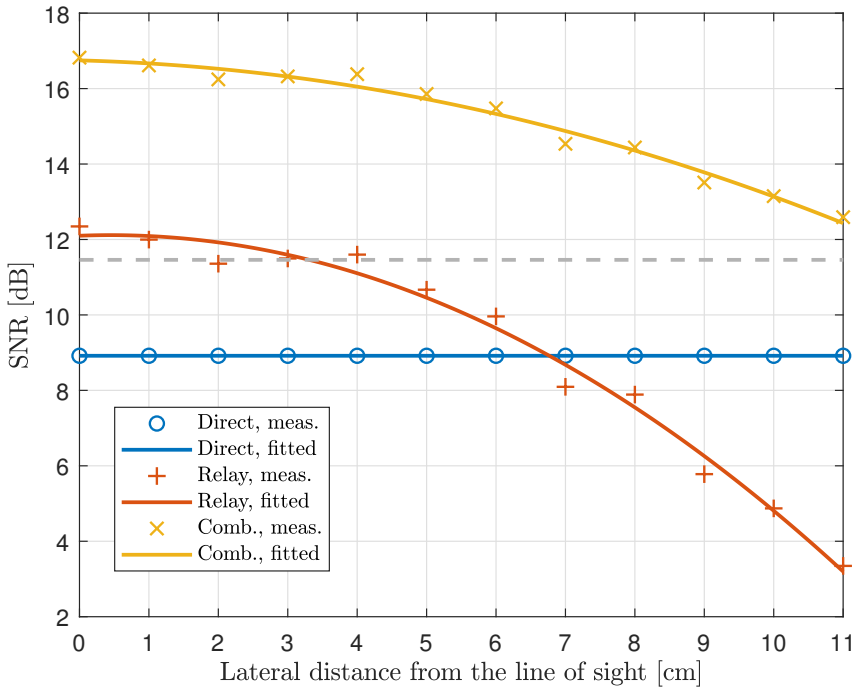

Source: The author.

systems because the VLC coverage may be expanded in an environment without additional backbone infrastructure. Improving the coverage by using relays may be cheaper and easier to install than, for instance, expanding cabling through inner walls or the roof of a house to connect all lamps to the network backbone. In that sense, experiment 2 shows such a scenario in which the transmission distance is limited to the length of the cable's between the relay receiver and the transmitter.

Experiment 3 may be interpreted as a scenario in which the user may control the position of the relay, while the distance between the relay receiver and transmitter is fixed. In a practical scenario, this could be a reading lamp, for instance, which has some flexibility to its height. It can be considered that the relay receiver is at the top of the structure of the reading lamp. Finally, experiment 4 suggests that communication performance quickly deteriorates with angle changes, by shifting the elements off the aligned line-of-sight.

4.3.2 Experimental setup for BER measurements

The experimental setup for BER measurements is slightly modified from that of SNR measurements, employing different equipment. The setup is presented in Figure 45.

In this setup, an OFDM signal (to be described below) is generated in MATLAB and sent to the arbitrary waveform generator (AWG), model Keysight M8195A, which physically generates the signal that is then connected to the AC input of the source bias-T, model ZFBT-4R2GW+ from MiniCircuits (Mini-Circuits, 2018a), with the same model employed at the relay as well. In this setup, a lens is employed at the receiver in order to improve the system performance, model ACL7560-A from Thorlabs (Thorlabs, 2015).

Figure 45 – Block diagram of the cooperative communication VLC experimental setup for BER measurement.

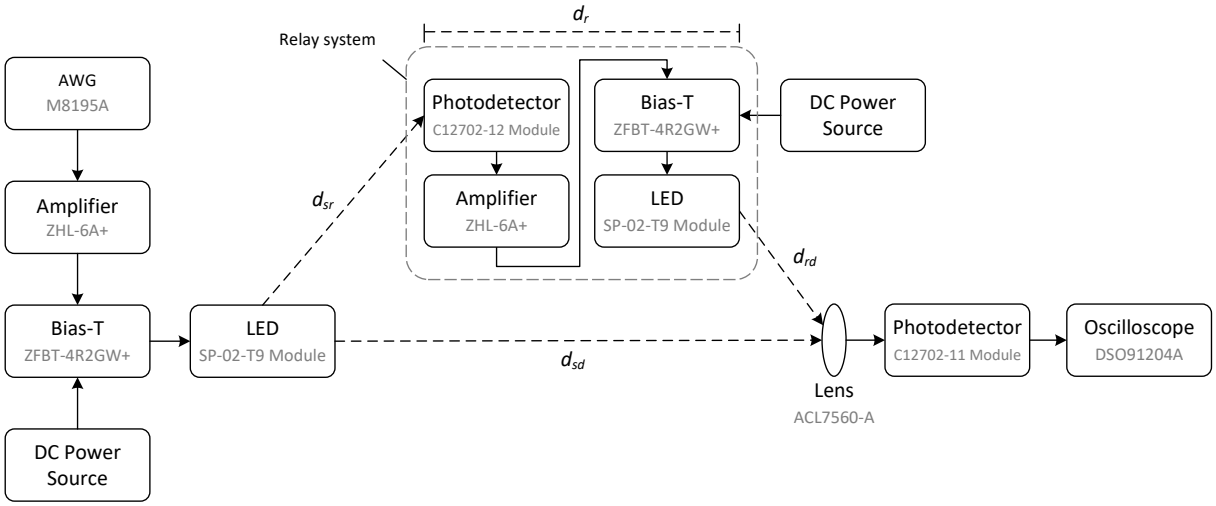

Source: The author.

As the signal generated at the AWG has a low amplitude, an amplifier is employed at the source before the bias-T, as well as in the relay, as in the previous setup. In both cases, amplifier ZHL-6A+ from Mini-Circuits is employed (Mini-Circuits, 2018b), which provides a linear gain of approximately 25 dB.

4.3.2.1 OFDM signal

For the evaluation of the BER of the cooperative VLC system, an OFDM signal is transmitted. OFDM is a multicarrier technique that has been frequently employed in the context of VLC systems (NA *et al.*, 2018; KAZEMI; HAAS, 2020). It is implemented by applying the inverse fast Fourier transform (IFFT) to a block of digitally modulated symbols, such as M-QAM or PSK. The QAM symbols are firstly mapped into different subcarriers in the frequency domain and then converted to time domain by the IFFT operation, resulting in complex-valued samples. However, as VLC systems are based on IM/DD links, the time domain OFDM signal must be real-valued and positive (unipolar). The most common technique is DCO-OFDM, which is the approach adopted in this setup.

To generate real-valued OFDM signals, the input symbols $X(k)$ are constrained to have Hermitian symmetry before being processed by the IFFT block. The real-valued time domain OFDM signal $x(n)$, at the IFFT output at time sample n, for $n = 0, 1, \cdots, N-1$, is given by

$$x(n) = \sqrt{\frac{1}{N}} \sum_{k=0}^{N-1} X(k) e^{j2\pi kn/N} \tag{24}$$

$$X(0) = X(N) = 0 \quad \text{and} \quad X(N-k) = X^*(k) \tag{25}$$

where $k = 0, 1, \cdots, N-1$ is the subcarrier index, N is the size of the IFFT, and $*$ denotes complex conjugation.

The block diagram of the DCO-OFDM transceiver used in the demonstration of the cooperative VLC scheme is shown in Fig. 46. The input data bits are encoded into 16-QAM symbols for data transmission. The training signals, used for the OFDM channel estimation, are generated using BPSK modulation. The resulting signal, after Hermitian symmetry, is processed by the IFFT block to create a real signal. The OFDM signal is generated with 88 data subcarriers, and IFFT size of 256. The number of data subcarriers is limited by the available bandwidth of the VLC link, around 2 MHz, which is ultimately set by the low bandwidth of the off-the-shelf LED source employed in the setup. The first subcarrier ($k = 0$) represents the DC term and no data is modulated on it. The subsequent 12 subcarriers are set to zeros to avoid strong signal-to-signal beating interference (SSBI) due to the square-law photodetector characteristic (CHEN *et al.*, 2015).

Figure 46 – Block diagram of the DCO-OFDM transceiver.

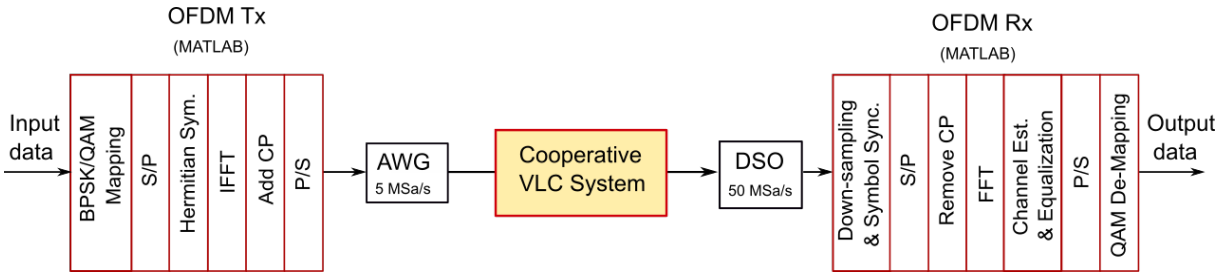

Source: The author.

In this work, an OFDM frame consists of 8 training signals and 200 data symbols. After the IFFT block, a cyclic prefix (CP) with a length of 32 is added and the OFDM signal is parallel-to-serial (P/S) converted and uploaded into AWG, which is configured with a DAC sample rate of 5 MS/s. The total OFDM bandwidth is 1.96 MHz and the

total bit rate (excluding CP) is $4 \times 5\text{M} \times 88/256 = 6.87$ Mbps (raw). Thus, the spectral efficiency is around 3.5 bit/s/Hz. After the AWG, the signal is properly amplified and biased and then transmitted over the VLC link. At the receiver end, after photodetection, the electrical signal is ADC converted by the oscilloscope, with a sample rate of 50 MS/s, and offline processed using MATLAB. Each OFDM sequence transmits 70,400 bits; as 15 sequences are captured to evaluate the BER, a total of 1,056,000 bits are obtained in each measurement. The BER is calculated by comparing these received bits with the generated ones. The code is not optimized to reach higher data rates.

The digital signal processing (DSP) flow at the receiver (see Figure 46) is described as follows. Firstly, the received signal is downsampled at a ratio of 10:1 and a symbol synchronization algorithm is employed to identify the start of each OFDM symbol. Then, after removing the CP, the signal is fed into the FFT block for OFDM demodulation. This is followed by channel estimation and equalization. Finally, the resulting signal is parallel-to-serial converted and QAM decoded for BER analysis.

To obtain the BER of the cooperative link, the waveforms of the received direct and relay OFDM signals are combined by means of software post-processing employing MRC, summing the amplitudes of each signals weighted according to each component's signal quality, considering a higher weight to the signal with a better SNR (GOLDSMITH, 2005), in order to achieve better BER.

4.3.2.2 Experimental configurations and results for BER measurements

For BER measurements, three configurations were employed, similar to configurations 1 to 3 for SNR measurements, but with different distances. These values are summarized in Table 9.

Table 9 – Distance between elements for the BER measurements. Values in centimeters.

Exp.	d_{sd}	d_{sr}	d_r	d_{rd}
1	$80 + d_{rd}$	40	40	20 to 100
2	120	10 to 50	$(50 - d_{sr}) + 30$	40
3	120	10 to 50	30	$(50 - d_{sr}) + 80$

In this Section, the diagram for each configuration will be presented, followed by the plot presenting BER results for direct, relay and combined links. In addition, at the end of the Section three constellation diagrams for each received OFDM signal, for each

configuration, will be presented.

The diagram for BER configuration 1 is presented in Figure 47, followed by BER plot in Figure 48. As with SNR results, the markers indicates the measured data, while fitted curves are provided for convenience.

Figure 47 – VLC cooperative communication experimental scheme for BER 1: varying distance of destination.

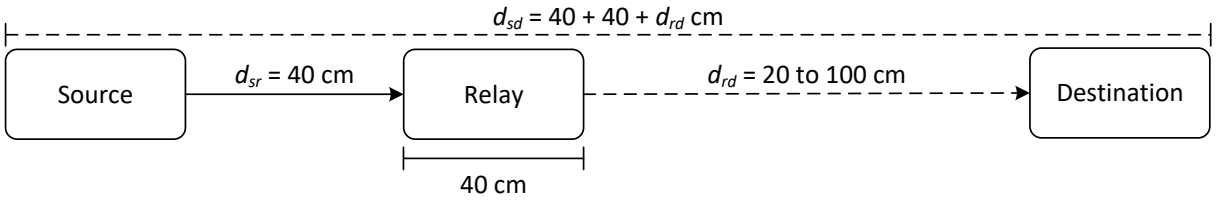

Source: The author.

Figure 48 – BER versus distance displaced distance for experimental scheme 1.

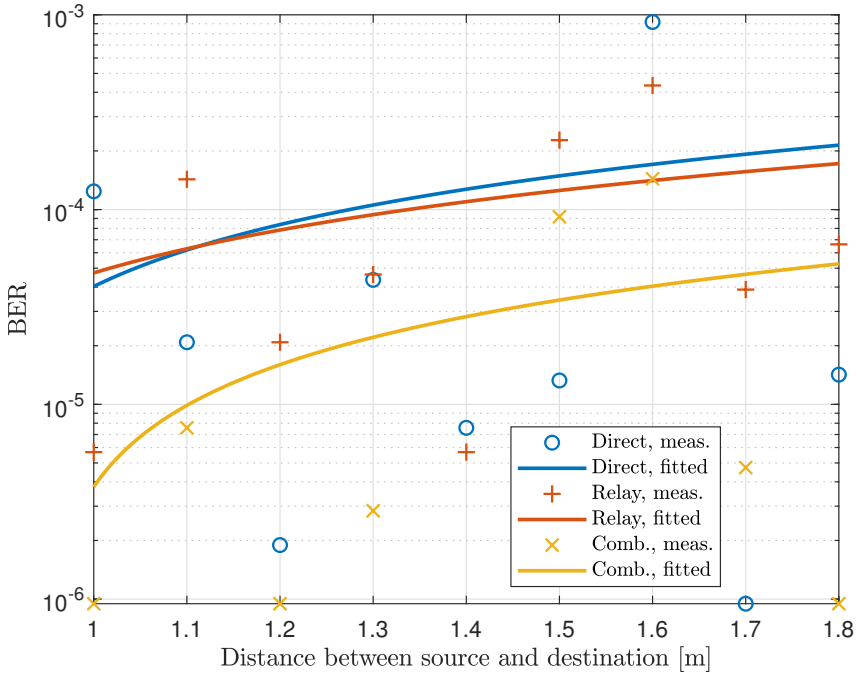

Source: The author.

With configuration 1, the fitted curves point out to an almost linear behavior of BER, showing a linear decrease in the performance as the distance increases. The combined curve, which represents the performance of the cooperative VLC link, follows similar pattern as the direct link curve, but achieving a lower BER. In practice, this improved BER can provide higher data rates, large maximum link distances or a more robust system overall. For configuration 1, the BER varies from 7.0×10^{-5} to 2.2×10^{-4} and from 6.5×10^{-6} to around 5.3×10^{-5} for the direct and the combined curves,

respectively, when the distance between source and destination increases from 1 to 1.8 m. This indicates that a BER improvement of at least one order of magnitude is observed when employing cooperation, in contrast with the direct link.

Next, the diagram for BER configuration 2 is presented in Figure 49, followed by BER plot in Figure 50.

Figure 49 – VLC cooperative communication experimental scheme for BER 2: varying position of the relay reception.

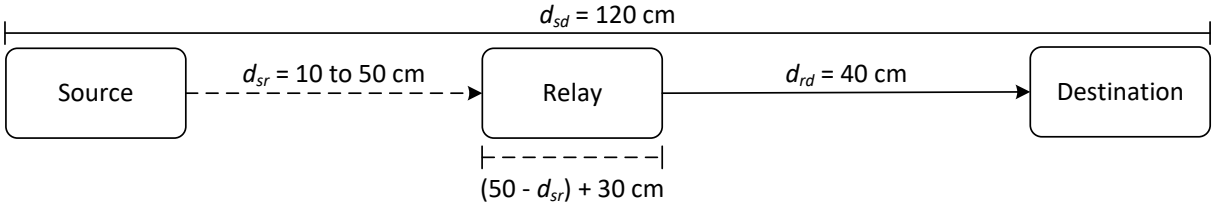

Source: The author.

Figure 50 – BER versus distance displaced distance for experimental scheme 1.

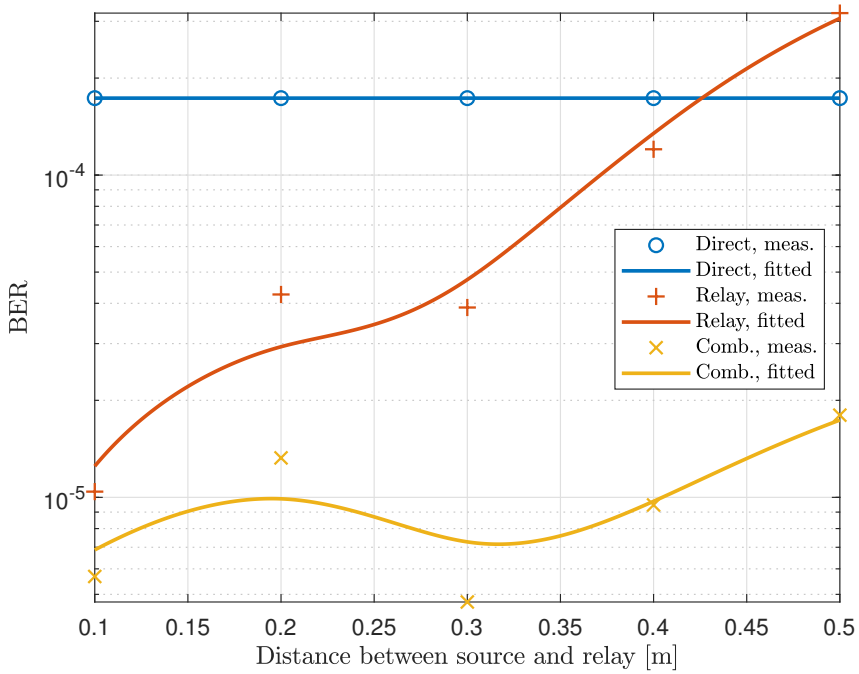

Source: The author.

In this case, for distances between source and relay up to 0.4 m, the measured BER of the relay link is better than that of the direct link. As with SNR, this indicates a case in which the relay may solely act as the VLC access point for a given area, under the condition that the receiver of the relay is close to the source (and considering that the relay is not a single device). As with configuration 1, for most of the measured results, BER improvements of more than one order of magnitude are achieved with the proposed

cooperative approach in comparison with the direct link case. The BER for the direct path is constant at 1.7×10^{-4}, while the combined BER values were in the range of the 10^{-5} mark.

Lastly, the diagram for BER configuration 3 is presented in Figure 51, followed by BER plot in Figure 52. In this scenario, the relay always presents a worse performance than the case for the direct link. As for the relay position, there is a trade-off between received power (better closer to the source) and path loss (better closer to the destination) that must be considered. In any case, however, when combining both received source and relay OFDM signals, the system performance improves. While the BER for the direct link is constant at 1.7×10^{-4} as in the previous scenario, the combined BER result ranges between 1.4×10^{-5} and 6.7×10^{-5}.

Figure 51 – VLC cooperative communication experimental scheme for BER 3: varying position of the relay reception and transmission.

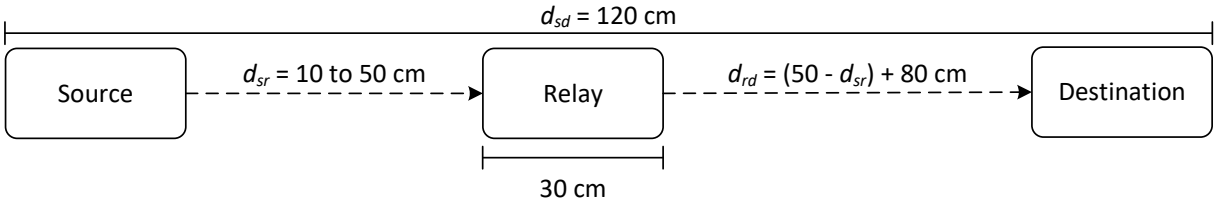

Source: The author.

Figure 52 – BER versus distance displaced distance for experimental scheme 1.

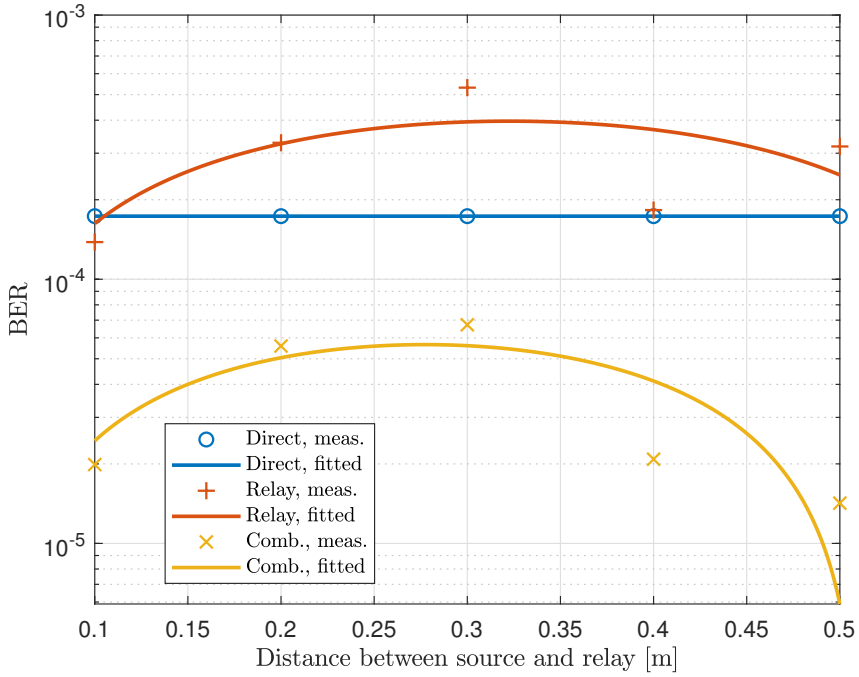

Source: The author.

Finally, constellation diagrams are presented in Figure 53. These plots refers to the maximum measured distance for each configuration. For instance, for the distance of $d_{sd} = 1.8$ m for configuration 1.

In these plots, we can observe the difference that the BER results have on the quality of the constellations. For instance, as presented in Fig. 48, the relay transmission has the poorest BER of the three links, which corresponds to its constellation, where symbols are spread over a larger area and closer to its neighbors. In the same sense, Fig.53c shows the combined transmission, which has the clearest constellation of the three, with the direct transmission showing a performance between these cases, but closer to the combined link than to the relay, as we expect from the analysis of the BER curves.

4.3.2.3 Frequency response and delay analysis

In order to obtain a clearer perception of the experimental VLC link, the frequency response of the link for both APD modules is measured, as well as the measurement of the delay time of the direct and relay links. A deeper analysis of the employed luminaire is reported in Oliveira *et al.* (2022).

The frequency responses for the LOS link between the LED and each APD module are presented in Figure 54. The frequency responses were obtained from 0.2 to 3 MHz, employing a sine wave from a function generator. This interval includes the frequency range of the OFDM signal employed in the BER measurements, from 0.24 to 1.96 MHz, which is highlighted at the plot. A decrease of 2.86 dB in power occurs between the lower and higher OFDM subcarriers. From the APDs datasheet (Hamamatsu Photonics, 2017), it can be seen that the frequency responses of the two APDs are relatively flat within the OFDM bandwidth. Thus, the measured power decrease is due to the uneven frequency response of the LED. Furthermore, the bandwidth of each OFDM subcarrier of the employed signal is around 19.5 kHz, which implies that the power fading within each subcarrier is much smaller than 2.86 dB, facilitating the equalization process.

As previously mentioned, the measurements of the direct and relay links happened separately and with the combination taking place offline, due to the delay that occurs at the relay link, causing the signal to reach the APD late. In practice, this meant that the performance were not as optimal as it can be for a cooperation system. In order to quantify this delay, the delay of each link is measured, in response to a step signal. Figure 55 presents the oscilloscope's screen capture of the delay analysis for both links,

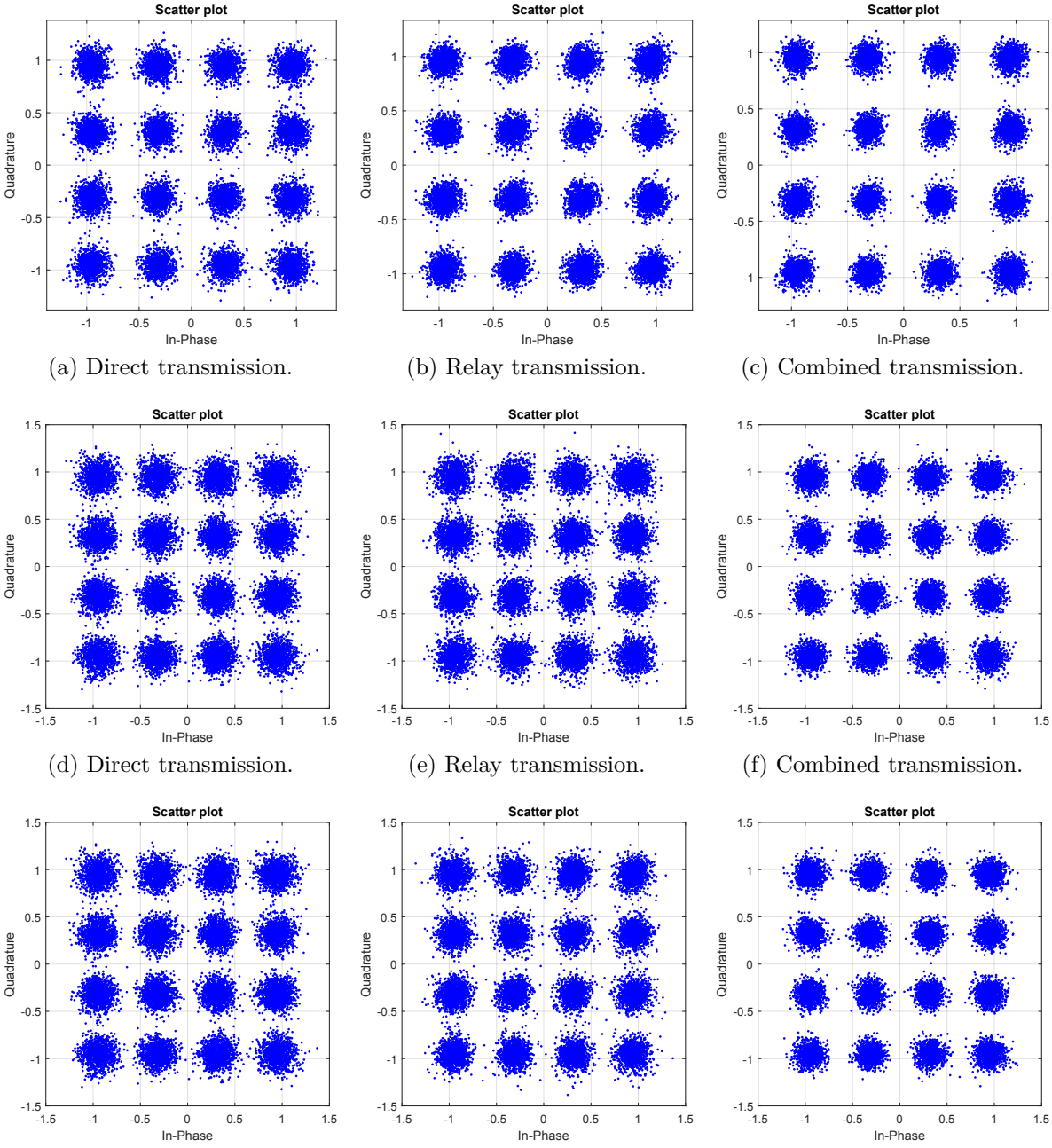

(a) Direct transmission. (b) Relay transmission. (c) Combined transmission.

(d) Direct transmission. (e) Relay transmission. (f) Combined transmission.

(g) Direct transmission. (h) Relay transmission. (i) Combined transmission.

Figure 53 – Constellations for received OFDM 16-QAM signals for direct, relay and combined links, respectively, for (a), (b) and (c): configuration 1; (d), (e) and (f): configuration 2; (g), (h) and (i): configuration 3;.

Figure 54 – Frequency response of the VLC BER setup. Shadowed area refers to the frequency of the employed OFDM signal.

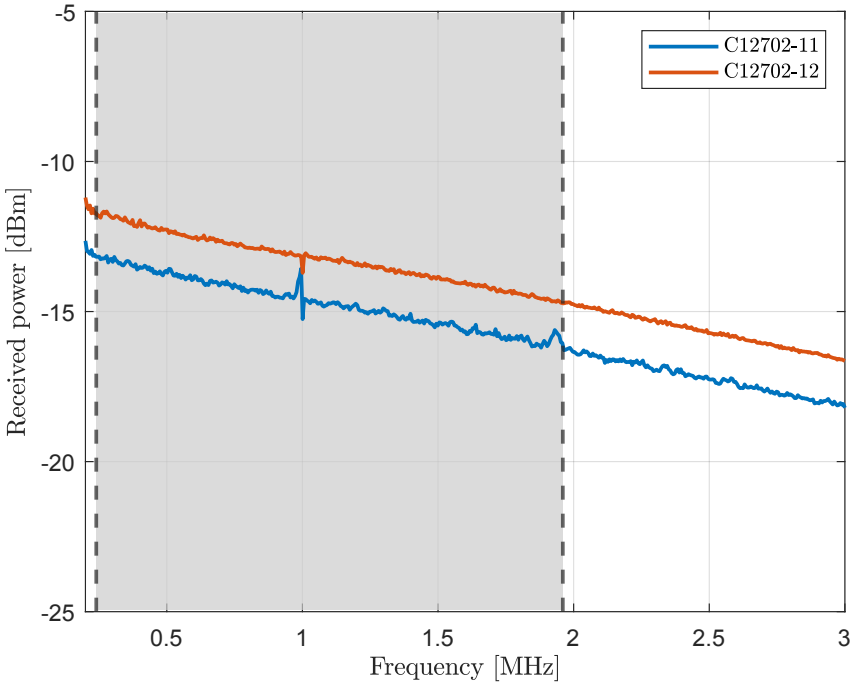

Source: The author.

including additional annotations of the time delays for better visualization.

For the measurement, the same setup from Figure 45 is employed, with the following distances: $d_{sd} = 1$ m, $d_{sr} = 0.4$ m and $d_{rd} = 0.2$ m. The measured time delays are around 30 ns and 63 ns for the direct and relay paths, respectively, thus resulting in a delay spread of around 33 ns due to the addition of the relay path. These values are useful for reference, though small variations are expected if different distances are employed.

(a) Direct transmission. (b) Relay transmission.

Figure 55 – Delay analysis for (a) direct and (b) relay links. Yellow curve refers to reference back-to-back signal and green line refers to VLC link.

4.4 CHAPTER CONCLUSIONS

The simulation model presented in Chapter 3 is also employed to evaluate the application of amplify-and-forward cooperative communication in VLC, with results showing that it improves the received BER and allow communication in areas in which the direct SNR is very low.

From all experiments, results demonstrate that VLC relaying and cooperative communication contribute to the communication performance of VLC systems, by increasing SNR by an amount varying from 4 to 8 dB at the destination and improving BER by at least one order of magnitude, across all configurations. In all cases, combining relay and source links significantly improves the resulting communication performance. Though most observed results are not as high as ideally expected from Equation (23), the combined SNR and BER provides more reliable communication. In the more extreme example, at the larger distances in Figure 48, both relay and source SNRs are relatively low, while the combined SNR still performs higher than the relay or source-only SNRs, at any distance. This is an example of a scenario in which only with the employment of both source and relay the communication becomes feasible.

As presented in this chapter, signal amplification is needed in order to deploy AF cooperative systems. To further analyze this matter, the next chapter addresses optical signal amplification, comparing the electrical and optical approaches.

5 AMPLIFICATION IN VLC

In this chapter, means are explored to perform visible light amplification. Amplification is not useful just for relaying, but also to increase link distance. For instance, scenarios such as those existing in large plants, exhibition halls, museums, shopping malls, airports, subway and train stations or even outdoor environments, such as public squares or streets, may require the optical signal to travel long distances and amplification may be necessary to overcome the strong attenuation in the optical path.

However, in using amplification there is the challenge of finding a suitable technique or means to boost signal power. The more conventional method is the amplification in the electrical domain, in which optoelectronic conversion is required. This method goes back to the early days of optical communication systems, when optoelectric and electrooptic conversion circuits were employed halfway between optical emitter and receiver.

Alternatively, to circumvent the need for optical-electrical conversion, an optical amplifier may be employed. Recent developments towards an optical amplifier in the visible spectrum have been reported (BASTOS *et al.*, 2018, 2020). In this chapter, from performance values reported in these works, theoretical analysis and comparisons are described.

These two methods are discussed based on theoretical simulations to compare their performances. For the simulation of both methods, refer to Figure 56. It is considered a VLC system with aligned, LoS transmitter and receiver with n amplifiers in between.

Figure 56 – Block diagram of VLC system with amplifiers.

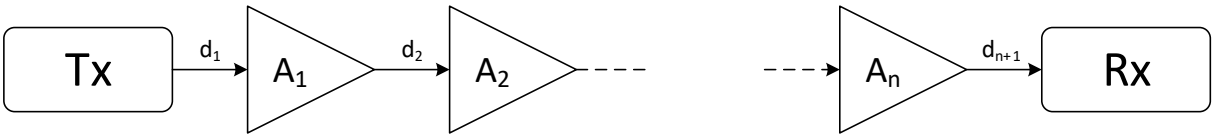

Source: The author.

From the analysis of Equation (5), the VLC path loss can be divided into two components: one fixed value for each transmission, regardless of the traveled distance, and one that varies as the light ray travels further in free space. This separation is useful for the optical amplification analysis and to compare it with electrical amplification. For

convenience, these values are separated and named H_{fix} and H_{var} as follows:

$$H_{fix} = \frac{A(m+1)}{2\pi} cos^{m}(\varphi) T_s(\theta) g(\theta) \cos(\theta), \tag{26}$$

$$H_{var} = \frac{1}{d^2}, \tag{27}$$

and

$$H(0) = H_{var} \times H_{fix}. \tag{28}$$

Remembering that A is the photodetector's area, m is the Lambertian order of the LED, φ is the emission angle, $T_s(\theta)$ is the gain of the optical filter, $g(\theta)$ is the gain of the concentrator and d is the distance between source and destination.

A setup with aligned components (transmitter, amplifiers and receiver) is considered, as in Figure 56. Therefore, $\varphi = \theta = 0°$. To illustrate these parameters, Figure 57 shows the path loss values H_{fix} and H_{var} for a transmission without amplification in a 1.5 m distance between transmitter and receiver, not including any filter or concentrator ($T_s(\theta)$ and $g(\theta)$ equals 1). This distance is considered in the remaining of this Chapter.

Figure 57 – H_{fix} and H_{var} for transmission without amplification.

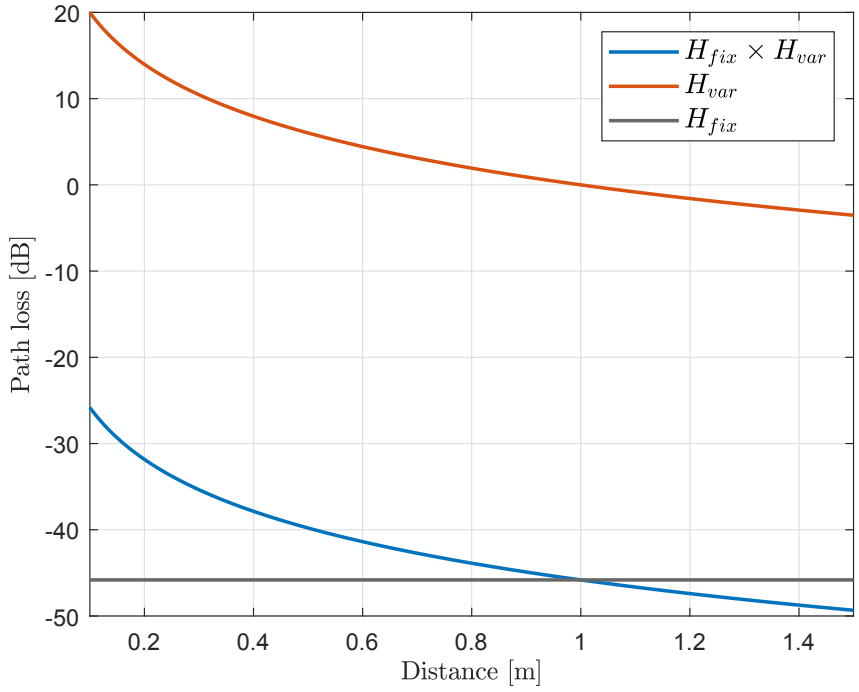

Source: The author.

For a numeric perspective, in the above examples, the

For a performance evaluation, SNR values are given for each scenario, with and without amplification, at the end of the measured distance (1.5 m). A reference transmission power P_t of 10 W is considered and the same values and parameters presented in Chapter 3. From now on, plots are presented only for the combined ($H_{fix} \times H_{var}$) path loss. The nomenclatures G_{el} and G_{op} refer to the gain values of electrical and optical amplification, respectively.

5.1 ELECTRICAL AMPLIFICATION

The well known and conventional solution to improve VLC signal strength is amplification in the electrical domain, which requires optoelectronic conversion.

An advantage of amplifying VLC signals (in comparison with other typical RF signals) is that they are typically in the order of relatively low frequencies, such as 1 to 10 MHz, in which case it is easier to amplify electrical signals without complex electronics to make up for high-frequency effects. However, any electronic treatment of the signal adds a delay to the whole system. Therefore, in practice, amplified signals from the relay reach the receiver with a delay, as discussed in Section 4.3.1. The noise model for electrical amplification is the one presented in Equation (12) in Section 2.1.4 (KOMINE; NAKAGAWA, 2004), considering thermal, shot and ISI noises.

The main limitation of electrical amplification is that each amplification process implies a "new" transmission. In mathematical terms, this means that H_{fix} (Equation (26)) is considered each time a transmission occurs, *i.e.*, each time an amplifier is employed. Therefore, the electrical amplifier gain needs not only to compensate the path loss, but also compensate this fixed loss value. To illustrate this, for a transmission considering the previously used parameters ($A = 1$ cm^2, $\varphi_{1/2} = 70°$) in Equation (26), the value for H_{fix} is in the order of 10^{-5}.

Even though each luminaire needs to be supplied with its own DC power to light it up, when concerning communication, the AC (modulated) amplitude is what is considered. That means that arbitrarily increasing the DC power won't improve the modulated signal; if any, an inadequate DC level may actually deteriorate the modulated signal, due to saturation in the LED or in the photodetector.

In Figure 58, a comparison of path losses for different gain values is presented. From the values of G_{el} it is possible to observe that relatively high gain values are necessary just to compensate the path losses. The SNR value for the direct transmission is -4.03

dB and for the three presented gain values the SNRs are −3.29, 4.70 and 12.70 dB, considering parameters from Tables 4 and 5.

Figure 58 – Path loss for different values of gains in electrical amplification with A_1 at 0.4 m and A_2 at 1.1 m.

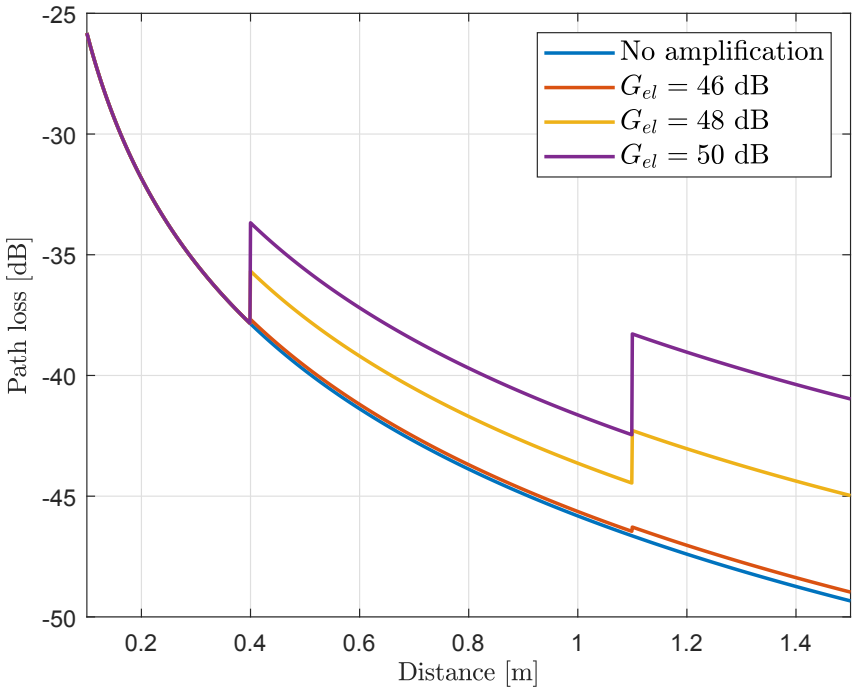

Source: The author.

These curves shows how electrical amplification requires high gain values for relaying or extending transmission distance. For an experimental comparison, the actual experimental setup, presented in Section 4.3, has an actual gain of (at least) 30 + 26 = 56 dB at the signal which is used to drive the relay, considering the gains from the photodetector module and the amplifier (not considering losses from cabling, connectors, etc).

5.2 OPTICAL AMPLIFICATION

Recently, an optical amplifier suitable for operation in the visible light spectrum has been developed (BASTOS *et al.*, 2018, 2020). It has potential do replace electrical amplification and boost the path extension in VLC links and also work as a relay node. The amplifier is a cylindrical flexible fiber with 1.5 cm ± 0.5 mm diameter and 3.5 cm ± 0.5 mm length. The material is a synthesized poly(fluorene)-based lumophore doped within a di-ureasil organic-inorganic hybrid (BASTOS *et al.*, 2020).

Optical amplification has some inherent advantages. Optical amplification is agnostic to bit rate and modulation format. The synthesized fiber is also flexible, enabling easy manipulation of the direction that the amplifier captures or redirects the light.

However, there are some limitations. As it is still an emerging technology, optical amplification in VLC is still limited to research laboratories and has a high cost. Also, in order to amplify light, the fiber requires some kind of excitation, such as by UV light, which may not be convenient for easy deployment in real scenarios (BASTOS *et al.*, 2018, 2020).

As for the noise model of optical amplification, it is necessary to account for the signal-ASE (amplified spontaneous emission) and ASE-ASE beating terms (AGRAWAL, 2010). The current noise induced from the ASE is originated in the beating of the signal field with the optical field and from the beating of the optical field with itself (AGRAWAL, 2010). Considering that the ASE-ASE beating is at least one order of magnitude smaller than the signal-ASE beating, that term can also be neglected. In this way, the total noise $\sigma^2_{total-optical}$ is given by

$$\sigma^2_{total-optical} = \sigma^2_{total-electric} + \sigma^2_{sig-ASE}, \tag{29}$$

where $\sigma^2_{total-electric}$ corresponds to Equation (12). In other words, the total noise when the optical amplifier is employed includes the ISI noise, the thermal and shot noises also present in the electrical amplification, plus the contribution of the signal-ASE beating from the amplifier.

The signal-ASE beating noise is given by (AGRAWAL, 2010)

$$\sigma^2_{sig-ASE} = \frac{2(q\eta_q G_{op})^2 P_r B}{h\nu}, \tag{30}$$

where q is the elementary charge, P_r is the received optical power, B is the noise equivalent bandwidth (or data rate), h is the Planck's constant, ν is the wave's frequency, G_{op} is the gain of the optical amplifier and η_q is the quantum efficiency. The value of η_q may be obtained from (AGRAWAL, 2010)

$$\eta_q = \frac{\gamma \times 1.24}{\lambda}, \tag{31}$$

where λ is the wavelength, given in microns. The values adopted in the simulations are $h = 6.626 \times 10^{-34}$ J·s, $\nu = 6.66 \times 10^{14}$ Hz, $\gamma = 0.54$ A/W and $\lambda = 450 \times 10^{-3}$ µm. From Equation (31) it is obtained $\eta_q = 1.488$.

Figure 59 shows the behavior of the noise mechanisms as a function of the data rate, as in Figure 12, but now including the signal-ASE beating noise from the optical amplifier. It can be inferred from the plot that the ISI noise remains the dominant noise source up to near 10 Gbps.

Figure 59 – Noise parameters as function of the data rate.

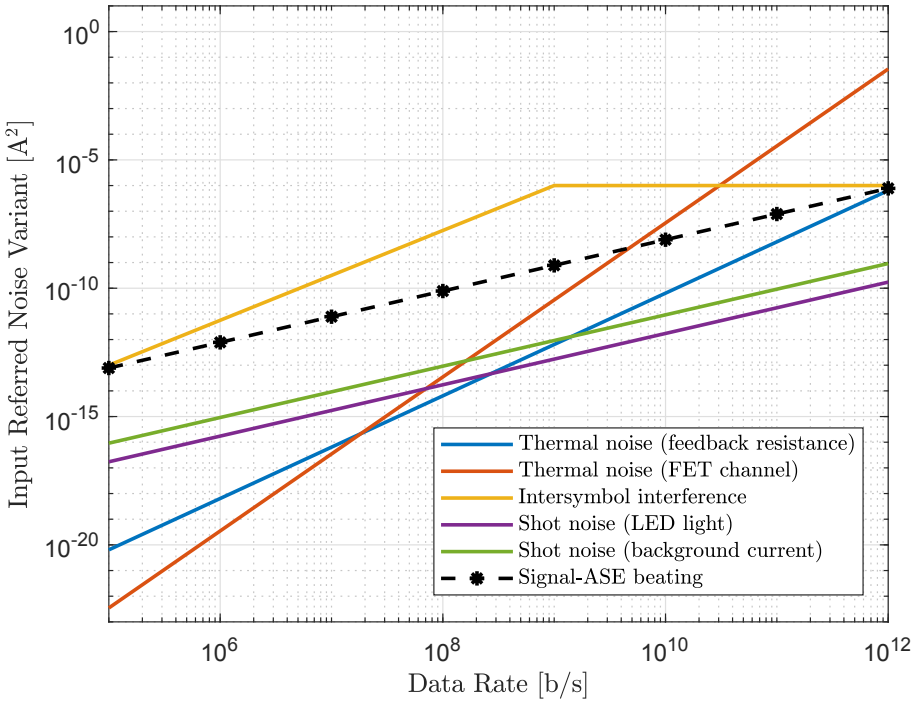

Source: The author, based on Komine and Nakagawa (2004).

As for experimental VLC optical amplification, Bastos *et al.* (2020) demonstrate a poly(fluorene)-based flexible fiber with a 5.9 ± 0.2 dB gain as a pre-amplifier and a 3.7 ± 0.2 dB gain as a relay node. Given the described simulation scenario, considering the amplification in the path between transmitter and receiver and the cooperative communication applications, it is considered the 3.7 dB gain value for the amplifiers.

The first simulation example uses the same distance as the previous, with one amplifier (A_1) positioned in the middle of the path (0.75 m). The resulting curves are presented in Figure 60. In this scenario, the SNR at the receiver without amplification is −4.03 dB and with the amplifier is 3.37 dB (both without considering lenses or other means to improve the received signal).

For the next two examples, the 1.5 m distance is maintained, but now two amplifiers are used: at 0.75 m and 1.25 m (Figure 61) and at 0.5 m and 1.1 m (Figure 62). The SNR in both cases is 10.77 dB.

Figure 60 – Path loss versus distance for A_1 at $d = 0.75$ m considering optical amplification.

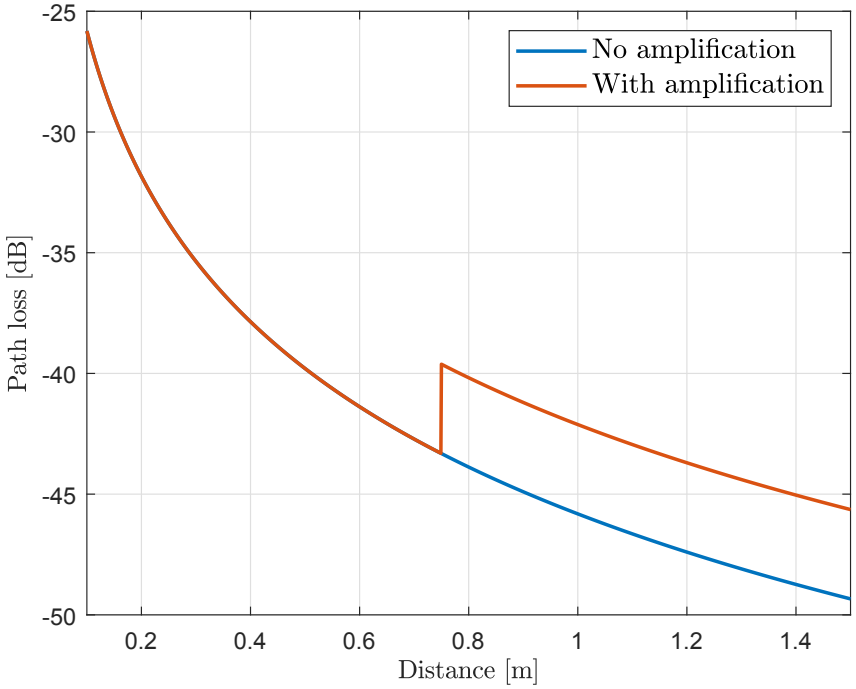

Source: The author.

5.3 COMPARISON

Lastly, a comparison of electrical and optical amplifications is presented. The main theoretical difference in performance between electrical and optical relaying is that, in optical relaying, H_{fix} is only calculated once. As seen in Figure 57, the fixed value is responsible for the majority of the path loss. Figure 63 presents a comparison of electrical and optical relaying in the same plot, with amplifiers in the same position as in Figure 62.

Electrical amplification needs orders of magnitude higher values of gain to achieve the same results as optical amplification. To achieve a similar performance considering the gain of 3.7 dB of the optical amplifier, the electrical amplification needs to be set to 50 dB, resulting in SNRs of 10.76 dB for optical and 12.70 for electrical amplification. This is due to the H_{fix} component of the transmission, as expressed in Equation (26) and illustrated in Figure 57, which only affects the electrical amplification at every retransmission and, therefore, needs to compensate for all this loss.

Figure 61 – Path loss versus distance for A_1 at $d = 0.75$ m and A_2 at $d = 1.25$ m considering optical amplification.

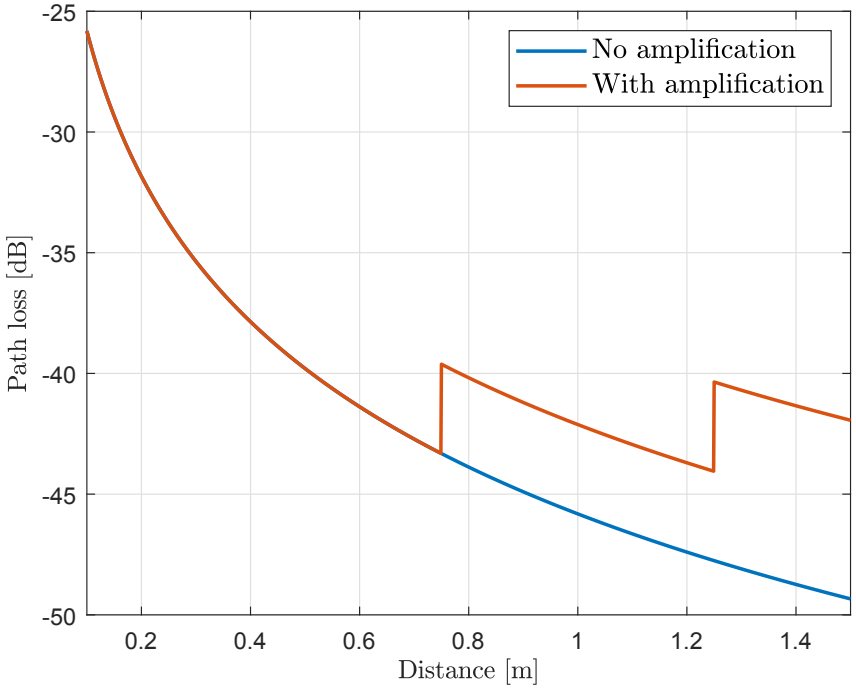

Source: The author.

5.4 CHAPTER CONCLUSIONS

Due to high path loss of visible light in free space, amplification is a fundamental aspect in amplify-and-forward cooperative VLC and also for hop-on-hop relaying communication. In this Chapter the traditional method of electrical amplification is analyzed and the novel optical amplifier for visible light is evaluated. The effects of path loss and the application of amplifiers were simulated. From mid- to high-range distances, this attenuation is so high that a amplification at the receiver is usually needed to demodulate the received signal, even if there is no intention of using cooperation.

Advantages, disadvantages and the performance of the optical amplification for visible light are presented. Although it is a new, experimental technology, further research is encouraged for optical amplification. Due to the nature of each technology, optical amplifiers with gain in the order of 3.7 dB are comparable with electrical amplification in the order of 50 dB, without the need of opto-electrical conversions. The performance results, as well as other practical advantages, suggests that it has potential to support the development and deployment of VLC systems in the future.

Figure 62 – Path loss versus distance for A_1 at $d = 0.5$ m and A_2 at $d = 1.1$ m considering optical amplification.

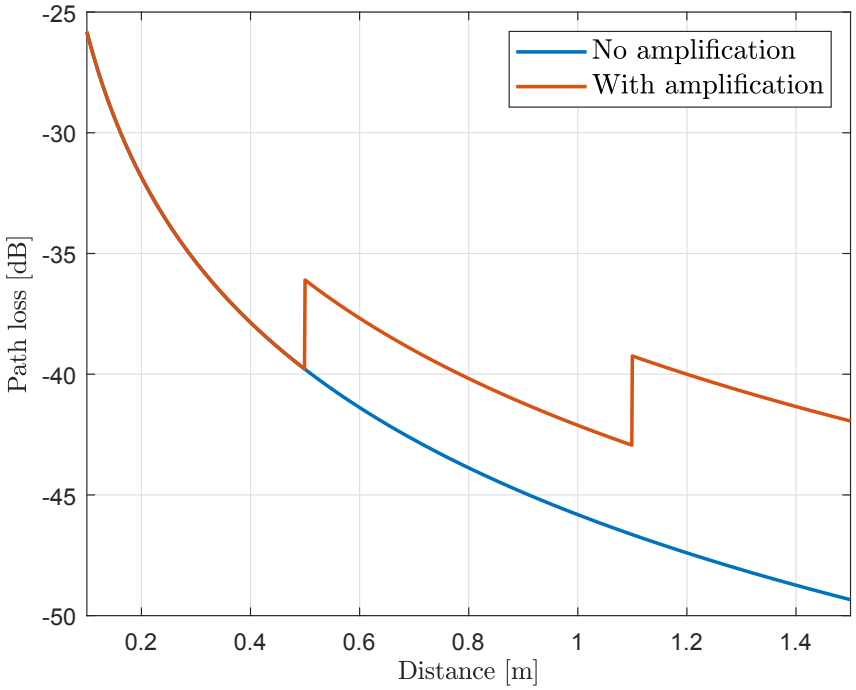

Source: The author.

Figure 63 – Path loss performance comparing optical and electrical amplification.

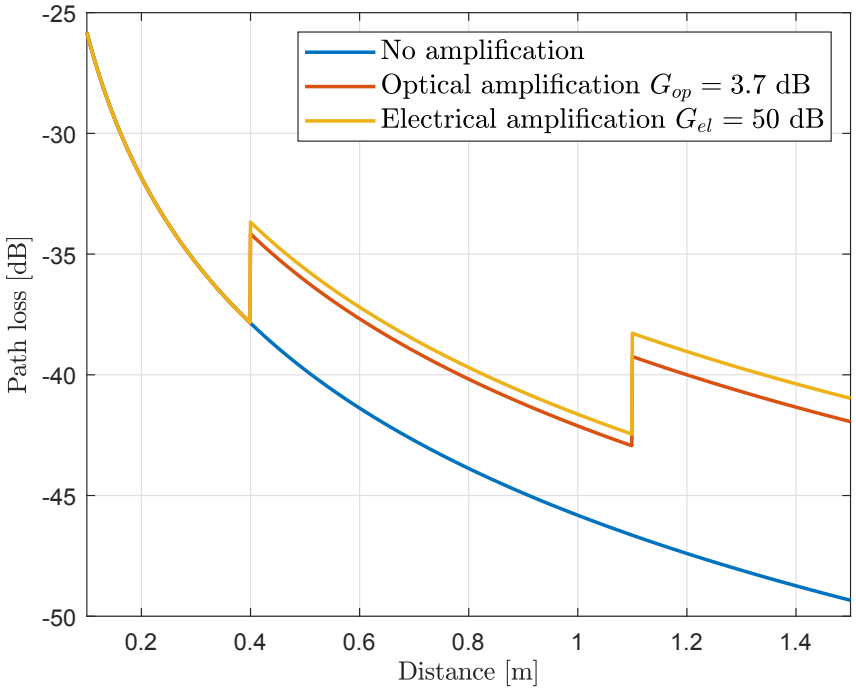

Source: The author.

6 4G AND 5G APPLIED TO VLC

The world has seen an urge for data traffic in the last years. Mobile data is estimated to increase sevenfold between 2017 and 2022 (CISCO, 2019). Also, it is estimated that around 80% of wireless data consumption happens indoors (FENG *et al.*, 2016). To supply this demand, mobile operators face the challenge of providing reliable and fast cellular connections, in more dense areas, specially with the advent of the Internet of Things, in which many more devices are expected to be connected. Hence, in this scenario, VLC is a suitable technology to support the deployment of cellular networks, such as LTE, 5G and beyond (HAAS *et al.*, 2016).

Since the third generation of mobile technology (3G), the dissemination of connected devices such as smartphones and tablets has quickly grown. The main source of traffic switched from voice calls to data transmission, which increased exponentially (ERICSSON, 2017).

To supply this demand, researchers worked on more robust technologies. The 3rd Generation Partnership Project (3GPP) developed the LTE (Long-Term Evolution) standard, which is colloquially referenced as 4G (fourth generation), although these terms are not technically synonyms. LTE proved to be the best candidate to succeed 3G networks (LOUÇÃO, 2013) and nowadays is a well established technology, with some countries providing over 90% signal availability and average data rates higher than 20 Mbps in most countries (OPENSIGNAL, 2018). This speed is limited due to factors such as user congestion, network density and the width of the spectrum devoted to LTE.

The 4G LTE standard has a flexible spectrum size, where the signal bandwidth for downlink or uplink may assume the sizes of 1.4, 3, 5, 10, 15 or 20 MHz; the higher the bandwidth, the higher the channel capacity. LTE uses OFDM as its basic waveform, modified as OFDMA (Orthogonal frequency division multiple access) in the downlink and SC-FDMA (Single channel orthogonal frequency division multiple access) in the uplink (ETSI, 2015). OFDM is a natural choice for LTE given that it offers robustness to interference, it is suitable for high data rates and has the capability of customization for LTE's specific requirements. Within the OFDM signal, possible modulations are QPSK (equivalent to 4QAM), 16QAM and 64QAM. The specific format chosen to a given transmission depends on factors such as SNR and bandwidth.

Architectures and models for LTE systems combined with VLC have been

proposed in the literature. Liang *et al.* (2016) propose a hybrid VLC-LTE (RF) system, focusing in evaluating handover algorithms. In this proposal, the objective is to take advantage of each technologies' features. It does not consider the transmission of LTE signals through VLC channel; rather, it is a system that employs a VLC (not specified) signal when there is a LOS link available and swaps for LTE when there is not. LTE signals would be received from the base station, while LTE would use another method to connect to the network's backbone. Results indicate that a vertical handover algorithm through prediction is the most suited for this transition.

Wu *et al.* (2017) propose the incorporation of VLC in vehicular communications to improve LTE-V2V systems. The concern of this technique is the interference between cellular links and the LTE-V2V links and, therefore, VLC is suggested as a method to support the V2V communication, taking advantage of the non-interference feature of VLC. However, as light is blocked by opaque structures, VLC-V2V is only thought as a complementary method to LTE-V2V. Simulation results show that the system supported by VLC significantly improves the performance, especially in dense areas.

As the VLC signal power sharply drops as distances grow and is subject to blocking, Hui Tian *et al.* (2015) propose a heterogeneous network model of a hybrid VLC-LTE system. To define which access technology the user equipment uses, the proposed model estimates the condition of each channel in the network via a water-filling algorithm to allocate power and uses the extremal method to allocate frequency. Comparing to uniform power allocation, throughput is improved in average by 59.23%, according to author's results.

Considering works such as the mentioned and the already comprehensive coverage and availability of 4G worldwide, there is an encouragement for the study of VLC applied in the LTE context, despite its successor, 5G, being on the horizon. Also, 5G is built reusing features and structures of LTE (COUTINHO, 2019), so know-how may be transferred.

While 3G introduced mobile broadband and 4G expanded the data rate, 5G is expected to unlock a true networked society not just to even higher data rates, but also because of scalability, connectivity and energy efficiency (MITRA; AGRAWAL, 2015). 5G is being deployed with the 5G NR (New Radio) access technology as the global standard air interface. 5G NR is capable of providing higher data rates (up to 20 Gbps), a massive number of connected devices (up to 1 million devices per km^2), low latency (1 ms maximum), among other features (COUTINHO, 2019). The 5G NR standard is also

developed by the 3GPP. By 2025, it is expected that 20% of global mobile communications will be carried over 5G networks (GSMA Intelligence, 2020).

Given the global mobile data traffic scenario and the advent of 5G, there is a strong need of resources to supply this demand. Millimeter waves (mmWaves), with frequencies between 3 and 300 GHz, have been given attention as one possible solution. Although providing higher data rates and smaller latencies, they show a limited penetration through walls and obstacles and a smaller coverage area per base station, contributing to a relatively slow deployment of 5G signal coverage. In this regard, VLC may contribute to extend the coverage in indoor environments.

As with LTE, works in the literature have considered 5G systems in a VLC context. VLC has features that addresses requirements of 5G. For instance, optical systems are suitable for low latency communication (CHOWDHURY *et al.*, 2019). Another key aspect for enabling 5G is massive MIMO (KATTI; PRINCE, 2019). For instance, Mitra and Bhatia (2018) proposed a precoding technique that induces diverse effective channel matrices for different users, resulting in interference cancellation for multiple users. Also in this regard, Xu *et al.* (2016) proposed a scheme for massive MIMO in VLC which consists of a channel adapted spatial modulation, that provides higher spectral efficiency than optical multi-stream spatial modulation, given that the channel state information is known at the receiver.

Feng *et al.* (2016) propose a heterogeneous multi-layer 5G architecture considering the sub-3 GHz spectrum, the mmWave spectrum and a VLC layer. Each layer is intended to cover a specific scenario, as, for instance, by which layers the user is covered at a given moment. Their simulation results show that the hybrid model has a better performance at distances up to 4 m, typical of indoor environments. Cosmas *et al.* (2018) propose a flexible 5G Internet Radio-Light architecture composed of four layers (Service, Access, Network Function Virtualisation and Software Defined Network), in a manner that it is simple to install, enabling quick deployment of 5G in indoor environments. Ulgen *et al.* (2018) proposes a hybrid access point that in ideal conditions uses VLC for downlink and mmWave for uplink, otherwise mmWave for both. The system continuously monitors the status of the two networks to decide which channel must me chosen. As these works suggest, VLC has potential to complement RF waves to distribute 5G NR technology and unlock its full potential.

Like LTE, 5G NR waveform is also based on OFDM, but in this case the same waveform is used in both downlink and uplink, a feature that simplifies the overall design.

For 5G NR, 3GPP selected cyclic prefix OFDM (CP-OFDM) waveform. Supported modulation formats are QPSK, 16QAM, 64QAM and 256 QAM. Channel bandwidths start from 5 MHz in frequency range 1 (FR1) up to 400 MHz in frequency range 2 (FR2) (ZAID *et al.*, 2018).

In this Chapter, experimental 4G and 5G transmissions over a VLC channel are described and results provided.

6.1 EXPERIMENTAL SETUP

In these experiments, the focus is on the receiver end of the cellular transmission, *i.e.*, the signal that reaches the UE, such as a mobile phone, from an indoor optical attocell (HAAS *et al.*, 2016) or access point, for instance. In this way, a distribution architecture must be adopted as backhaul for the optical cell, such as radio-over-fiber, coaxial cables, power over Ethernet or power line communication (COSSU *et al.*, 2016; FENG *et al.*, 2016; LIANG *et al.*, 2016).

The experimental setup employed to transmit signals in both technologies is presented in Figure 64.

Figure 64 – Block diagram of the experimental 4G and 5G setups.

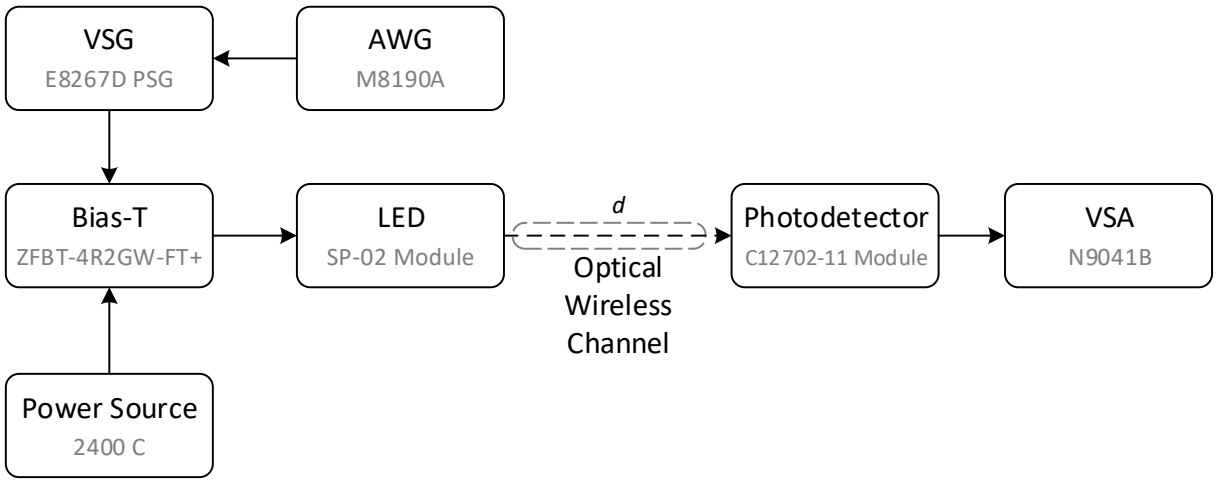

Source: The author.

A 5 MHz wide LTE or 5G signal is generated by proprietary software bundled with the equipment. This bandwidth is chosen due to the low bandwidth of commercial LEDs; the next possible band (10 MHz) provides poor performance results. The signal is sent to an arbitrary waveform generator (AWG, Keysight M8190A) that physically generates the

desired signal which is then sent to a vector signal generator (VSG, Keysight E8297D) that converts it to the chosen carrier frequency.

As LEDs have a very low bandwidth when compared to RF devices, a down conversion is needed. In this way, the mobile signals are modulated at a carrier frequency of 3.5 MHz, which provided the best EVM performances for within the consraints of the setup. The signal is then mixed with DC level at a bias-T (Mini-Circuits ZFBT-4R2GW). The output of the bias-T acts as the input driver current for the LED module. The transmission distance is varied from 20 cm to 3 m.

At the receiver side, the C12702 module is employed (receiver area of 7.06 mm^2). In order to improve the strength of the received signal, in this setup it is also employed an optical lens before the photodetector to collect more light and improve the gain of the incident light. Finally, the received signal is demodulated and analyzed at a vector signal analyzer (VSA, Keysight N9041B). Figure 65 is a picture of the 4G and 5G setup in the laboratory.

Figure 65 – VLC LTE and 5G setup in the laboratory.

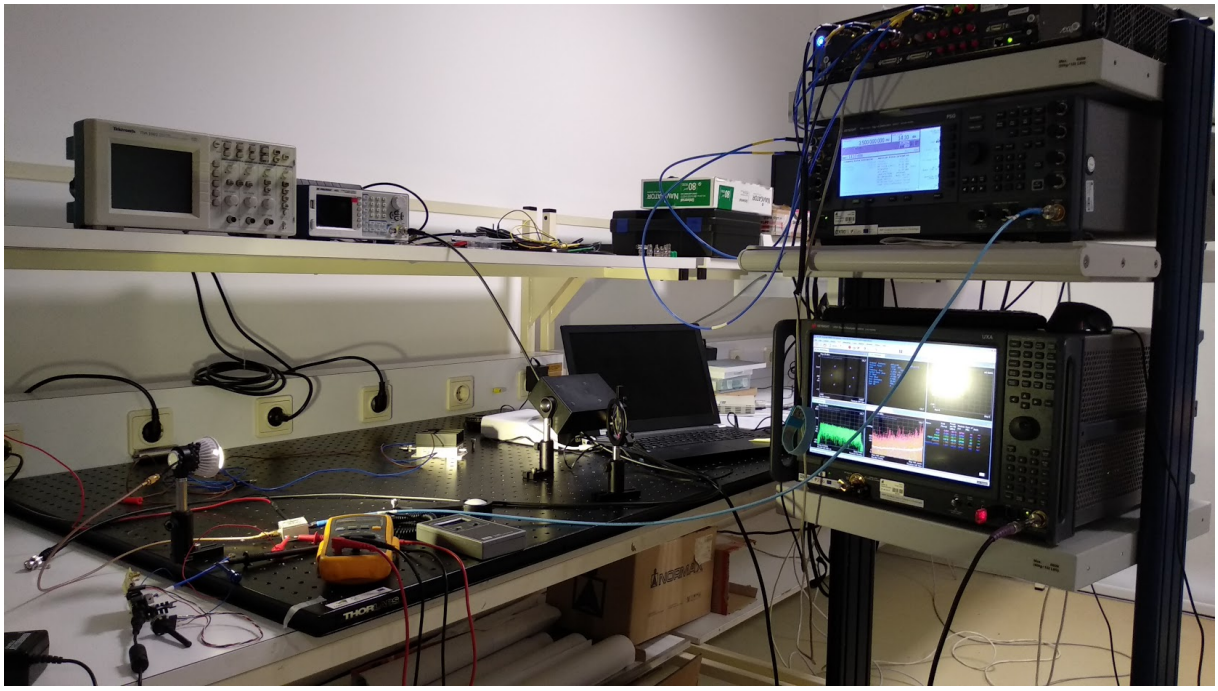

Source: The author.

The performance of the transmission is evaluated by measuring the EVM, as obtained from the VSA.

6.2 CONFIGURATION OF THE 4G SIGNAL

The transmitted downlink LTE signal contains the following signals and channels (and their modulation formats) (ETSI, 2015):

- Primary synchronization signal (PSS): Zadoff-Chu;
- Secondary synchronization signal (SSS): BPSK;
- Cell specific reference signal (CRS): QPSK;
- Physical broadcast channel (PBCH): QPSK;
- Physical control format indicator channel (PCFICH): QPSK;
- Physical HARQ indicator channel (PHICH): BPSK;
- Physical downlink control channel (PDCCH): QPSK;
- Physical downlink shared channel (PDSCH): 64-QAM.

In Figure 66, the EVM results for the experiment are presented. For LTE using 64-QAM in the PDSCH (the channel that carries user data), the threshold EVM is -22 dB (or 8%) (ETSI, 2015).

As a reference, in Figure 67 it is presented the constellation diagram and the received spectrum of the 4G transmission at the maximum measured distance of 3 m.

Compared to previous results in the literature (COSSU *et al.*, 2016), the presented setup shows a better performance while employing a smaller photodetection area (7.06 mm^2 versus 1 cm^2) in a distance of up to 3 m compared to 2 m, albeit in this work it was measured only a 5 MHz-wide signal, against a signal of 10 MHz in the work of Cossu *et al.* (2016).

6.3 CONFIGURATION OF THE 5G SIGNAL

The transmitted downlink 5G-NR signal contains the following signals and channels (and their modulation formats) (COUTINHO, 2019):

- Primary synchronization signal (PSS): BPSK;

Figure 66 – Experimental EVM variation over distance for VLC 4G transmission.

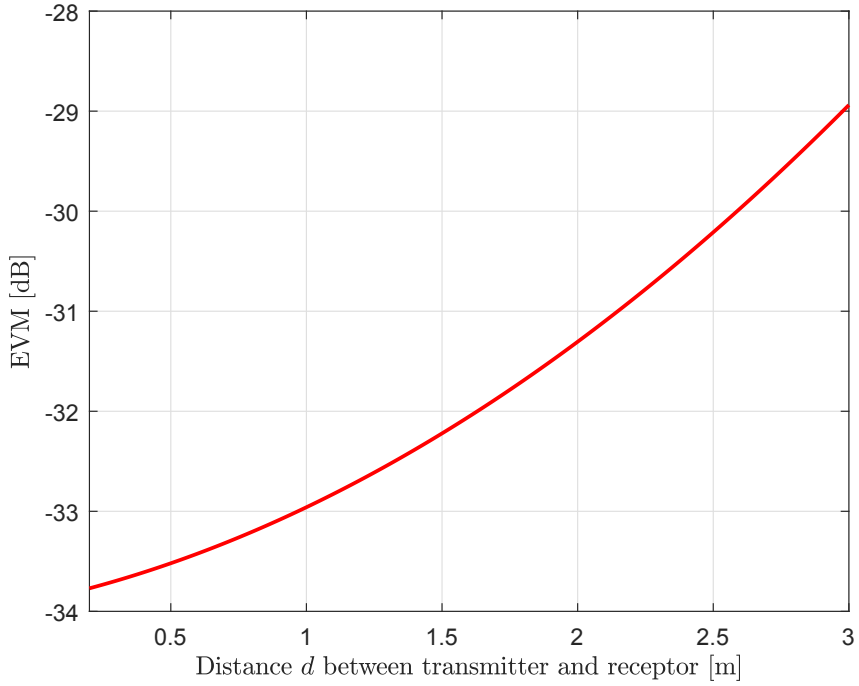

Source: The author.

- Secondary synchronization signal (SSS): BPSK;
- Physical broadcast channel and PBCH demodulation reference signal (PBCH and PBCH-DRMS): QPSK;
- Physical data shared channel and PDSCH demodulation reference signal (PDSCH and PDSCH-DRMS): QPSK.

For 5G, a comparison with theoretical EVM values is presented. The EVM can be expressed as a function of the SNR (SHAFIK *et al.*, 2006a):

$$\mathrm{EVM_{RMS}} = \sqrt{\frac{1}{\mathrm{SNR}}}. \tag{32}$$

To calculate the SNR, it is used the transmission power employed in the practical setup for each distance (from 3 to 18 dBm), as well as other experimental parameters, summarized in Table 10. For the noise value, it is employed the value in Figure 12 referring to the carrier frequency of 3.5 MHz.

Figure 68 presents both theoretical and experimental curves. For QPSK modulation at the PBCH, the required EVM is -15 dB (17.5%), according to the 3GPP Standard (3GPP TS 38.101-1, 2018).

Figure 67 – Received (a) constellation and (b) spectrum for VLC 4G transmission at 3 m distance.

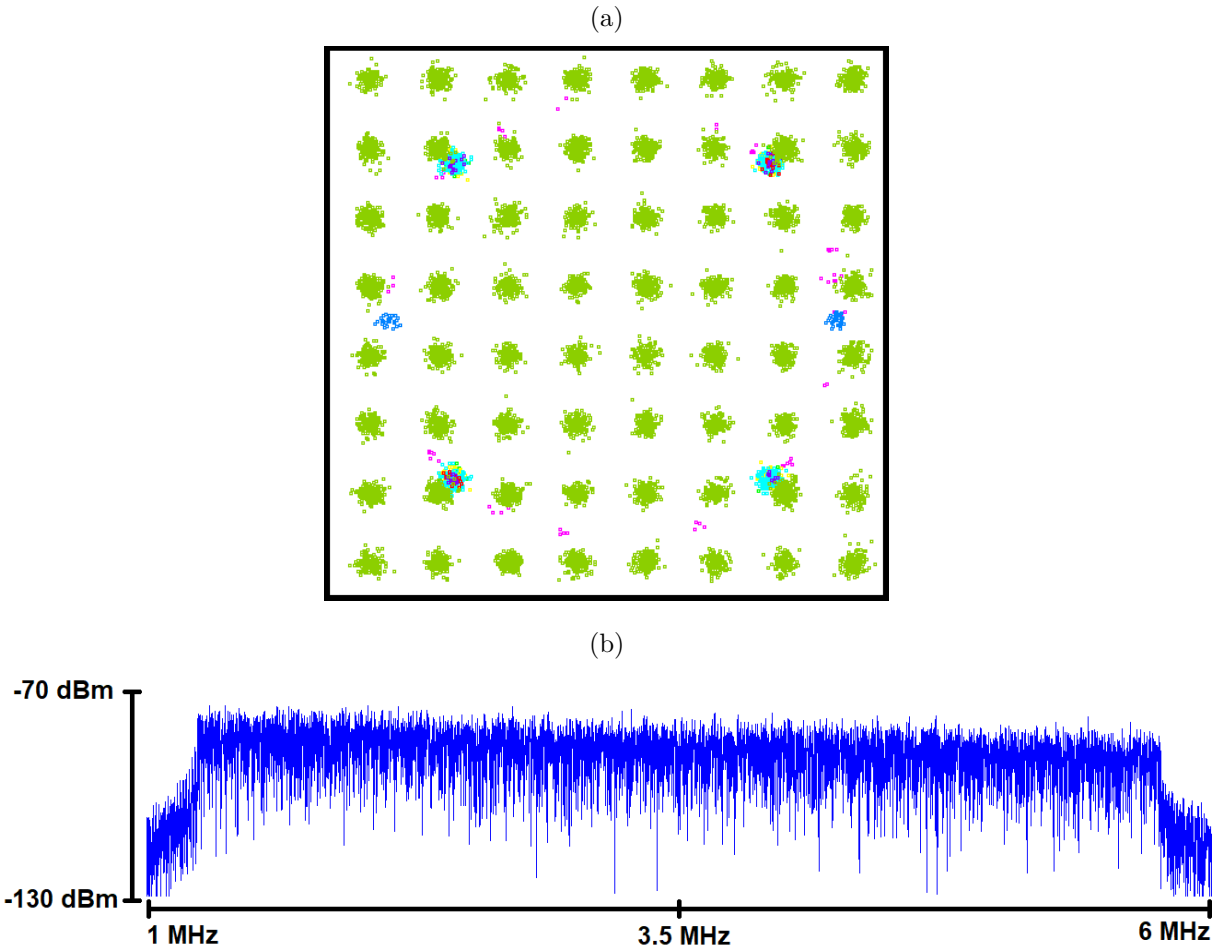

Source: The author.

As previously presented for LTE, in Figure 69 the constellation diagram and the received spectrum for the 5G transmission at the maximum measured distance of 3 m are shown.

Compared to the previous work of Shi *et al.* (2019), the presented setup shows a higher measured distance (55 cm versus 3 m) while keeping lower EVM values.

6.4 CHAPTER CONCLUSIONS

Among the variety of potential VLC applications, mobile communications attracts attention due to how widespread cellular networks are worldwide and how VLC may benefit this field. With the ever growing expansion of connected users to LTE networks, the incoming expansion of 5G and the expectation for the deployment of large

Table 10 – Experimental parameters of 5G VLC transmission.

Parameter	Value	Unit
Tranmission power (P_r)	3 to 18	dBm
Distance (d)	0.15 to 3	m
Photodetection area (A)	0.78	mm^2
Half-power semiangle ($\varphi_{1/2}$)	20	°
PD responsivity (γ)	0.42	A/W

Figure 68 – Comparison between theoretical and experimental EVM for 5G-NR VLC transmission.

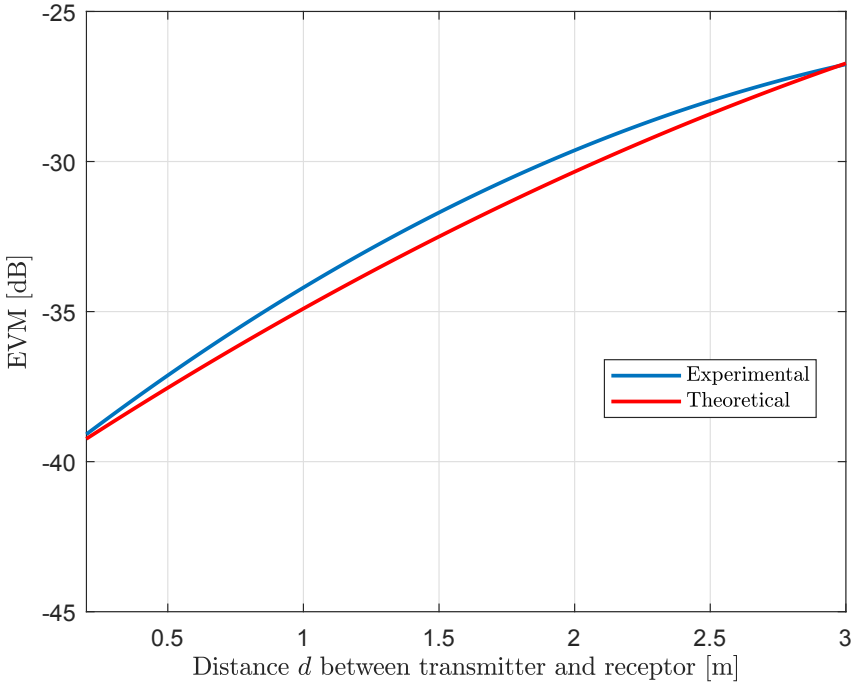

Source: The author.

quantities of IoT devices, solutions are needed to supply this demand, and VLC is a candidate to support it.

In order to contribute to this field, the signal is transmitted both with the LTE and 5G downlink configurations using VLC and measured performance results. In the context in which VLC is most suitable, *i.e.*, indoor medium-range communications, the results suggests that VLC is capable of transmitting mobile signals. For both technologies, the EVM results, measured up to 3 m, are below the standard's minimum, suggesting that it may be expanded to cover most indoor scenarios, such as offices or houses.

Figure 69 – Received (a) constellation and (b) spectrum for VLC 4G transmission at 3 m distance.

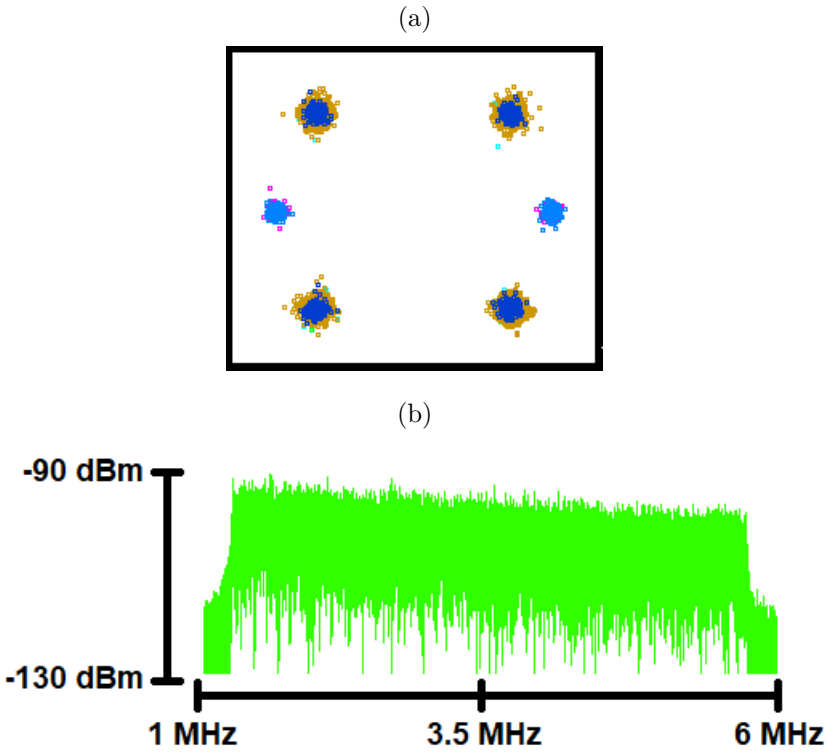

Source: The author.

7 CONCLUSIONS AND CLOSING COMMENTS

In a world that is hungry for information and data consumption, specially considering the convenience of fast wireless communication in portable devices, the research on means to improve these technologies is a hot topic. In this sense, this work aims to contribute to the field of visible light communications, an upcoming technology that has potential to address limitations of RF communications. VLC also encourages the adoption of LED illumination, a green technology, which is highly desirable in a society that urges to reduce its carbon footprint.

This study begins with the development of a simulation environment based on the VLC channel model described in the literature. This allows an initial familiarization with the field and the model is later employed in other developments in this work. In order to evaluate different parameters of VLC system, the model described in Ghassemlooy *et al.* (2018) is employed and developed further to also visualize SNR and BER values in a surface of a given height of a room. Also in MATLAB, a intuitive graphical interface for VLC simulation is developed, allowing for quick simulation of different scenarios, without the need of coding.

Besides the examples of the simulation model presented in this work, the model allows the evaluation of other scenarios by adjusting environment parameters such as room size, position of luminaires and receivers, and component's parameters such as transmission power, half-power semiangle, photodetection area, field of view, responsivity etc. Not all parameters and features of a real system are considered, such as amplitude deterioration due to transmission frequency, photodetector's cutoff frequency and others, limiting the simulation model to some extent.

The application of cooperative communication in the context of VLC is next described. It is the previously developed simulation model, now considering the use of a relay. This device, positioned between the source and transmission, improves performance of VLC systems by using the amplify-and-forward protocol to amplify the signal and retransmit it. The destination, if it receives both signals, combines them. The simulations results show that the cooperation contribute to improve SNR in diverse situations, *i.e.*, different positions of the transmission elements. For instance, in a room illuminated by one central lamp, in which the corners do not receive enough light to communicate, cooperation enables communication by raising SNR from 0 to 12 dB.

Experiments are set up for cooperative communication. Four different configurations are evaluated for SNR analysis and three for BER analysis employing an OFDM signal, with the purpose of analyzing scenarios that may happen in real deployments. The configurations consists of variations of the position of the setup's elements (source, relay and destination). Measured received power values were employed to calculate the SNRs and comparison of transmitted and received bits were performed to measure BER for each scenario and evaluate the benefits of cooperation. Results demonstrate that cooperation act as a support means for the deployment of VLC systems, improving the SNR and the BER by combining the source and relay signals and by enabling communication when the source-destination line of sight link is blocked. Overall, results presents SNR values increasing from 4 to 8 dB in the evaluated scenarios and, for BER measurements, the signal combination improved the BER by up to one order of magnitude, while the relay alone may be used as the access point at certain distances.

Next, VLC amplification is analyzed. As optical amplifiers for visible light begins to be developed, its advantages and limitations are analyzed and compared it with electrical amplification. The noise models are compared and simulation results for VLC amplification are presented, including a comparison of both methods. VLC relaying requires high values of gain in electrical amplification, while optical amplification requires lower values and presents inherent advantages.

Lastly, an application of VLC is presented, the transmission of downlink LTE (4G) and 5G signals. 5 MHz-wide signals are transmitted, due to LEDs' bandwidth limitations, for both standards, for distances up to 3 m. EVM values are measured for performance evaluation, which are well within the EVM limits for both cases at 3 m: -29 dB (limit: -22 dB) for 4G and -26 dB (limit: -15 dB) for 5G. These results suggests that larger distances are reachable and that VLC is a technology suitable to support 5G networks and beyond in indoor environments.

7.1 FUTURE DEVELOPMENTS

As VLC is a technology still mostly restricted to research laboratories, with few commercial deployments so far, the possibilities for research are manifold. On what concerns the themes approached in this thesis, future developments on cooperative cooperation includes the real time combination of source and relay signals. Possible approaches for this are the use of different frequencies for source and relay, which is a challenge for low-bandwidth LEDs, as most off-the-shelf devices are. Other possibility

is the use of RGB LEDs (CHUN *et al.*, 2016), in which different signals are assigned to different colors. As optical amplifiers for visible light evolves, its application in VLC is further encouraged. Development of materials with higher gains could be used for experimental cooperative VLC setups and compared with electrical relaying.

The simulation model can be expanded by implementing other features, such as MIMO systems, embed modulations and consider more reflections. The graphical interface (and the whole simulation model as well) can be reprogrammed in another language, such as Python or C, enabling the distribution of easy-to-use VLC simulators, allowing research groups and other interested parties to quickly simulate and evaluate VLC scenarios.

Cooperative communication and relay-assisted VLC can be employed to support the deployment of LiFi networks. As LiFi intends to be a complete wireless network solution, it is necessary to cover as much as possible of the environment. In such matter, cooperative and relay-assisted VLC is capable of expanding coverage without backbone infrastructure. Nodes in the network may also be configured to act as relays, as proposed in the RF cooperative communication literature (LANEMAN *et al.*, 2004). As well as amplify-and-forward cooperation, covered in this work, the decode-and-forward protocol also can be experimentally investigated in the VLC context, comparing the performance results and costs of deployment for AF and DF cooperative VLC.

The employed OFDM signal may be optimized to achieve better results while still employing the same bandwidth. The duration of the cyclic prefix is larger than the measured delay between the direct and relay channels, suggesting an opportunity for optimization and to aim for real-time signal combination. On the channel analysis, another aspect that may be studied is the LED nonlinearity (EIGALAT *et al.*, 2009; DENG *et al.*, 2018), which is an important concern in OFDM systems due to the high PAPR of OFDM, which may severely impact high data rate systems. This analysis is then suggested as a future work and as an important issue to be addressed for commercial applications.

Investigation of specific applications and scenarios of cooperation are suggested as future works. For instance, the application of cooperative VLC in a low power context, such as uplink or in contexts in which there is not a permanently guaranteed line of sight between source and destination, as vehicular communication. In uplink, there is the issue that a high power light next to the user is visually unpleasant and not expected to be accepted; with cooperation or a relay-assisted system, a lower power is required, enabling to reach the required distances using less electrical power. As for vehicular communication,

it is a context in which there is a high variation in the position of the users (vehicles), including blocking in the line of sight link between users and users and infrastructure. In such context, each user can act as a relay, enabling that every user reaches other users and infrastructure, regardless of its current position and the availability or not of a LOS link.

High-bandwidth LEDs (YEH *et al.*, 2019; ZHANG *et al.*, 2019) may also be employed for future research for mobile links in VLC. With higher available bandwidth, LTE and 5G signals with larger than 5 MHz bandwidths may be investigated and performance measured. Experimental setups of uplink LTE and 5G signals transmission are also encouraged.

BIBLIOGRAPHY

3GPP TS 38.101-1. User Equipment (UE) radio transmission and reception; Part 1: Range 1 Standalone (Release 15). v. 0, p. 0–244, 2018.

ABOU-RJEILY, C.; SLIM, A. Cooperative diversity for free-space optical communications: Transceiver design and performance analysis. **IEEE Transactions on Communications**, v. 59, n. 3, p. 658–663, 2011.

AGRAWAL, G. P. **Fiber-Optic Communication Systems**. 4th. ed. Hoboken, NJ, USA: John Wiley & Sons, Inc., 2010. 626 p. ISBN 9780470918524.

ALRESHEEDI, M. T.; HUSSEIN, A. T.; ELMIRGHANI, J. M. Uplink design in VLC systems with IR sources and beam steering. **IET Communications**, v. 11, n. 3, p. 311–317, 2017. ISSN 1751-8628.

Analysys Mason Limited. **Wireless network traffic worldwide: forecasts and analysis 2013-2018**. New Delhi, 2013. Available: <http://www.analysysmason.com/About-Us/News/Insight/Mobile-data-Oct2013/>.

ANGELOVA, M.; RAJBHANDARI, S.; GHASSEMLOOY, Z. Bit error performance of diffuse indoor optical wireless channel pulse position modulation system employing artificial neural networks for channel equalisation. **IET Optoelectronics**, v. 3, n. 4, p. 169–179, 2009.

AZHAR, A. H.; TRAN, T. A.; O'BRIEN, D. A gigabit/s indoor wireless transmission using MIMO-OFDM visible-light communications. **IEEE Photonics Technology Letters**, v. 25, n. 2, p. 171–174, 2013.

BALDWIN, H. **Wireless bandwidth: Are we running out of room?** 2012. Available: <https://www.computerworld.com/article/2500312/mobile-wireless/wireless-bandwidth–are-we-running-out-of-room-.html>.

BALEJA, R. *et al.* Comparison of LED properties, compact fluorescent bulbs and bulbs in residential areas. **Proceedings of the 2015 16th International Scientific Conference on Electric Power Engineering, EPE 2015**, p. 566–571, 2015.

BARRY, J. R. *et al.* Simulation of Multipath Impulse Response for Indoor Wireless Optical Channels. **IEEE Journal on Selected Areas in Communications**, v. 11, n. 3, p. 367–379, 1993. ISSN 07338716.

BASTOS, A. *et al.* Flexible Optical Amplifier for Visible-Light Communications Based on Organic-Inorganic Hybrids. **ACS Omega**, v. 3, n. 10, p. 13772–13781, oct 2018. ISSN 2470-1343.

BASTOS, A. R. *et al.* Flexible Blue-Light Fiber Amplifiers to Improve Signal Coverage in Advanced Lighting Communication Systems. **Cell Reports Physical Science**, v. 1, n. 4, p. 100041, 2020. ISSN 26663864.

BELL, A. G. Selenium and the Photophone. **Nature**, v. 22, n. 569, p. 500–503, sep 1880.

BESSHO, M.; SHIMIZU, K. Latest trends in LED lighting. **Electronics and Communications in Japan**, v. 95, n. 1, p. 1–7, 2012.

BIAN, R.; TAVAKKOLNIA, I.; HAAS, H. 15.73 Gb/s Visible Light Communication with Off-the-Shelf LEDs. **Journal of Lightwave Technology**, IEEE, v. 37, n. 10, p. 2418–2424, 2019. ISSN 07338724.

BOROGOVAC, T. *et al.* "Lights-off" visible light communications. **IEEE Globecom 2011 2nd Workshops on Optical Wireless Communications (OWC 2011)**, p. 797–801, 2011.

BRENNAN, D. Linear diversity combining techniques. **Proceedings of the IEEE**, v. 91, n. 2, p. 331–356, feb 2003. ISSN 0018-9219.

BUI, T. C. *et al.* A Comprehensive Lighting Configuration for Efficient Indoor Visible Light Communication Networks. **International Journal of Optics**, v. 2016, 2016.

CARBONELLI, C.; CHEN, S. H.; MITRA, U. Error propagation analysis for underwater cooperative multi-hop communications. **Ad Hoc Networks**, Elsevier B.V., v. 7, n. 4, p. 759–769, 2009.

CHANG, R. W. Synthesis of Band-Limited Orthogonal Signals for Multichannel Data Transmission. **Bell System Technical Journal**, v. 45, n. 10, p. 1775–1796, 1966.

CHEN, C. *et al.* Visible light communication using the microphone jack of the smart phone as an optical receiver and its application in the indoor localization system. **2017 International Conference on Electron Devices and Solid-State Circuits (EDSSC)**, p. 1–2, 2017.

CHEN, M. *et al.* Experimental Demonstration of Real-Time High-Level QAM-Encoded Direct-Detection Optical OFDM Systems. **Journal of Lightwave Technology**, IEEE, v. 33, n. 22, p. 4632–4639, 2015. ISSN 07338724.

CHINTALAPUDI, K.; Padmanabha Iyer, A.; PADMANABHAN, V. N. Indoor localization without the pain. **Proceedings of the sixteenth annual international conference on Mobile computing and networking - MobiCom '10**, p. 173, 2010.

CHOWDHURY, M. Z. *et al.* The role of optical wireless communication technologies in 5G/6G and IoT solutions: Prospects, directions, and challenges. **Applied Sciences (Switzerland)**, v. 9, n. 20, 2019. ISSN 20763417.

CHUN, H. *et al.* LED Based Wavelength Division Multiplexed 10 Gb/s Visible Light Communications. **Journal of Lightwave Technology**, v. 34, n. 13, p. 3047–3052, jul 2016. ISSN 0733-8724.

CISCO. **Cisco Visual Networking Index: Global Mobile Data Traffic Forecast Update, 2017-2022 White Paper**. 2019. Available: <https://www.cisco.com/c/en/us/solutions/collateral/service-provider/visual-networking-index-vni/white-paper-c11-738429.html>.

COSMAS, J. *et al.* A Scalable and License Free 5G Internet of Radio Light Architecture for Services in Homes & Businesses. In: **2018 IEEE International Symposium on Broadband Multimedia Systems and Broadcasting (BMSB)**. Valencia: IEEE, 2018. v. 4, p. 1–6. ISBN 978-1-5386-4729-5.

COSSU, G. *et al.* Demonstrating practical indoor LTE-over-optical wireless. **2016 10th International Symposium on Communication Systems, Networks and Digital Signal Processing, CSNDSP 2016**, IEEE, p. 1–4, 2016.

COSSU, G. *et al.* 3.4 Gbit/s visible optical wireless transmission based on RGB LED. **Optics Express**, v. 20, n. 26, p. B501, 2012.

COSSU, G. *et al.* Design and characterization of the optical layer of a novel pair of underwater VLC modems. **International Conference on Transparent Optical Networks**, n. 1, p. 3–6, 2017.

COUTINHO, F. D. L. **FPGA implementation of a 5G-NR DU Rx Uplink chain**. Tese (Dissertation) — Universidade de Aveiro, 2019. Available: <https://ria.ua.pt/handle/10773/29637>.

COVER, T. M.; GAMAL, A. A. E. Capacity Theorems for the Relay Channel. **IEEE Transactions on Information Theory**, v. 25, n. 5, p. 572–584, 1979.

CUI, Z.; YUE, P.; JI, Y. Study of cooperative diversity scheme based on visible light communication in VANETs. **2016 International Conference on Computer, Information and Telecommunication Systems (CITS)**, n. 60902038, p. 1–5, 2016.

DENG, J. *et al.* Graph-based multi-user scheduling for indoor cooperative visible light transmission. **Optics Express**, v. 28, n. 11, p. 15984, 2020. ISSN 1094-4087.

DENG, X. *et al.* Mitigating LED nonlinearity to enhance visible light communications. **IEEE Transactions on Communications**, IEEE, v. 66, n. 11, p. 5593–5607, 2018. ISSN 15580857.

DIMITROV, S.; HAAS, H. Optimum signal shaping in OFDM-based optical wireless communication systems. **IEEE Vehicular Technology Conference**, p. 0–4, 2012.

DIMITROV, S.; HAAS, H. **Principles of LED Light Communications**. 1st. ed. Cambridge: Cambridge University Press, 2015.

DING, D. qiang; KE, X. zheng. A new indoor VLC channel model based on reflection. **Optoelectronics Letters**, v. 6, n. 4, p. 295–298, 2010.

DISSANAYAKE, S. D.; ARMSTRONG, J. Comparison of ACO-OFDM, DCO-OFDM and ADO-OFDM in IM/DD systems. **Journal of Lightwave Technology**, v. 31, n. 7, p. 1063–1072, 2013.

EIGALAT, H.; MESLEHT, R.; HAAST, H. A Study of led nonlinearity effects on optical wireless transmission using OFDM. **2009 IFIP International Conference on Wireless and Optical Communications Networks, WOCN 2009**, 2009.

ERGEN, M. Critical penetration for vehicular networks. **IEEE Communications Letters**, v. 14, n. 5, p. 414–416, 2010.

ERICSSON. **Ericsson Mobility Report Ericsson Mobility Report: Central and Estern Europe Key Figures**. 2017. Available: <https://www.ericsson.com/assets/local/mobility-report/documents/2017/ericsson-mobility-report-november-2017-central-and-eastern-europe.pdf>.

ETSI. **TS 136 141 - V12.6.0 - LTE; Evolved Universal Terrestrial Radio Access (E-UTRA); Base Station (BS) conformance testing (3GPP TS 36.141 version 12.6.0 Release 12)**. 2015.

FENG, L. *et al.* Applying VLC in 5G Networks: Architectures and Key Technologies. **IEEE Network**, n. December, p. 77–83, 2016. ISSN 08908044.

GFELLER, F. R.; BAPST, U. Wireless In-House Data Communication via Diffuse Infrared Radiation. **Proceedings of the IEEE**, v. 67, n. 11, p. 1474–1486, 1979.

GHASSEMLOOY, Z.; POPOOLA, W. O.; RAJBHANDARI, S. **Optical Wireless Communications: System and Channel Modelling with MATLAB**. 1. ed. Boca Raton: CRC Press, 2013. 575 p.

GHASSEMLOOY, Z.; POPOOLA, W. O.; RAJBHANDARI, S. **Optical Wireless Communications System and Channel Modelling with MATLAB**. 2nd. ed. Boca Raton: CRC Press, 2018. 541 p. ISBN 9781498742696.

Global Market Insights. **Li-Fi Market size forecast worth $75.5 billion by 2023**. 2016. Available: <https://www.gminsights.com/pressrelease/LiFi-market>.

GOLDSMITH, A. **Wireless Communications**. New York, NY, USA: Cambridge University Press, 2005.

GSMA Intelligence. **The Mobile Economy 2020**. Barcelona, 2020. Available: <https://www.gsma.com/mobileeconomy/>.

GUPTA, A. *et al.* Cascaded FSO-VLC communication system. **IEEE Wireless Communications Letters**, v. 6, p. 810–813, 2017.

HAAS, H. High-speed wireless networking using visible light. **SPIE Newsroom**, p. 2–4, 2013.

HAAS, H. *et al.* What is LiFi? **Journal of Lightwave Technology**, v. 34, n. 6, p. 1533–1544, mar 2016.

Hamamatsu Photonics. **APD modules: C12702 series**. 2017. 1–5 p. Available: <https://www.hamamatsu.com/jp/en/product/type/C12702-04/index.html>.

HAN, J.-W. *et al.* A Study on the Cooperative Diversity Technique with Amplify and Forward for Underwater Wireless Communication. In: **OCEANS 2008 - MTS/IEEE Kobe Techno-Ocean**. IEEE, 2008. p. 1–3.

HAO, X. *et al.* Design and performance analysis of indoor cooperative IHDAF protocol-based spatial modulation-index modulation visible light communication system. **Applied Optics**, v. 59, n. 19, p. 5821, 2020. ISSN 1559-128X.

HONG, W.; BAEK, K. H.; KO, S. Millimeter-Wave 5G Antennas for Smartphones: Overview and Experimental Demonstration. **IEEE Transactions on Antennas and Propagation**, v. 65, n. 12, p. 6250–6261, 2017. ISSN 0018926X.

HSIEH, C. C.; SHIU, D. S. Single carrier modulation with frequency domain equalization for intensity modulation-direct detection channels with intersymbol interference. **IEEE International Symposium on Personal, Indoor and Mobile Radio Communications, PIMRC**, n. 2, p. 0–4, 2006.

Hui Tian; Bo Fan; Lu Li. A joint resources allocation approach for hybrid visible light communication and LTE system. In: **11th International Conference on Wireless Communications, Networking and Mobile Computing (WiCOM 2015)**. Institution of Engineering and Technology, 2015. p. 6 .–6 . ISBN 978-1-78561-034-9.

HUSSAIN, B. *et al.* Visible Light Communication System Design and Link Budget Analysis. **J. Lightwave Technol.**, v. 33, n. 24, p. 1–1, 2015.

HUSSEIN, A. T.; ALRESHEEDI, M. T.; ELMIRGHANI, J. M. H. Fast and Efficient Adaptation Techniques for Visible Light Communication Systems. **Journal of Optical Communications and Networking**, OSA, v. 8, n. 6, p. 382, 2016. ISSN 1943-0620.

Institute of Electrical and Electronics Engineers. **802.15.7-2011 - IEEE Standard for Local and Metropolitan Area Networks–Part 15.7: Short-Range Wireless Optical Communication Using Visible Light**. 2011.

ISLIM, M. S.; HAAS, H. Modulation Techniques for Li?Fi. **ZTE Communications**, n. 2, p. 29–40, 2016.

JAMALI, M. V.; AKHOUNDI, F.; SALEHI, J. A. Performance Characterization of Relay-Assisted Wireless Optical CDMA Networks in Turbulent Underwater Channel. **IEEE Transactions on Wireless Communications**, v. 15, n. 6, p. 4104–4116, 2016.

JHA, M. K. *et al.* Channel coding performance of optical MIMO indoor visible light communication. In: **2015 International Conference on Advances in Computing, Communications and Informatics (ICACCI)**. IEEE, 2015. p. 97–102.

JOHNSON, L. J.; GREEN, R. J.; LEESON, M. S. Hybrid Underwater Optical / Acoustic Link Design. **International Conference on Transparent Optical Networks (ICTON)**, n. 2, p. 1–4, 2014.

JOVICIC, A.; LI, J.; RICHARDSON, T. Visible light communication: Opportunities, challenges and the path to market. **IEEE Communications Magazine**, v. 51, n. 12, p. 26–32, 2013.

KADAM, K.; DHAGE, M. R. Visible Light Communication for IoT. **2016 2nd International Conference on Applied and Theoretical Computing and Communication Technology (iCATccT)**, n. Vl, p. 275–278, 2016.

KAHN, J. M.; BARRY, J. R. Wireless Infrared Communications. v. 9219, n. 97, 1997.

KARUNATILAKA, D. *et al.* LED Based Indoor Visible Light Communications: State of the Art. **IEEE Communications Surveys & Tutorials**, v. 17, n. 3, p. 1649–1678, 2015.

KATTI, R.; PRINCE, S. A survey on role of photonic technologies in 5G communication systems. **Photonic Network Communications**, Springer US, v. 38, n. 2, p. 185–205, 2019. ISSN 15728188.

KAUSHAL, H.; KADDOUM, G. Underwater Optical Wireless Communication. **IEEE Access**, v. 4, p. 1518–1547, 2016. ISSN 2169-3536.

KAVEHRAD, M. Sustainable Energy-Efficient Wireless Applications Using Light. **Consumer Communications and Networking, IEEE**, v. 48, n. December, p. 66–73, 2010.

KAZEMI, H.; HAAS, H. Downlink cooperation with fractional frequency reuse in DCO-OFDMA optical attocell networks. **2016 IEEE International Conference on Communications, ICC 2016**, 2016.

KAZEMI, H.; HAAS, H. On the performance of single side-band OFDM for band-limited visible light communication. **2020 IEEE International Conference on Communications Workshops, ICC Workshops 2020 - Proceedings**, 2020.

KHALID, A. M. *et al.* 1-Gb/s transmission over a phosphorescent white LED by using rate-adaptive discrete multitone modulation. **IEEE Photonics Journal**, v. 4, n. 5, p. 1465–1473, 2012.

KHALIGHI, M. A.; UYSAL, M. Survey on Free Space Optical Communication: A Communication Theory Perspective. **IEEE Communications Surveys & Tutorials**, v. 16, n. 4, p. 2231–2258, 2014. ISSN 1553-877X.

KIM, J. K.; SCHUBERT, E. F. Transcending the replacement paradigm of solid-state lighting. **Optics Express**, v. 16, n. 26, p. 21835, dec 2008.

KIZILIRMAK, R. C.; NARMANLIOGLU, O.; UYSAL, M. Relay-Assisted OFDM-Based Visible Light Communications. **IEEE Transactions on Communications**, v. 63, n. 10, p. 3765–3778, 2015.

KIZILIRMAK, R. C.; UYSAL, M. Relay-assisted OFDM transmission for indoor visible light communication. **2014 IEEE International Black Sea Conference on Communications and Networking, BlackSeaCom 2014**, p. 11–15, 2014.

KOMINE, T.; HARUYAMA, S.; NAKAGAWA, M. A study of shadowing on indoor visible-light wireless communication utilizing plural white LED lightings. **Wireless Personal Communications**, v. 34, n. 1-2, p. 211–225, 2004.

KOMINE, T.; NAKAGAWA, M. Fundamental analysis for visible-light communication system using LED lights. **IEEE Transactions on Consumer Electronics**, v. 50, n. 1, p. 100–107, 2004.

KUMAR, N.; LOURENÇO, N. **LED based visible light communication: A brief survey and investigation**. 2010. 296–307 p.

KUNG, F.; SIM, M.; LEE, I. Performance enhancement of outdoor visible-light communication system using selective combining receiver. **IET Optoelectronics**, v. 3, n. 1, p. 30–39, feb 2009.

LANEMAN, J. N.; TSE, D. N. C.; WORNELL, G. W. Cooperative Diversity in Wireless Networks: Efficient Protocols and Outage Behavior. **IEEE Trans. Inf. Theory**, v. 50, n. 12, p. 3062–3080, 2004.

LEE, K.; PARK, H. Channel model and modulation schemes for visible light communications. **2011 IEEE 54th International Midwest Symposium on Circuits and Systems (MWSCAS)**, v. 00, p. 1–4, 2011.

LEE, S. J.; JUNG, S. Y. A SNR analysis of the visible light channel environment for visible light communication. **APCC 2012 - 18th Asia-Pacific Conference on Communications: "Green and Smart Communications for IT Innovation"**, p. 709–712, 2012.

LI, Y. *et al.* A VLC Smartphone Camera Based Indoor Positioning System. **IEEE Photonics Technology Letters**, v. 30, n. 13, p. 1171–1174, jul 2018. ISSN 1041-1135.

LIANG, S. *et al.* A novel vertical handover algorithm in a hybrid visible light communication and LTE system. In: **2015 IEEE 82nd Vehicular Technology Conference, VTC Fall 2015 - Proceedings**. 2016. ISBN 9781479980918.

LIFI.CO. **LiFiMAX Flex**. 2022. Available: <https://lifi.co/lifi-product/lifimax-flex/>.

LIN, B. *et al.* Interleaved frequency division multiple access for uplink VLC. In: **2016 15th International Conference on Optical Communications and Networks (ICOCN)**. IEEE, 2016. p. 1–3.

LOUÇÃO, L. P. S. **Iterative Space-Frequency Equalization Techniques for LTE**. Tese (Dissertation) — Universidade de Aveiro, 2013. Available: <https://ria.ua.pt/handle/10773/11779>.

Lumileds Holding B.V. **LUXEON Rebel Plus**. 2017. Available: <https://www.luxeonstar.com/lx18-p150-3-ansi white-luxeon-rebel-led-186lm>.

Luxeon Star LEDs. **SinkPAD-II 7 Rebel LED 40mm Round Module**. 2015. Available: <https://www.luxeonstar.com/ansi-white-5000K-sinkpad-ii-40mm-7-led-round-led-module-558lm>.

Mini-Circuits. **Coaxial Bias-Tee ZX85-12G-S+**. 2013. Available: <https://www.minicircuits.com/pdfs/ZX85-12G-S+.pdf>.

Mini-Circuits. **ZFBT-4R2GW+ Coaxial Bias-T**. 2018. Available: <https://www.minicircuits.com/pdfs/ZFBT-4R2GW+.pdf>.

Mini-Circuits. **ZHL-6A+ Coaxial Amplifier**. 2018. Available: <https://www.minicircuits.com/pdfs/ZHL-6A+.pdf>.

Mini-Circuits. **ZHL-72A+ Pulse Amplifier**. 2019. Available: <https://www.minicircuits.com/WebStore/dashboard.html?model=ZHL-72A%2B>.

MITRA, R.; BHATIA, V. Precoding Technique for Ill-Conditioned Massive MIMO-VLC System. **IEEE Vehicular Technology Conference**, IEEE, v. 2018-June, p. 1–5, 2018. ISSN 15502252.

MITRA, R. N.; AGRAWAL, D. P. 5G mobile technology: A survey. **ICT Express**, Elsevier B.V., v. 1, n. 3, p. 132–137, 2015. ISSN 24059595.

Mobile World Live. **Studio Demo: Pure LiFi**. 2018. Available: <https://www.mobileworldlive.com/mwl-tv-18/mwl-tv-18-monday/studio-demo-pure-lifi>.

NA, Z. *et al.* Modeling and Throughput Analysis of an ADO-OFDM Based Relay-Assisted VLC System for 5G Networks. **IEEE Access**, v. 6, p. 17586–17594, 2018.

NAKAMURA, S.; MUKAI, T.; SENOH, M. Candela-class high-brightness InGaN/AlGaN double-heterostructure blue-light-emitting diodes. **Applied Physics Letters**, v. 64, n. 13, p. 1687–1689, 1994.

NAMONTA, P.; CHERNTANOMWONG, P. The improvement of repeater system for Visible Light Communication. **2016 13th International Conference on Electrical Engineering/Electronics, Computer, Telecommunications and Information Technology, ECTI-CON 2016**, p. 0–5, 2016.

NARMANLIOGLU, O. *et al.* Cooperative visible light communications with full-duplex relaying. **IEEE Photonics Journal**, v. 9, n. 3, 2017.

NARMANLIOGLU, O.; KIZILIRMAK, R. C.; UYSAL, M. Relay-assisted OFDM-based visible light communications over multipath channels. **International Conference on Transparent Optical Networks**, v. 2015-August, p. 2–5, 2015.

NOSRATINIA, A.; HUNTER, T. E.; HEDAYAT, A. Cooperative Communication in Wireless Networks. **IEEE Commun. Mag.**, v. 42, n. 10, p. 74–80, 2004.

OH, E. *et al.* Toward dynamic energy-efficient operation of cellular network infrastructure. **IEEE Communications Magazine**, v. 49, n. 6, p. 56–61, 2011.

OH, M. A flicker mitigation modulation scheme for visible light communications. **Advanced Communication Technology (ICACT), 2013 15th International Conference on**, p. 933–936, 2013.

OKUDA, K. *et al.* Information delivery tactile pavings using visible light communication. In: **IEEE International Conference on Consumer Electronics (ICCE) Information**. 2014. p. 327–328.

OLIVEIRA, M.; MONTEIRO, P. P.; POHL, A. d. A. P. Performance Improvement of VLC Systems Employing an Amplify-and-Forward Scheme. In: **2019 22nd International Symposium on Wireless Personal Multimedia Communications (WPMC)**. IEEE, 2019. v. 53, n. 9, p. 1–5.

OLIVEIRA, M. *et al.* Theoretical and Experimental Analysis of LED Lamp for Visible Light Communications. **Wireless Personal Communications**, Springer US, n. 0123456789, 2022. ISSN 0929-6212.

OPENSIGNAL. **The State of LTE (February 2018)**. 2018. Available: <https://www.opensignal.com/reports/2018/02/state-of-lte>.

PATHAK, P. *et al.* Visible Light Communication, Networking and Sensing: Potential and Challenges. **IEEE Communications Surveys & Tutorials**, v. 17, n. c, p. 1–1, 2015.

PEREZ-JIMENEZ, R. *et al.* Visible light communication systems for passenger in-flight data networking. **Consumer Electronics (ICCE), 2011 IEEE International Conference on**, p. 445–446, 2011.

PEŠEK, P. *et al.* Mobile user connectivity in relay-assisted visible light communications. **Sensors (Switzerland)**, v. 18, n. 4, p. 1–16, 2018.

POHL, V.; JUNGNICKEL, V.; HELMOLT, C. Integrating-sphere diffuser for wireless infrared communication. **IEE Proceedings - Optoelectronics**, v. 147, n. 4, p. 281–285, 2000.

PREMACHANDRA, H. C. N. *et al.* High-speed-camera image processing based LED traffic light detection for road-to-vehicle visible light communication. In: **Intelligent Vehicles Symposium IV 2010 IEEE**. San Diego: IEEE, 2010. p. 793–798.

QIU, Y.; CHEN, H.-H.; MENG, W.-X. Channel modeling for visible light communications-a survey. **Wireless Communications and Mobile Computing**, v. 16, n. 14, p. 2016–2034, oct 2016.

RAHAIM, M. B.; VEGNI, A. M.; LITTLE, T. D. A hybrid Radio Frequency and broadcast Visible Light Communication system. **2011 IEEE GLOBECOM Workshops, GC Wkshps 2011**, p. 792–796, 2011.

RAHMAN, M. T. *et al.* Review of advanced techniques for multigigabit visible light communication. **IET Optoelectronics**, v. 14, n. 6, p. 359–373, 2020. ISSN 17518768.

RAJAGOPAL, S.; ROBERTS, R. D.; LIM, S. K. IEEE 802.15.7 visible light communication: Modulation schemes and dimming support. **IEEE Communications Magazine**, v. 50, n. 3, p. 72–82, 2012.

Real Wireless. **Study on the future UK spectrum demand for terrestrial mobile broadband applications**. 2014. 1–129 p.

SEJAN, M. A. S.; CHUNG, W.-Y. Lightweight multi-hop VLC using compression and data-dependent multiple pulse modulation. **Optics Express**, v. 28, n. 13, p. 19531, 2020.

SENDONARIS, A.; ERKIP, E.; AAZHANG, B. User cooperation diversity-part I: system description. **IEEE Transactions on Communications**, v. 51, n. 11, p. 1927–1938, 2003.

SHAFIK, R. A.; RAHMAN, M. S.; ISLAM, A. H. On the extended relationships among EVM, BER and SNR as performance metrics. **Proceedings of 4th International Conference on Electrical and Computer Engineering, ICECE 2006**, n. December, p. 408–411, 2006.

SHAFIK, R. A. *et al.* On the error vector magnitude as a performance metric and comparative analysis. **Proceedings - 2nd International Conference on Emerging Technologies 2006, ICET 2006**, n. November, p. 27–31, 2006.

SHARMA, R. *et al.* Performance analysis of LED based indoor VLC system under receiver mobility. In: **2017 International Conference on Computing, Communication and Automation (ICCCA)**. IEEE, 2017. p. 945–950.

SHI, L. *et al.* Experimental 5G New Radio integration with VLC. **2018 25th IEEE International Conference on Electronics Circuits and Systems, ICECS 2018**, IEEE, p. 61–64, 2019.

SIMON, M. K.; ALOUINI, M.-S. **Digital Communication over Fading Channels, 2nd Edition**. 2005. 936 p.

SINDHUBALA, K.; VIJAYALAKSHMI, B. Simulation of VLC system under the influence of optical background noise using filtering technique. **Materials Today: Proceedings**, Elsevier Ltd, v. 4, n. 2, p. 4239–4250, 2017.

TANAKA, Y. *et al.* Indoor visible communication utilizing plural white LEDs as lighting. In: **12th IEEE International Symposium on Personal, Indoor and Mobile Radio Communications. PIMRC 2001. Proceedings (Cat. No.01TH8598)**. IEEE, 2001. v. 2, p. F–81–F–85.

TANAKA, Y. *et al.* Indoor visible light data transmission system utilizing white led lights. **IEICE Transactions on Communications**, E86-B, n. 8, p. 2440–2454, 2003.

Tektronix. **PSPL5865 12.5 Gb/s Driver Amplifier**. 2015. Available: <https://www.tek.com/datasheet/amplifiers-and-drivers/pspl5865-datasheet-1>.

Thorlabs. **ACL7560, ACL7560-A, ACL7560-B**. 2015. Available: <https://www.thorlabs.com/catalogpages/Obsolete/2015/ACL7560.pdf>.

TIWARI, S. V.; SEWAIWAR, A.; CHUNG, Y. H. An Efficient Repeater Assisted Visible Light Communication. **European Wireless 2015; 21th European Wireless Conference; Proceedings of**, p. 1–5, 2015.

TOSTA, F. C. B.; OLIVEIRA, M.; POHL, A. d. A. P. Análise e caracterização de luminária LED aplicada em comunicação por luz visível. In: **XXXVIII Simpósio Brasileiro de Telecomunicações e Processamento de Sinais - SBrT 2020**. Florianópolis, 2020. p. 1–4.

TUENGE, J. **SSL pricing and efficacy trend analysis for utility program planning**. Washington, D.C., 2013. Available: <http://apps1.eere.energy.gov/buildings/publications/%0Apdfs/ssl/ssl_trend-analysis_2013.pdf>.

UCAR, S. *et al.* Dimming support for visible light communication in intelligent transportation and traffic system. In: **Proceedings of the NOMS 2016 - 2016 IEEE/IFIP Network Operations and Management Symposium**. 2016. p. 1193–1196.

ULGEN, O.; OZMAT, U.; GUNAYDIN, E. Hybrid Implementation of Millimeter Wave and Visible Light Communications for 5G Networks. In: **2018 26th Telecommunications Forum (TELFOR)**. IEEE, 2018. p. 1–4. ISBN 978-1-5386-7171-9.

UYSAL, M.; NOURI, H. Optical wireless communications - An emerging technology. **2014 16th International Conference on Transparent Optical Networks (ICTON)**, p. 1–7, 2014.

VATS, A.; AGGARWAL, M.; AHUJA, S. Outage analysis of AF relayed hybrid VLC-RF communication system for E-health applications. In: **2017 International Conference on Computing, Communication and Automation (ICCCA)**. IEEE, 2017. p. 1401–1405. ISBN 978-1-5090-6471-7.

VAVOULAS, A.; SANDALIDIS, H. G.; VAROUTAS, D. Underwater Optical Wireless Networks: A k-Connectivity Analysis. **IEEE Journal of Oceanic Engineering**, v. 39, n. 4, p. 801–809, oct 2014.

VUCIC, J. *et al.* 803 mbit/s visible light wdm link based on dmt modulation of a single rgb led luminary. In: **2011 Optical Fiber Communication Conference and Exposition and the National Fiber Optic Engineers Conference**. 2011. p. 1–3.

VUCIC, J. *et al.* 513 Mbit/s Visible Light Communications Link Based on DMT-Modulation of a White LED. **Journal of Lightwave Technology**, v. 28, n. 24, p. 3512–3518, dec 2010.

WANG, S. W. *et al.* A high-performance blue filter for a white-led-based visible light communication system. **IEEE Wireless Communications**, v. 22, n. 2, p. 61–67, 2015.

WANG, Y. *et al.* 4.5-Gb/s RGB-LED based WDM visible light communication system employing CAP modulation and RLS based adaptive equalization. **Optics Express**, v. 23, n. 10, p. 13626, may 2015.

WU, J. *et al.* Energy-efficient base-stations sleep-mode techniques in green cellular networks: A survey. **IEEE Communications Surveys and Tutorials**, v. 17, n. 2, p. 803–826, 2015.

WU, L.; YUE, P.; CUI, Z. Integrating LTE-D2D and VLC Techniques to Support V2V Communication. In: **2017 IEEE/CIC International Conference on Communications in China (ICCC)**. 2017. ISBN 9781538645024.

XU, K.; YU, H.; ZHU, Y. J. Channel-Adapted Spatial Modulation for Massive MIMO Visible Light Communications. **IEEE Photonics Technology Letters**, v. 28, n. 23, p. 2693–2696, 2016. ISSN 10411135.

YANG, H.; PANDHARIPANDE, A. Full-duplex relay VLC in LED lighting linear system topology. In: **IECON 2013 - 39th Annual Conference of the IEEE Industrial Electronics Society**. IEEE, 2013. p. 6075–6080.

YANG, H.; PANDHARIPANDE, A. Full-duplex relay VLC in LED lighting triangular system topology. **ISCCSP 2014 - 2014 6th International Symposium on Communications, Control and Signal Processing, Proceedings**, p. 85–88, 2014.

YANG, Y. *et al.* An Amplify-and-Forward Based OFDM System for VLC Uplink Transmission. **2017 IEEE Global Communications Conference, GLOBECOM 2017 - Proceedings**, v. 2018-January, p. 1–6, 2018.

YEH, C. H. *et al.* 1.7 to 2.3 Gbps OOK LED VLC transmission based on 4x4 color-polarization-multiplexing at extremely low illumination. **IEEE Photonics Journal**, IEEE, v. 11, n. 4, p. 1–6, 2019. ISSN 19430655.

YOSHINO, M.; HARUYAMA, S.; NAKAGAWA, M. High-accuracy positioning system using visible LED lights and image sensor. **2008 IEEE Radio and Wireless Symposium, RWS**, p. 439–442, 2008.

YU, S. H. *et al.* Smart automotive lighting for vehicle safety. **IEEE Communications Magazine**, v. 51, n. 12, p. 50–59, 2013.

ZAID, A. *et al.* **5G Physical Layer: Principles, Models and Technology Components**. 1st. ed. London: Elsevier, 2018. 312 p. ISBN 9780128145791.

ZENG, L. *et al.* Improvement of date rate by using equalization in an indoor visible light communication system. **2008 4th IEEE International Conference on Circuits and Systems for Communications, ICCSC**, n. 0, p. 678–682, 2008.

ZHANG, Z. *et al.* Over 700 MHz -3 dB Bandwidth UOWC System Based on Blue HV-LED with T-Bridge Pre-Equalizer. **IEEE Photonics Journal**, v. 11, n. 3, 2019. ISSN 19430655.

ZHOU, Z.; CHEN, C.; KAVEHRAD, M. Impact Analyses of High-Order Light Reflections on Indoor Optical Wireless Channel Model and Calibration. **Journal of Lightwave Technology**, v. 32, n. 10, p. 2003–2011, 2014.

ZWAAG, K. M. V. D. *et al.* A Manchester-OOK Visible Light Communication System for Patient Monitoring in Intensive Care Units. **IEEE Access**, IEEE, v. 9, p. 104217–104226, 2021. ISSN 21693536.

ZWAAG, K. M. vd *et al.* Adaptation to the LEDs flicker requirement in visible light communication systems through CE-OFDM signals. **Optics Communications**, Elsevier Ltd., v. 441, n. February, p. 14–20, 2019. ISSN 00304018.